CONTRACT REPORT NO. 1-170

A COMPARISON OF PLANE AND SPHERICAL TRANSIENT VOIGT WAVES WITH EXPLOSION GENERATED WAVES IN ROCK MASSES

by

G. B. Clark

G. B. Rupert

J. E. Jamison

April 1967

Sponsored by

Defense Atomic Support Agency

NWER Subtask 13.191C

Conducted for

U. S. Army Engineer Waterways Experiment Station

CORPS OF ENGINEERS

Vicksburg, Mississippi

Under

Contract No. DA-22-079-eng-464

by

George B. Clark and Associates

Rolla, Missouri

ARMY-MRC VICKSBURG, MISS.

ABSTRACT

Plane and spherical waves in a Voigt medium were investigated to compare the calculated wave forms with observed waves generated by large contained HE and NE explosions. Interest is centered on wave forms in what is usually considered to be the elastic region around an explosion. Plane waves do not apply at this distance because of geometry.

The plane Voigt wave equation has been previously solved for particle velocity, stress and strain for a unit impulse forcing function. However, solutions for the displacement for a unit impulse and for the four wave parameters for a unit step and a decay exponential involve multipliers in the operational form for which no transform pairs have been published. A method of solution is presented which utilizes a Heaviside expansion of the multipliers in the transform plane which results in products of two infinite series which may be inverted term by term. These may be further resolved as single series with polynomial coefficients for purposes of computation.

A similar method of solution of Voigt spherical waves was found for unit impulse, unit step and decay exponential forcing functions for displacement, particle velocity, strain and radial stress. Appropriate recursion formulas make them readily adaptable to computer evaluation. Oscillations occur for a spherical wave whereas for a plane wave they do not.

Calculations were performed for particle velocity for three values of the Voigt viscoelastic parameter ω_o and comparisons made with pulse forms for waves in granite, tuff and salt.

FOREWORD

This work was supported by the Defense Atomic Support Agency and was conducted as a part of the U. S. Army Engineer Waterways Experiment Station's (WES) Nuclear Weapons Effects Research program, Subtask 13.191C, Rock Mechanics Research Relating to Deep Underground Protective Construction, Wave Propagation in Rock.

Contract monitoring was under the direction of Mr. G. L. Arbuthnot, Jr., Chief, Nuclear Weapons Effects Division, with Messrs. L. F. Ingram, J. L. Kirkland, and J. L. Drake providing assistance.

Director of WES was Colonel John R. Oswalt, Jr., CE; Technical Director was Mr. J. B. Tiffany.

TABLE OF CONTENTS

	Page Number
Abstract	3
Foreword	4
List of Symbols	6
Introduction	8
Voigt Model	9
Plane Waves	12
Spherical Wave	20
Computation Procedures	27
Comparison of Voigt Waves and Observed Waves	28
Plane Waves	29
Forcing Functions	29
Rock Properties	29
Wave Velocity	30
Rise and Fall Time	30
Attenuation	31
Conclusions	32
Table I - Rock Properties	33
Figs. 1-49	34-82
Appendix A Wave Parameter Formulas	83
References	102

List of Symbols

a_i = constants
b_m = constants from Heaviside expansion
c = elastic velocity of sound
$c = \sqrt{E/\rho}$ for plane wave
$c = \sqrt{(\lambda+2\mu)/\rho}$ for spherical wave
c_i = constants
D_{-n} = Weber function of negative integral order
e = exponential
E = Young's modulus of elasticity
k = summation index
m = summation index
n = summation index
P = notation for plane wave
P_o = pressure
P' = pressure multiplier for $\delta(t)$
P'' = pressure multiplier for $1(t)$
$q = s^{\frac{1}{2}}$
r = radial length
r_o = radius of cavity
$R = \omega_o(r-r_o)/c$, dimensionless distance
s = transform variable
S = notation for spherical wave
t = time
T = dimensionless time = $\omega_o t$
u = displacement
v = particle velocity
x = linear distance
$X = \omega_o x/c$, dimensionless distance
ϵ = strain

λ = Lame's constant - elastic

λ' = viscoelastic modulus

μ = shear modulus - elastic

ρ = density

σ = stress

ω_o = transition frequency = $(\lambda+\mu)/(\lambda'+\mu')$

$\sum$ = summation

A Comparison of Plane and Spherical Transient Voigt Waves With Explosion Generated Waves in Rock Masses

Introduction

The Voigt model yields responses to transient forcing functions which are different from the standard elastic model, and earlier (Ref. 1) mathematical analyses of plane waves in Voigt materials indicated pulse lengthening and attenuation somewhat similar to that observed in waves generated by large explosions in rock.

While the theory of elasticity provides a good first approximation to many problems in rock mechanics, in the solution to close-in wave mechanics in rock it does not give an accurate description of the behavior of peak stress, strain, displacement, velocity or pulse length. The Voigt viscoelastic model is among the many physical analogs which have been investigated in an attempt to find valid mathematical representations of wave parameters in rock. The only solutions for a plane Voigt wave in the literature appears to be those of Collins (Ref. 1) and Hanin (Ref. 2) in which they solved for the particle velocity in response to a unit impulse.

Lee (Ref. 3) solved the spherical Voigt equation for stress for a continuous harmonic forcing function. However, in solving for response to transient loading he introduced a "constant loss factor" into the transform which changed the problem from a Voigt model to essentially a solid friction model.

The objectives of this investigation are to arrive at and present solutions to both the plane and spherical wave equations for parameters of interest, i.e., particle velocity, strain, displacement and stress, and to compare the calculated results with those obtained in observations of waves in rocks from large HE and nuclear explosions.

There have been many approaches made to the solution of transient Voigt waves, but apparently the first

successful solution was made by Collins (Ref. 1) for particle velocity for a unit impulse. Clark and Rupert (Ref. 4 and 5) obtained stress and strain by Collins' method and the displacement by numerical integration. The method employed by Collins was to normalize and shift the Laplace transform solution for the Voigt wave equation, expand the positive part of a resulting exponential in a series, and obtain a term by term inversion expressed as negative order parabolic cylinder functions multiplied by a factorial, an exponential and a power term.

Operational solutions for the displacement for a unit impulse and for forcing functions such as a unit step or a decay exponential require that the transform solution also contain an appropriate multiplier. No transform pairs for the resulting expressions exist in published tables.

The transformed multipliers may, however, be expressed as Heaviside expansions, yielding a transformed solution in the s-plane composed of the product of two infinite series. These may be inverted term by term into the time plane, expressed as a product of two series in the time variable and by proper arrangement utilized for computer evaluation. Some of the double series may be expressed as Cauchy products, which clarifies the mathematical operations and assists materially in computer programming.

Voigt Model: The basic Voigt model for an aeolotropic solid was conceived for a substance in which it was assumed that the stress components could be expressed as the sum of two sets of terms, the first being proportional to the strains and the second proportional to the rate of change of the strains. (Ref. 6) For an aeolotropic solid the stress equations are of the form (Ref. 7)

$$\sigma_x = (c_{11}+d_{11}\frac{\partial}{\partial t})\varepsilon_x + (c_{12}+d_{12}\frac{\partial}{\partial t})\varepsilon_y + (c_{13}+d_{13})\varepsilon_z$$

$$+ (c_{14}+d_{14}\frac{\partial}{\partial t})\gamma_{yz} + (c_{15}+d_{15}\frac{\partial}{\partial t})\gamma_{zx} + (c_{16}+d_{16}\frac{\partial}{\partial t})\gamma_{xy} \qquad (1)$$

where σ_y, σ_z, τ_{yz}, τ_{xz} and τ_{xy} are of similar form with appropriate c_{ij} and d_{ij} multiplying constants. If energy is to be an univalued function then $c_{rs} = c_{sr}$ and $d_{rs} = d_{sr}$. This reduces the number of independent constants from 72 to 42. In an isotropic medium there are only three elastic constants and three viscoelastic constants. Thus,

$$
\begin{aligned}
&c_{12} = c_{13} = c_{21} = c_{31} = c_{32} = \lambda \\
&d_{12} = d_{13} = d_{21} = d_{31} = d_{32} = \lambda' \\
&c_{44} = c_{55} = c_{66} = \mu \\
&d_{44} = d_{55} = d_{66} = \mu' \\
&c_{11} = c_{22} = c_{33} = \lambda+2\mu \\
&d_{11} = d_{22} = d_{33} = \lambda'+2\mu'
\end{aligned}
\qquad (2)
$$

Thus, the stresses for a Voigt solid become

$$\sigma_x = \left(\lambda+\lambda' \frac{\partial}{\partial t}\right) \Delta + 2\left(\mu+\mu' \frac{\partial}{\partial t}\right) \varepsilon_x$$

$$\sigma_y = \left(\lambda+\lambda' \frac{\partial}{\partial t}\right) \Delta + 2\left(\mu+\mu' \frac{\partial}{\partial t}\right) \varepsilon_y$$

$$\sigma_z = \left(\lambda+\lambda' \frac{\partial}{\partial t}\right) \Delta + 2\left(\mu+\mu' \frac{\partial}{\partial t}\right) \varepsilon_z \qquad (3)$$

$$\tau_{yz} = \left(\mu+\mu' \frac{\partial}{\partial t}\right) \gamma_{yz}$$

$$\tau_{xz} = \left(\mu+\mu' \frac{\partial}{\partial t}\right) \gamma_{xz}$$

$$\tau_{xy} = \left(\mu+\mu' \frac{\partial}{\partial t}\right) \gamma_{xy}$$

where

$$\Delta = \varepsilon_x + \varepsilon_y + \varepsilon_z \qquad \text{(dilatation)}$$

Thus, the wave equation may be obtained for a Voigt solid by substituting $\left(\lambda+\lambda' \frac{\partial}{\partial t}\right)$ and $\left(\mu+\mu' \frac{\partial}{\partial t}\right)$ for μ.

Plane Waves

The basic wave equation for a plane Voigt wave may be derived in different ways and in terms of alternative parameters:

$$\left(1+\frac{1}{\omega_o}\frac{\partial}{\partial t}\right)\frac{\partial^2 z}{\partial x^2} = \frac{1}{c^2}\frac{\partial^2 z}{\partial t^2} \tag{4}$$

where z represents either displacement, velocity, stress or strain.

Where,

ω_o = viscoelastic or transition frequency factor

c = bar velocity = E/ρ

x = distance

t = time

Collins, (Ref. 1), however, derived the operational form of the equation directly for particle velocity utilizing the force acceleration relation

$$\frac{\partial \sigma}{\partial x} = \rho \frac{\partial v}{\partial t} \tag{5}$$

in which particle velocity is

$$v = \frac{\partial u}{\partial t} \tag{6}$$

and the relationship of strain to displacement

$$\varepsilon = \frac{\partial u}{\partial x} \tag{7}$$

together with the following. The Voigt relationship between stress and strain is

$$\sigma = E\left(\varepsilon + \frac{1}{\omega_o}\frac{\partial \varepsilon}{\partial t}\right) \tag{8}$$

which in operational form is

$$\sigma = E(1+s/\omega_o)\varepsilon \tag{9}$$

Equation (5) in operational form becomes

$$\frac{\partial \bar{\sigma}}{\partial x} = \rho s \bar{v} \tag{10}$$

where the bar indicates that the Laplace transform has been taken and (6) is

$$\bar{u} = s\bar{v} \tag{11}$$

For a delta function input the boundary condition at $t \geq o$ is

$$\sigma = - P'\delta(t) \tag{12}$$

which is unity in operational form, i.e.,

$$\bar{\sigma} = -P' \tag{13}$$

From (10) and (11)

$$\frac{\partial \bar{\sigma}}{\partial x} = \rho s^2 \bar{u} \tag{14}$$

or differentiating

$$\frac{\partial^2 \bar{\sigma}}{\partial x^2} = \rho s^2 \frac{\partial \bar{u}}{\partial x} = \rho s^2 \bar{\varepsilon} \tag{15}$$

which, with (9) becomes

$$\frac{\partial^2 \bar{\sigma}}{\partial x^2} = \frac{\rho}{E} \frac{s^2}{(s/\omega_o+1)} \bar{\sigma} \tag{16}$$

The solution to this, after satisfying the boundary conditions is

$$\bar{\sigma} = \exp[-xs/c(s/\omega_o+1)^{\frac{1}{2}}] \tag{17}$$

Differentiating once with respect to x and using (10) gives the velocity equation

$$\bar{v} = \frac{P'}{\rho c} \frac{\exp[-xs/c(s/\omega_o+1)^{\frac{1}{2}}]}{\sqrt{s/\omega_o+1}} \tag{18}$$

The notation of Collins and van der Pol is used herein for the symbol connecting a function to its transform:

$$v(x,t) \doteq \bar{v}(x,s) \tag{19}$$

The transform expression in (18) is then "normalized" by substituting $\omega_o s$ for ω_o, or multiplying s by ω_o. This is equivalent to dividing the time and the velocity function by ω_o, thus

$$\frac{1}{\omega_o} v(x,t/\omega_o) \doteq \frac{P'}{\rho c} \frac{\exp[-x\omega_o s/c(s+1)^{\frac{1}{2}}]}{\sqrt{s+1}} \tag{20}$$

The shift theorem is then used to place the transform

solution in a form which can be inverted by use of tabulated transform pairs, i.e.,

$$v(x,t/\omega_o)e^t \doteq \frac{P'\omega_o}{\rho c} \frac{\exp[-X(s-1)/s^{\frac{1}{2}}]}{\sqrt{s}} \tag{21}$$

where $X = \frac{\omega_o x}{c}$

The second half of the exponential is then expanded:

$$e^{-X/\sqrt{s}} = \sum_{n=o}^{\infty} \frac{X^n}{n!} \frac{1}{s^{n/2}} \tag{22}$$

which gives

$$v(x,t/\omega_o)e^t \doteq \frac{P'\omega_o}{\rho c} \sum_{n=o}^{\infty} \frac{X^n}{n!} \frac{\exp(-x\sqrt{s})}{s^{n/2+1/2}} \tag{23}$$

By use of formula (9) page 246 of Ref.(8) equation (23) may be inverted term by term to give

$$v(x,t/\omega_o)e^t = \frac{P'\omega_o}{\rho c} \sum_{n=o}^{\infty} \frac{X^n 2^{n/2} t^{n/2-1/2}}{n!\sqrt{\pi}} \exp(-X^2/8t) \; D_{-n}\left(\frac{X}{\sqrt{2t}}\right) \tag{24}$$

or, rearranging and substituting $\omega_o t$ for t and letting $\omega_o t = T$

$$v(x,t) = \frac{P'\omega_o}{\rho c\sqrt{\pi}} \exp(-T-X^2/8T) \sum_{n=o}^{\infty} \frac{X^n}{n!} 2^{n/2} T^{(n-1)/2} D_{-n}\left(\frac{X}{\sqrt{2T}}\right) \tag{25}$$

Similarly, from equation (24)

$$\sigma(x,t/\omega_o)e^{t} \doteq - P'\omega_o \exp[-X(s-1)/s^{\frac{1}{2}}] \qquad (26)$$

or

$$\sigma(x,t/\omega_o)e^{t} \doteq - P'\omega_o \sum_{n=o}^{\infty} \frac{X^n}{n!} \frac{e^{-X\sqrt{2}}}{s^{n/2}} \qquad (27)$$

whose solution is

$$\sigma(x,t) = \frac{-P'\omega_o}{\sqrt{\pi}} \sum_{n=o}^{\infty} \frac{X^n}{n!} 2^{(n-1)/2} T^{n/2-1} D_{-n+1}\left(\frac{X}{\sqrt{2T}}\right) \qquad (28)$$

The displacement is the integral of the velocity with respect to time, which is obtained by multiplying equation (11) by 1/s. This operation is valid only for zero displacement at t = o. Hence

$$u(x,t) \doteq \frac{P'}{\rho c} \frac{\exp[-xs/c(s/\omega_o+1)^{\frac{1}{2}}]}{s\sqrt{s/\omega_o+1}} \qquad (29)$$

Normalizing and shifting gives

$$\frac{1}{\omega_o} u(x,t/\omega_o)e^{t} \doteq \frac{P'}{\rho c} \frac{\exp[-X(s-1)/s^{\frac{1}{2}}]}{\omega_o(s-1)\sqrt{s}} \qquad (30)$$

In this case $1/(s-1)$ must be expanded and the final operational solution is a double series, i.e.,

$$\frac{1}{s-1} = \frac{1}{s}\sum_{m=o}^{\infty}\frac{1}{s^m} \tag{31}$$

which yields

$$u(x,t/\omega_o)e^{t\cdot} = \frac{P'}{\rho c}\sum_{m=o}^{\infty}\sum_{m=o}^{\infty}\frac{X^n}{n!}\frac{\exp(-x\sqrt{s})}{s^{n/2+m+3/2}} \tag{32}$$

which may be inverted term by term to give

$$u(x,t) = \frac{P'}{\rho c\sqrt{\pi}}\exp(-T-X^2/8T)\sum_{m=o}^{\infty}\sum_{n=o}^{\infty}\frac{X^n}{n!}\,2^{n/2+m+1}{}_{T}{}^{n/2+m=1/2} \tag{33}$$

$$D_{-n-2m-2}\left(\frac{X}{\sqrt{2T}}\right)$$

The double series is readily amenable to evaluation by computer methods for small values of X and T.

The expression for strain is found by differentiating equation (29) with respect to x, which gives

$$\varepsilon(s,t) = \frac{P'}{\rho c^2}\frac{\exp[-xs/c(s/\omega_o+1)^{\frac{1}{2}}]}{(s/\omega_o+1)} \tag{34}$$

which yields

$$\frac{1}{\omega_o}\,\varepsilon(x,\frac{t}{\omega_o})\;e^{t} \doteq \frac{P'}{\rho c^2}\sum_{n=o}^{\infty}\frac{X^n}{n!}\;\frac{\exp(-X\sqrt{s})}{s^{n/2+1}} \tag{35}$$

Equation (35) may be inverted term by term to give

$$\varepsilon(x,t) = \frac{P'}{\rho c^2\sqrt{n}}\exp(-T-X^2/8t)\sum_{n=o}^{\infty}\frac{X^n}{n!}\;2^{(n+1)/2}T^{n/2}D_{-n-1}(\frac{X}{\sqrt{2T}}) \tag{36}$$

The solutions for an exponential decay input can be obtained by multiplying the transform for each particular parameter before normalizing and shifting by $P_o/(s+\beta)$, which is the transform of $P(t) = P_o\exp(-\beta t)$. This is illustrated by the derivation of the velocity equation:

$$v(x,t) \doteq \frac{P_o}{c}\cdot\frac{1}{(s+\beta)}\cdot\exp(-\frac{x}{c}\frac{s}{\sqrt{s/\omega_o+1}}) \tag{37}$$

Upon shifting and normalizing this becomes

$$\frac{1}{\omega_o}\,v(x,\frac{t}{\omega_o})\;e^{t} \doteq \frac{P_o}{\rho c}\,\frac{1}{\omega_o[s-(1-\frac{\beta}{\omega_o})]}\;\frac{\exp[-x(s-1)/\sqrt{s}]}{\sqrt{s}} \tag{38}$$

Let

$$[s-(1-\frac{\beta}{\omega_o})] = (s-\alpha) \tag{39}$$

and expanding the positive exponential as previously done, and letting

$$\frac{1}{s-\alpha} = \frac{1}{s} \sum_{m=o}^{\infty} \left(\frac{\alpha}{s}\right)^m \tag{40}$$

The transform then becomes

$$\frac{1}{\omega_o} v(x,\frac{t}{\omega_o})e^{t} = \frac{P_o}{\rho c \omega_o} \cdot \frac{1}{s} \sum_{m=o}^{\infty} \left(\frac{\alpha}{s}\right)^m \sum_{n=o}^{\infty} \frac{X^n}{n!} \frac{\exp(-X\sqrt{s})}{s^{n/2+1/2}} \tag{41}$$

which may be rewritten

$$\frac{1}{\omega_o} v(x,\frac{t}{\omega_o})e^{t} = \frac{P_o}{\rho c \omega_o} \sum_{m=o}^{\infty} \sum_{n=o}^{\infty} \frac{X^n}{n!} \alpha^m \frac{\exp(-X\sqrt{s})}{s^{n/2+m+1/2}} \tag{42}$$

The inverse is found term by term to be

$$v(x,t) = \frac{P_o}{\rho c \sqrt{\pi}} \exp(-T-X^2/8T) \sum_{m=o}^{\infty} \sum_{n=o}^{\infty} \frac{X^n}{n!} \alpha^m 2^{n/2+m+1} T^{n/2+m+1/2} D_{-n-2m-1}\left(\frac{X}{\sqrt{2T}}\right) \tag{43}$$

which can be evaluated by computer methods.

The other parameters are determined in a like manner each resulting in a double series. The values for a unit step input can be readily determined by letting $\beta = 0$ which makes $\alpha = 1$.

Spherical Wave

Collins (Ref. 1) presented a Laplace transform solution for particle velocity in terms of the s-variable for a spherical Voigt wave with a unit impulse, $\delta(t)$, input, but did not invert it.

The spherical Voigt wave equation may be developed in more than one way (Ref. 4), but is probably in its most tractable form when expressed in terms of the displacement potential, ϕ:

$$\left(1 + \frac{1}{\omega_o} \frac{\partial}{\partial t}\right) \frac{\partial^2 r\phi}{\partial r^2} = \frac{1}{c^2} \frac{\partial^2 r\phi}{\partial t^2} \tag{44}$$

The boundary condition pressure equation for a cavity of radius r_o is:

$$\left[(\lambda+2\mu) + (\lambda'+2\mu') \frac{\partial}{\partial t}\right] \frac{\partial^2 \phi}{\partial r^2} + \frac{2(\lambda+\lambda'\partial/\partial t)}{r} \frac{\partial \phi}{\partial r} = \sigma_r(t) \tag{45}$$

No experimental values are available for the viscoelastic moduli, hence, for purposes of computation it is assumed that $\lambda = \mu$ and $\lambda' = \mu'$, although the following methods are applicable without this assumption.

Equation (45) then reduces to

$$\mu\left(1 + \frac{1}{\omega_o} \frac{\partial}{\partial t}\right)\left(3 \frac{\partial^2 \phi}{\partial r^2} + \frac{2}{r} \frac{\partial \phi}{\partial r}\right) = -\sigma_r(t) \tag{46}$$

For a Dirac delta forcing function, $P(t) = P'\delta(t)$,

the operational solution of equation (44) becomes

$$r\phi(r,t) = -\frac{P'r_o \exp[-s(r-r_o)/c(s/\omega_o+1)^{\frac{1}{2}}]}{rus\ (s/\omega_o+1)\left[\frac{3s^2}{c^2(s/\omega_o+1)} + \frac{4s}{r_o c(s/\omega_o+1)^{\frac{1}{2}}} + \frac{r}{r_o^2}\right]} \tag{47}$$

However, interest is centered on parameters such as displacement, particle velocity, stress and strain. The displacement is

$$u = \frac{\partial \phi}{\partial r} \tag{48}$$

or

$$u(r,t) = \frac{P'r_o \exp[-s(r-r_o)/c(s/\omega_o+1)^{\frac{1}{2}}]}{\mu(s/\omega_o+1)\quad [B]}\left[\frac{1}{r^2} + \frac{s}{rc(s/\omega_o+1)^{\frac{1}{2}}}\right] \tag{49}$$

where

$$[B] = \left[\frac{3s^2}{c^2(s/\omega_o+1)} + \frac{4s}{r_o c(s/\omega_o+1)^{\frac{1}{2}}} + \frac{4}{r_o^2}\right] \tag{50}$$

Let $s = \omega_o s$ (normalize) and then $s = s-1$(shift), and equation (49) becomes

$$\frac{1}{\omega_o} u(r,t/\omega_o)e^{t} = \frac{P'r_o \exp(-R\sqrt{s}+R/\sqrt{s})}{\mu\omega_o^2[A]}\left[\frac{1}{r^2} + \frac{\omega_o(s-1)}{rc\sqrt{s}}\right] \tag{51}$$

where

$$[A] = [s^2 + \frac{4c}{3r_o\omega_o} s^{3/2} + (\frac{4c^2}{3r_o^2\omega_o^2} - 2)s - \frac{4c}{3r_o\omega_o} s^{\frac{1}{2}} + 1] \qquad (52)$$

and $R = \omega_o(r-r_o)/c$ (53)

The fraction involving the quadratic in s may be expanded as follows:

$$1/[A] = \frac{1}{s^2} \sum_{m=o}^{\infty} b_m \frac{1}{s^{m/2}} \qquad (54)$$

where the coefficients b_m are functions of the coefficients of the quadratic. The positive exponential may likewise be expanded to yield:

$$\exp R/\sqrt{s} = \sum_{n=o}^{\infty} \frac{R^n}{n!} \frac{1}{(s)^{n/2}} \qquad (55)$$

Substituting in (51) and separating into appropriate terms gives the operational solution in terms of double infinite series:

$$u(r,t/\omega_o)e^t = \frac{P'r_oc^2}{\mu\omega_o} \{\frac{1}{r^2} \sum_{m=o}^{\infty}\sum_{n=o}^{\infty} \frac{R^n}{n!} b_m \frac{\exp(-R\sqrt{s})}{s^{n/2+m/2+2}} \qquad (56)$$

$$[\sum_{m=o}^{\infty}\sum_{n=o}^{\infty} \frac{R^n}{n!} b_m \frac{\exp(-R\sqrt{s})}{s^{n/2+m/2+3/2}} - \sum_{m=o}^{\infty}\sum_{n=o}^{\infty} \frac{R^n}{n!} b_m \frac{\exp(-R\sqrt{s})}{s^{n/2+m/2+5/2}}]\}$$

Equation (56) may then be inverted term by term (Ref. 7) to yield the solution in the time plane.

The velocity for a unit impulse may be found by differentiating the displacement with respect to t, or multiplying (49) by s. The strain is determined by differentiating the displacement equation (49) with respect to r, and the stress by substituting into equation (46). All of these lead to solutions consisting of double series similar to equation (56), which may be inverted and evaluated by computer methods.

For example:

$$u(r,t) = \frac{P' r_o c^2}{\mu\omega_o} \exp(-T-R^2/8T)\left\{\frac{1}{r^2}\sum_{m=o}^{\infty}\sum_{n=o}^{\infty}\frac{R^n}{n!}b_m\, 2^{n/2+m/2+5/2}\right.$$

$$T^{n/2+m/2+2} D_{-n-m-5}\left(\frac{R}{\sqrt{2T}}\right) + \frac{\omega_o}{rc}\left[\sum_{m=o}^{\infty}\sum_{n=o}^{\infty}\frac{R^n}{n!}b_m\, s^{n/2+m/2+2}\right. \qquad (57)$$

$$T^{n/2+m/2+3/2} D_{-n-m-4}\left(\frac{R}{\sqrt{2T}}\right) - \sum_{m=o}^{\infty}\sum_{n=o}^{\infty}\frac{R^n}{n!}b_m\, 2^{n/2+m/2+3}$$

$$\left.\left. T^{n/2+m/2+5/2} D_{-n-m-6}\left(\frac{R}{\sqrt{2T}}\right)\right]\right\}$$

where

$T = \omega_o t$

D_{-n-m-z} = Weber functions of negative integral order

The expansion of fractions has been shown to be valid for both rational (Ref. 8) and fractional exponents (Ref. 9) of the denominator terms of the fraction (see below). Some of the expansions in series converge slowly for large values of dimensionless distance and dimensionless time. The limits of convergence for real time are therefore dependent upon the value of ω_o, as well as the programming techniques employed and the capacity of the computer. Several other methods of obtaining a function which could be inverted were investigated but none offered a means of solution.

In every term in the inverted equations, there are essentially five components an exponential, a power-factorial term, 2 to an exponential value, T to an exponential value, and a cylinder function of negative integral order. The exponential decreases rapidly with increasing values of T, and the cylinder functions also decrease with an increase in order or an increase in value of the argument. The power-factorial term increases rapidly until n = R and then it decreases. Cylinder functions are calculated by means of an appropriate recursion formula (Ref. 4).

The factor $(2T)^n$ increases without bound as n increases. The behavior of all of these functions must be considered in programming inasmuch as some of the numbers may become very large, in excess of 10^{100}, and some very small, less than 10^{-100}. In some cases the order of multiplication becomes important so that two small or two large numbers are not multiplied in succession.

For computation of the double series, it is more convenient to find the multipliers of each successive cylinder function. These are found to be increasing truncated series of power-factorial terms. That is, a double series may be expressed as a Cauchy product:

$$\sum_{n=o}^{\infty} \sum_{m=o}^{\infty} b_m \frac{R^n}{n!} 2^{(n+m+z)/2} T^{(n+m+z-1)/2} D_{-n-m-z} = \tag{58}$$

$$\sum_{n=o}^{\infty} \left(\sum_{k=o}^{n} \frac{b_k R^{n-k}}{(n-k)!} \right) 2^{(n+z)/2} T^{(n+z-1)/2} D_{-n-z}$$

The infinite series all converge rapidly for relatively small values of R and T, but not so rapidly for larger values. Specific values must also be chosen for r, r_o, ω_o, and c, which was not necessary in the case of plane waves.

A rational function of the following type may be expanded (Ref. 9) in an infinite series, and has a zero or order n at ∞, i.e.,

$$y(s) = \frac{1}{a_o s^n + a_1 s^{n-1} + \cdots a_n} \tag{59}$$

may be expanded as

$$y(s) = \frac{1}{a_o s_n} - \frac{a_1}{a_o^2} \frac{1}{s^{n+1}} + \frac{a_1 - a_o a_2}{a_o^3} \frac{1}{s^{n+2}} t\cdots \tag{60}$$

and inverting term by term yields

$$y(t) = c_o \frac{t^{n-1}}{(n-1)!} + c_1 \frac{t^n}{n!} + c_2 \frac{t^{n+1}}{(n+1)!} + \cdots \tag{61}$$

However, the individual coefficients of the terms in the series rapidly become very cumbersome to develop and to use in computation. For digital computer calculations, on the other hand, a simple sequential loop procedure can be employed to determine the successive coefficients.

Let equation (60) be written in the following infinite series form:

$$y(s) = \frac{c_o}{s^n} + \frac{c_1}{s^{n+1}} + \frac{c_2}{s^{n+2}} + \cdots \frac{c_n}{s^{2n}} + \cdots \tag{62}$$

The same process may be carried out for irrational fractions (Ref. 10):

$$y(q) = \frac{1}{a_o q^n + a_1 q^{n-1} + \cdots a_n} \tag{63}$$

where

$$q = s^{\frac{1}{2}}$$

This may likewise be expanded in the form

$$y(q) = \frac{c_o}{q_n} + \frac{c_1}{q^{n-1}} + \frac{c_2}{q^{n-2}} + \cdots \qquad (64)$$

and may also be inverted term by term to give a solution in the time plane.

Thus, the inversion of the double series resolves itself into the inversion of a single series with a polynomial coefficient, each term of the series having a valid inversion. The inverted terms are similarly expressed and are in a convenient form for computation.

The operational solutions for unit step and decay exponentials are obtained in a similar manner. In these cases the operational expression is multiplied into the quadratic in s before it is expanded.

It is notable that there is an oscillation of all parameters for the spherical wave, while the plane Voigt wave does not exhibit oscillations (Ref. 3). The behavior is somewhat similar to an elastic wave, but with greater damping and a difference in wave shape. For a unit impulse and a decay exponential forcing function the oscillations are about the zero axis. For a unit step, however, the oscillations are about a curve which is parallel to the zero axis. In an elastic material, a wave caused by a unit step function also oscillates about a line parallel to the zero axis.

For larger travel distances the wave spreads out and becomes somewhat more symmetrical. However, very small disturbances which are characteristic of a "diffusion model" are indicated before the arrival of the main wave.

Computation Procedures

A generalized flow diagram for the computer program is given in Fig. I . The cylinder functions are evaluated by use of the following recursion:

$$(n+1)D_{-n-2}(z) = - zD_{-n-1}(t) + D_{-n}(z) \tag{65}$$

where

$$D_o(z) = e^{-z^2/4} \tag{66}$$

and

$$D_{-1}(z) = \sqrt{\frac{\pi}{2}}\, e^{z^2/4}\ \text{erfc}\ \frac{z}{\sqrt{2}} \tag{67}$$

The complementary error function is computed from

$$\text{erfc} = 1.0\text{-erf} \tag{68}$$

and the error function may be determined from several appropriate formulas (Ref. 11), including an infinite series expansion. For large arguments the error function rapidly approaches a value of 1.0 and the value of erfc becomes very small, which restricts the use of equation (68) and the upper limit of argument which may be employed in computation procedures, i.e., above a value of about 3.0.

The argument of the cylinder function is

$R/\sqrt{2T} = \omega_o(r-r_o)/c\sqrt{2\omega_o t}$, which means that any combination of the quantities in the expression such as large r, large ω_o or very small t, which yields values of the argument larger than 3.0 leads to computing difficulties. Further, large values of ω_o in the expression

$e^{-T-R^2/8T} = -\omega_o\left\{t-\left(\frac{r-r_o}{c}\right)^2/8t\right\}$ yield very small values for this function. The cylinder functions of high order also are very small. On the other hand the factor

$(2T)^n=(2\omega_o t)^n$

increases very rapidly for large values of ω_o to 3000 for the ranges of r and t shown in Fig.33 . Also, the terms in the polynomial in R increase very rapidly for large values of ω_o (Eq. 58).

Thus, the series expressions are well adapted for small values of the parameters involved with the exception of very

small t. Numerical integration of the wave equations was also considered, but this method also becomes unwieldy for large values of ω_o.

Comparison of Voigt Waves and Observed Waves

The important parameters of waves in natural earth materials are arrival time, rise time, fall time, rate of attenuation with distance and oscillating characteristics. In this study the observed waves of interest are radial pulses generated by underground nuclear explosions, i.e., in the HARDHAT, AIRVENT, LONG SHOT, and GNOME events.

There are several types of energy losses, dispersion, etc. in the transmission of dilatation waves through natural rock masses which cause the waves to differ from those predicted by elastic theory. Two immediate evidences of this are greater attenuation, and lengthening of the initial pulse with distance. In many rocks the pulse length has been found to increase approximately with the first power of travel distance. As indicated earlier one of the primary purposes of this investigation was to ascertain whether the spherical Voigt wave equation would demonstrate any of the characteristics found in observed pulses created by under ground nuclear explosions.

Since there have been only approximated values for ω_o for rocks published in the literature, a range of values was used which would demonstrate the possible applicability of the Voigt equation. The values employed for ω_o were 600, 2000, and 3000, having the dimensions of t^{-1}. Larger values could not be handled by the computer program, and smaller values represent large effective coefficients of viscosity which do not appear to be applicable. That is, the higher the viscosity of the dashpot element, the more nearly the Voigt model acts as a single rigid member. This results in very high velocities of the wave front which velocities are not characteristic of rock or other natural materials.

For lower viscosities the Voigt wave forms do demonstrate some of the important properties of natural waves, i.e., attenuation and pulse lengthening. For high viscosities, (small ω_o), they exhibit velocities of the wave front which are, as indicated above, velocities which exceed the velocity of both elastic and observed waves in rock.

Plane Waves. Plane Voigt waves were investigated in the process of developing procedures for solving the transformed spherical wave equation. Close to the source of disturbance these waves demonstrate a significant attenuation of peak velocity and strain, etc., whereas a plane elastic wave is propagated without loss of amplitude or change in shape. While the behavior of plane Voigt waves (Figs.2 to 13) is not of direct importance in this study, the principles evolved in their solution were valuable aids in solving and programming the spherical wave equations.

Forcing Functions. As previously discussed, three forcing functions were employed in calculating wave forms, a unit impulse, a unit step and a decay exponential. Each of these functions makes the transformed solutions successively more complicated, and the first two were used primarily as a means of developing procedures for obtaining inverse transforms, working from the less to the more complex forms. For simulation of a real pressure function, the decay exponent is the more realistic of the three, but has too sharp a rise time for most field conditions. Finally, solutions obtained for the unit impulse, $\delta(t)$, forcing function serves as a basis for solutions for other forcing functions by means of convolution.

Rock Properties. Available data on properties of rocks which constituted the environment of the nuclear events discussed are listed in Table I. No data were available for AIRVENT. The data for LONG SHOT are limited to strength and ultrasonic pulse velocity. Data on salt and granite are more complete. However, no values for viscoelastic properties are available inasmuch as methods have not been devised for measuring such properties of rock masses.

Physical property data and viscoelastic wave analyses are not complete enough to derive any quantitative relationships between them. However, for rocks with lower moduli and a significant porosity, the pulse forms are of shapes similar to those obtained from a Voigt model. Also, the Voigt wave shows some lengthening with travel distance, but is not as great as that found in natural rock.

Wave Velocity. A detailed frequency-wave velocity analysis has not been made, but an inspection of the particle velocity pulses indicates that the macro-wave front velocity for ω_c = 600 (Fig. 27, for example), 2000, and 3000 is greater than the elastic velocity, decreasing with an increase of ω_o. The actual first disturbance at the distances investigated are extremely small, and they occur at very small times. That is, there is no well defined arrival time for either plane or spherical Voigt waves. This is not the case for an elastic wave, however, where the arrival time is defined by the elastic velocity, i.e., for $\tau' = t-(r-r_o)/c$, and no wave is defined for $\tau \leq 0$.

For larger values of ω_o the velocity at the wave front decreases, but in each case approximately one-fourth of the "measurable" use time has passed before the corresponding elastic pulse would have arrived. For very large viscosity the Voigt model would indicate a small disturbance at ∞ for a very small time. For low viscosities the behavior approaches that of an elastic wave.

The forcing function of greatest interest in this study is the decay exponential, $P_o e^{-\beta t}$. The early arrival times of waves for this function are in part due to the abrupt (zero) rise time in pressure. The dashpot in the viscoelastic model tends to respond as a rigid segment to instantaneous change in pressure or force. Thus, in a Maxwell element the first response to a sharp pressure front is almost totally in the spring. In the Voigt model where the spring and dashpot are in parallel, however, one element cannot respond without the other. Consequently, for even moderate values of viscosity the Voigt model will act as a rigid element in its immediate response to high magnitude, short changes in force. For a less abrupt rise the wave velocity and the rise time approach those of an elastic wave.

Rise and Fall Time. The spherical pulses in the Voigt model show a marked symmetry in their first positive phase. These are similar in shape to the pulses in GNOME (salt) and AIR-VENT (andesite), (Figs. 35 to 43) and are also symmetrical in their first positive phase. The pulses for HARD HAT (granite) and LONG SHOT (andesite) on the other hand have a shorter rise time and a longer fall time. Exact scaled comparisons cannot be made at the present stage of developments with the Voigt results primarily because of the uncertainty of the choice of a radius of equivalent cavity, r, at which either elastic or viscoelastic behavior could be

assumed to become effective. The Voigt equation is linear, but will scale only if the viscosity varies as the scale factor. This condition does not occur for small and large events in the same earth material.

It would appear that for somewhat porous types of rock such as those of GNOME and AIRVENT that certain properties of the rock mass cause a damping out of the higher frequencies more rapidly than in granite and andesite. Porosity, water content, and geologic structure, as well as elastic properties of intact specimens all have their effect in varying but unknown degrees. No quantitative coefficients for the damping properties of large rock masses for high order transients have been found in the literature, however. Hence, this would be a fruitful area for further research.

The value of c for the wave velocity employed in the Voigt wave calculations was 20,000 fps, or a value equal to that of a dense granite with large shear and Young's moduli. However, the shape of the Voigt pulses corresponds more nearly to that of low moduli materials such as salt.

Attenuation. Both the relative magnitude and the rate of attenuation of the normalized particle velocity pulse are affected by the value of ω_o (Fig. 34). For larger values of ω_o, i.e., for smaller viscosity, the normalized peak particle velocity becomes larger and the attenuation is lower. The rate of attenuation decreases somewhat with travel distance, which is not the case for actual velocity pulses in salt, granite and tuff. However, the slope of the peak velocity curve for larger values of ω_o is somewhat lower than that of observed values in natural rock, which is about 1.65 (Fig. 49).

It should be noted that the calculated peak velocities are for a wave input form of $P(t) = P_o e^{-\beta t}$, which has an infinitely steep rise in pressure. The shape of the input pulse affects the attenuation as well as the magnitude of the peak velocity as shown above. At the radial distance from the disturbance at which either the elastic, viscoelastic or similar wave equation becomes effective (radius of equivalent cavity), the shape of the pulse crossing this surface is also affected by the properties of the rock medium. That is, pressures generated by explosive sources are so intense that there may be vaporization and melting (nuclear explosives) as well as pulverization, fracturing and flow. The limit of this volume is described by the distance called radius of equivalent cavity, and energy and pressure losses will be determined by the porosity, strength and various properties of the rock which contribute to its ability

to successfully sustain an intense pressure pulse. Thus, fractured granite apparently can sustain a pulse with sharper rise time than porous rocks and salt, as well as transmitting the same general shape of pulse beyond the fracture zone. Further, the pulse to be considered for possible viscoelastic applications would have a more gentle rise time than a simple exponential. Pulses of the form $P(t) = P_o(e^{-\alpha t}-e^{-\beta t})$ will be investigated in a continuation of the study of viscoelastic waves.

Conclusions. The Voigt spherical wave generated by a single decay exponential forcing function exhibits some characteristics which are similar to those of pulses observed in some kinds of natural rock masses. The Voigt pulse form tends to become symmetrical and lengthens somewhat with travel distance. However, the velocities of the frequency components of the Voigt pulse are frequency dependent, and hence, the wave spreads in both directions, rather than lengthening from an arrival time described by the elastic velocity. Observed pulses in salt and porous andesite likewise tend to become symmetrical, but lengthen more than the Voigt pulse does and only in one direction. The attenuation of this type of viscoelastic wave is somewhat greater than the average of attenuation rates observed in rocks in which contained nuclear explosions have been carried out, but is comparable for tuff and salt. Waves generated by pulses with longer rise times will undoubtedly more nearly approximate waves in natural rock.

For all values of ω_o investigated and for the single exponential decay pressure function the arrival times of Voigt waves are considerably smaller than for either observed or elastic waves. This is due to the abrupt rise in magnitude of the pressure function and to the rigid response of the viscoelastic model to abrupt changes in face.

Thus, while a change in the pressure function will make the Voigt wave more closely approximate natural waves, a decrease in the viscosity factor causes the viscoelastic pulse to approach the character of an elastic pulse, which does not lengthen with travel distance. It appears, therefore, that while for certain parameters the Voigt model may more closely approximate observed pulses in attenuation and pulse lengthening, it does not offer sufficient advantages, except for a few special cases, to justify its use for predicting wave parameters for design purposes in comparison with elastic waves or empirical procedures.

These analyses of the Voigt model indicate that a configuration other than one incorporating a dashpot element will be required to represent rock materials.

TABLE I - Rock Properties

Physical Property Data

LONG SHOT - andesite (Ref. 12)

Compressive strength:	2260 - 5260 psi
Specific gravity:	2.27 - 2.36
Ultrasonic pulse velocity:	6100 - 10,645 fps

HARD HAT - granite (Ref. 13)

Compressive strength:	19,835 psi
Tensile split strength:	1,915 psi
Bulk density:	2.69
Ultrasonic velocity (20 kc):	19,450 fps
Modulus of elasticity, E:	11.3 x 10^6 psi
Poisson's ratio:	0.20

GNOME - salt (Ref. 14)

Compressional wave velocity:	4.08 km/sec
Shear wave velocity:	2.88 km/sec
Density (dry, bulk):	2.13 - 2.46
Poisson's ratio:	0.28 - 0.32
Young's modulus:	2.41 x 10^{11} dynes/cm^2
Porosity (% volume):	0.76 - 5.1%
Water content (% wt):	1%

AIRVENT - data not available

COMPUTER FLOW SHEET

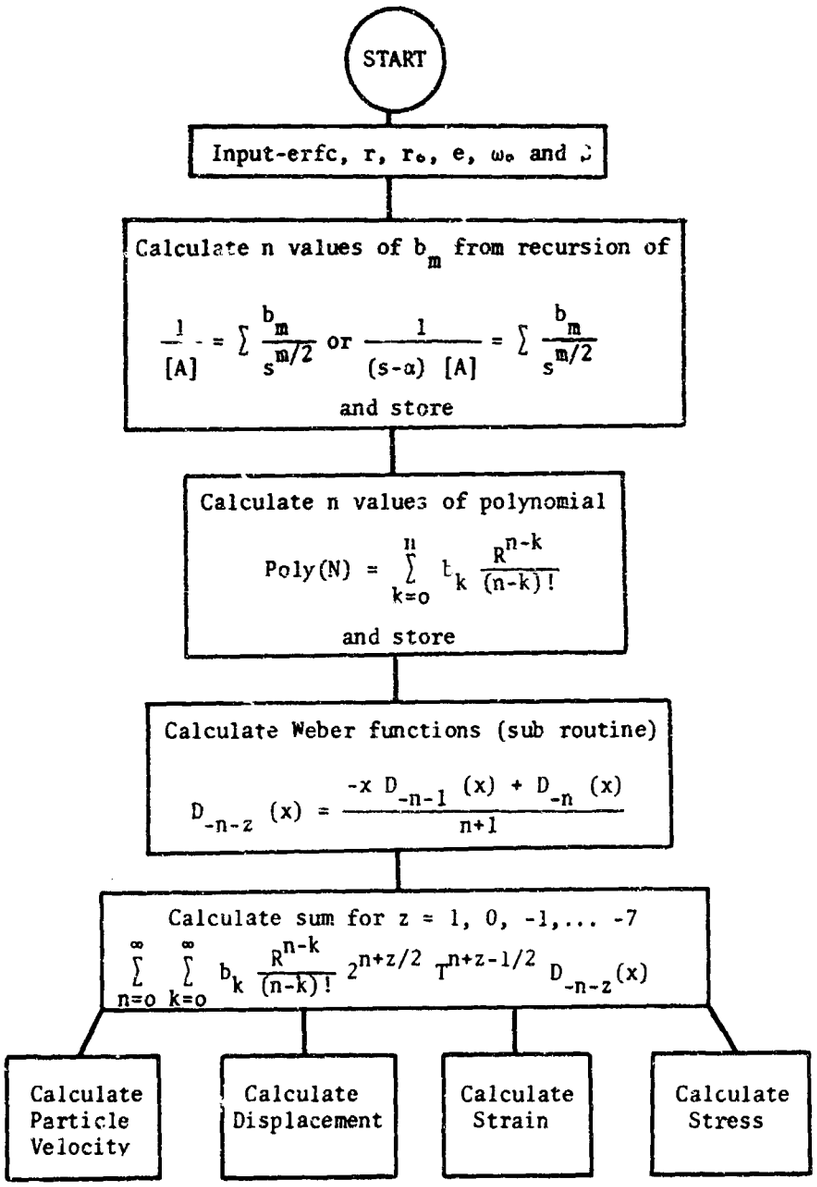

Fig. 1. Generalized Computer Flow Sheet

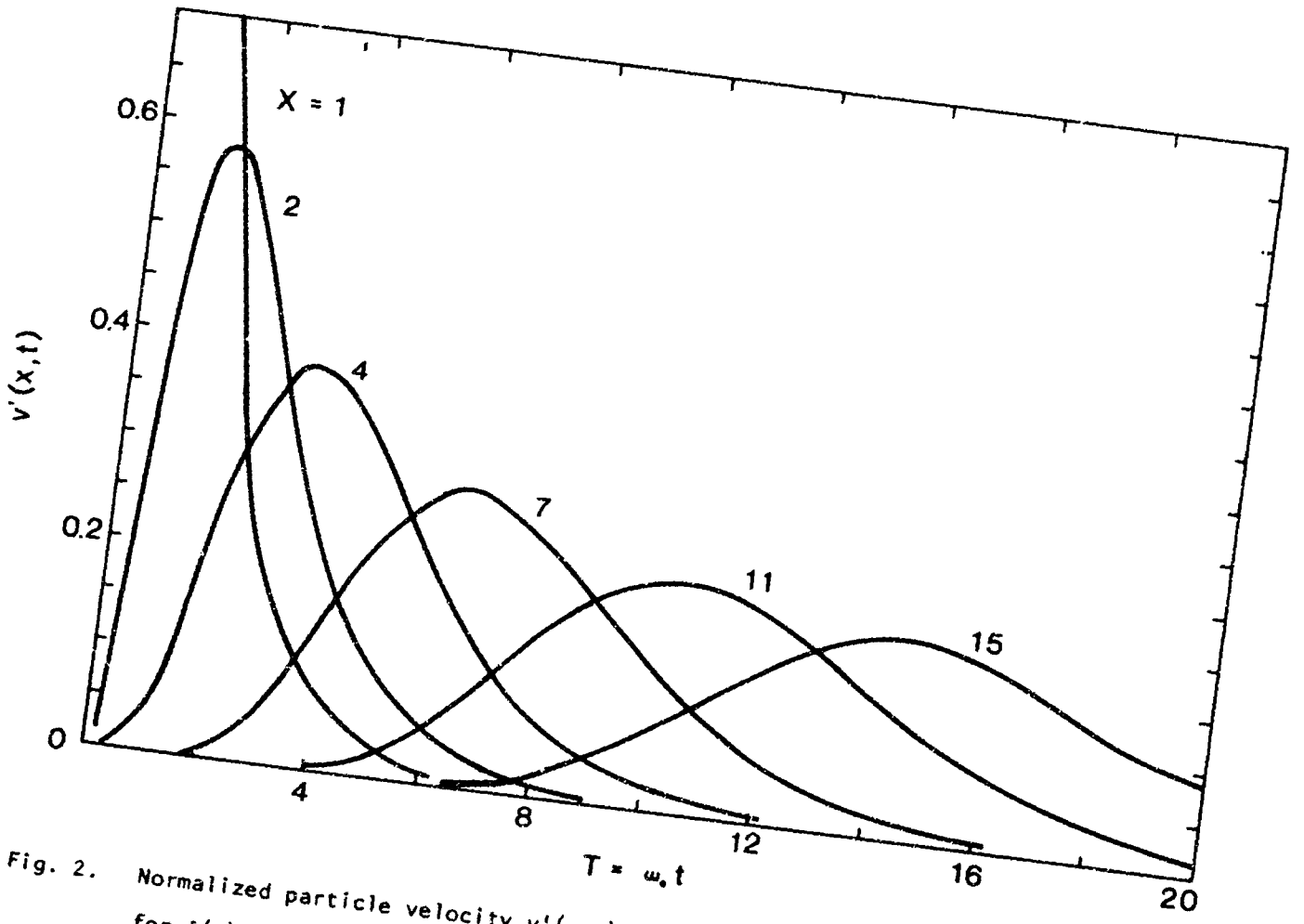

Fig. 2. Normalized particle velocity $v'(x,t) = v(x,t) \pm \frac{\omega_0}{\rho c\sqrt{\pi}}$ for plane Voigt wave for $\delta(t)$ forcing function.

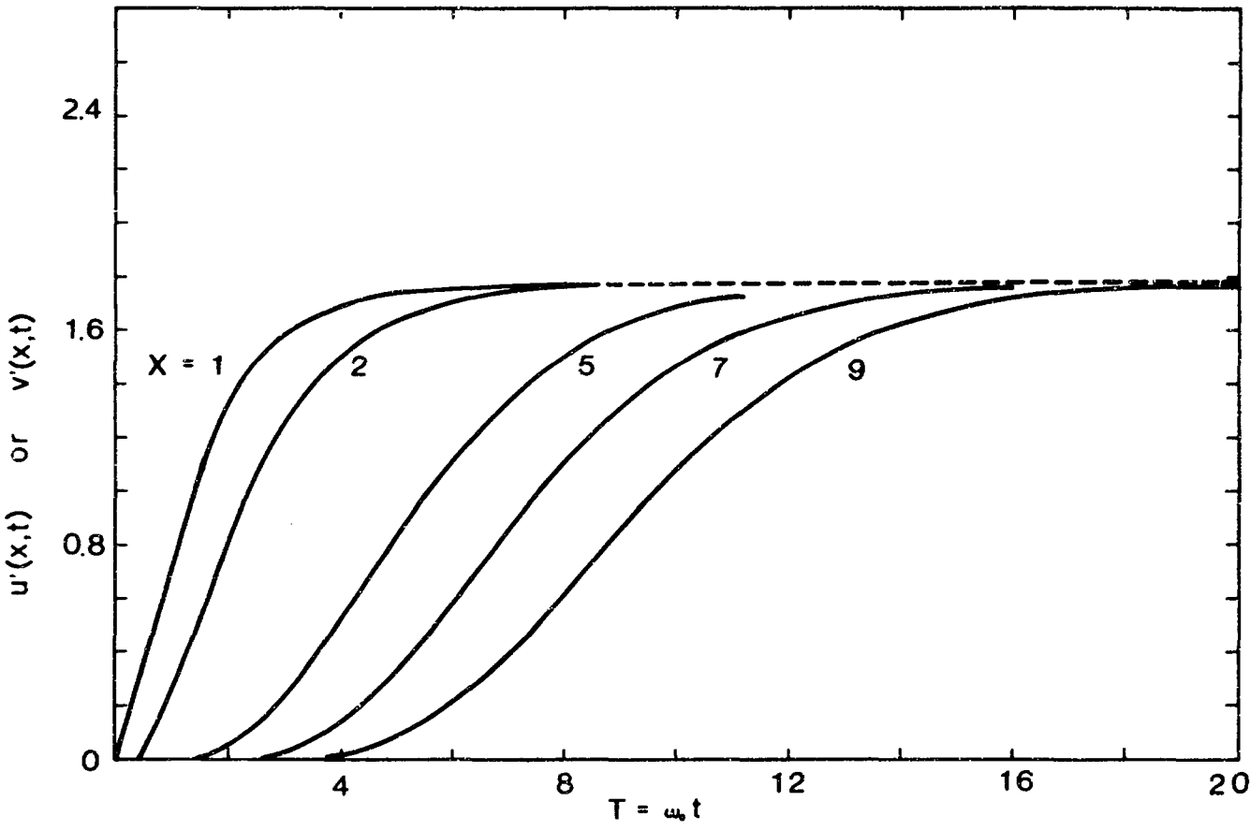

Fig. 3. Normalized displacement $u'(x,t) = u(x,t) \div \frac{1}{\rho c\sqrt{\pi}}$ for $\delta(t)$ forcing function, and normalized particle velocity $v'(x,t) = v(x,t) \div \frac{1}{\rho c\sqrt{\pi}}$ for $1(t)$ forcing function for Voigt plane wave.

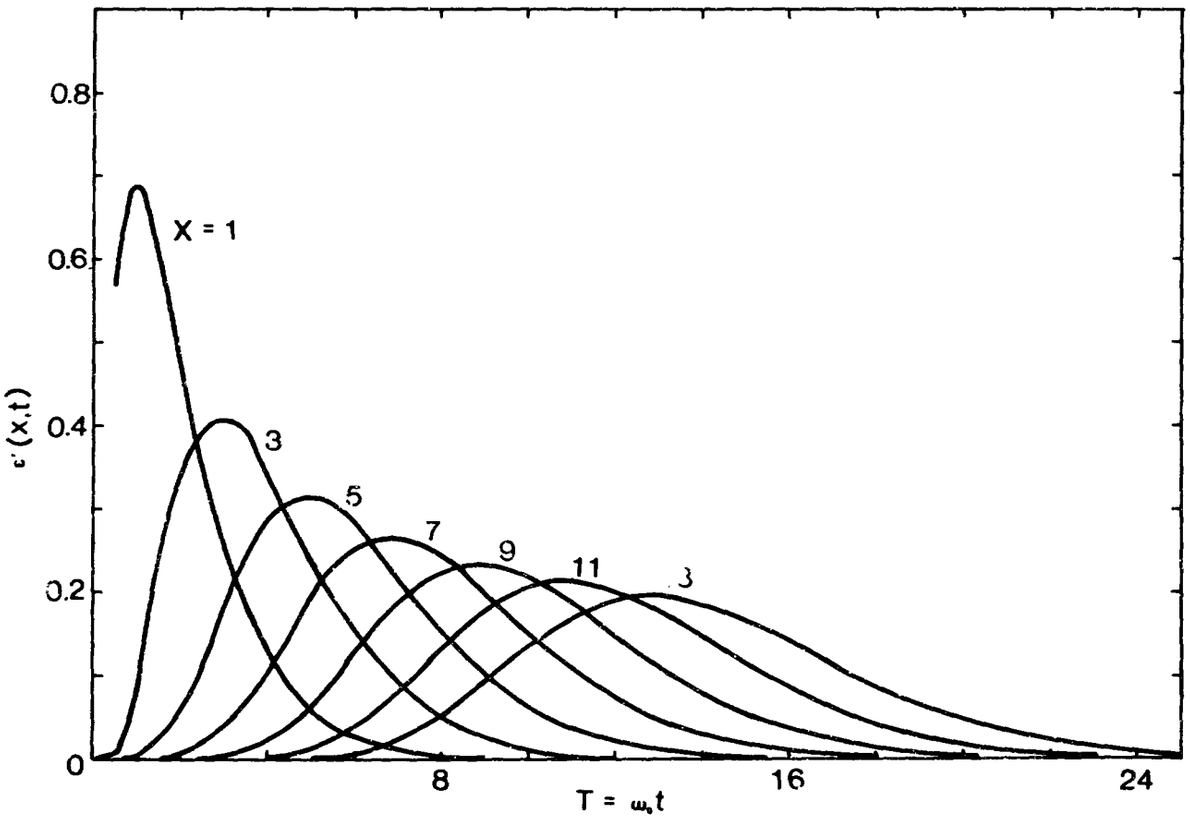

Fig. 4. Normalized strain $\varepsilon'(x,t) = \varepsilon(x,t) \div -\frac{\omega_o}{\rho c^2 \sqrt{\pi}}$ for $\delta(t)$ forcing function for Voigt plane wave.

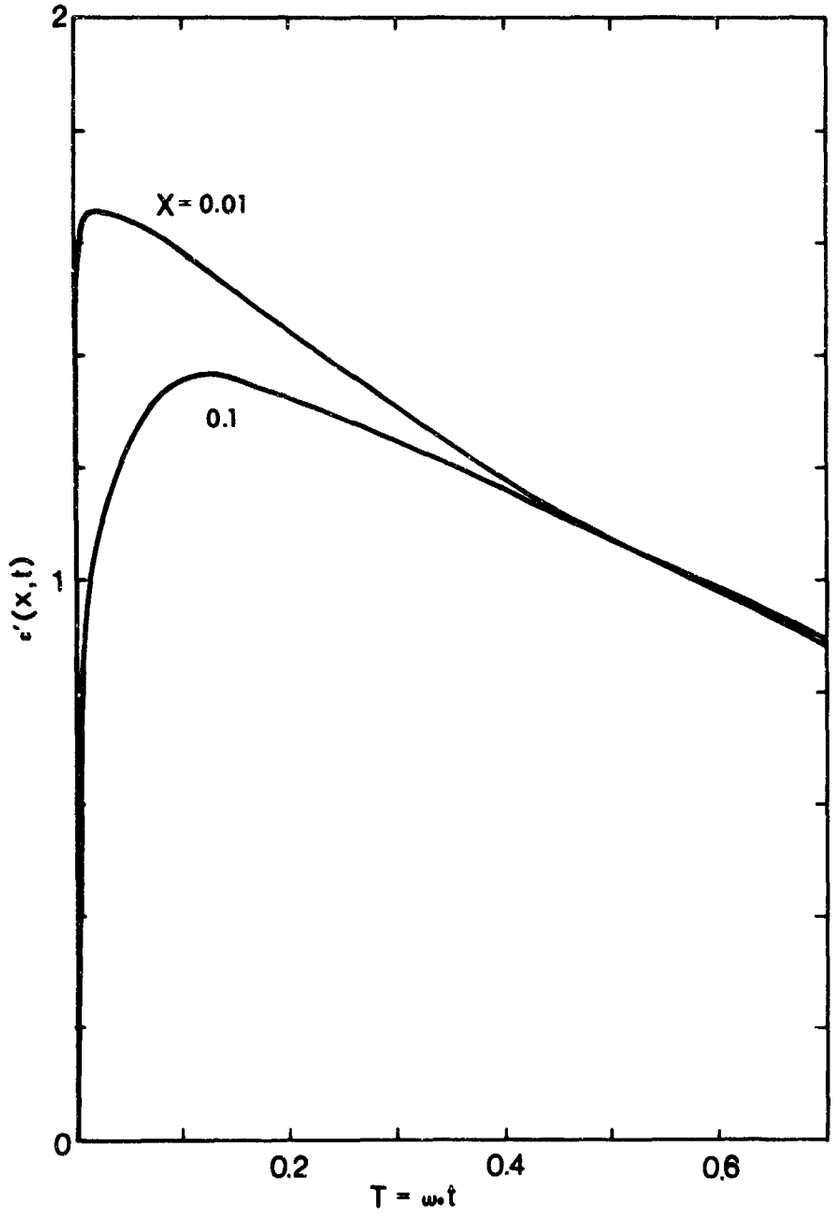

Fig. 5. Normalized strain $\varepsilon'(x,t) = \varepsilon(x,t) \div -\frac{\omega_o}{\rho c^2 \sqrt{\pi}}$ for small x for $\delta(t)$ forcing function.

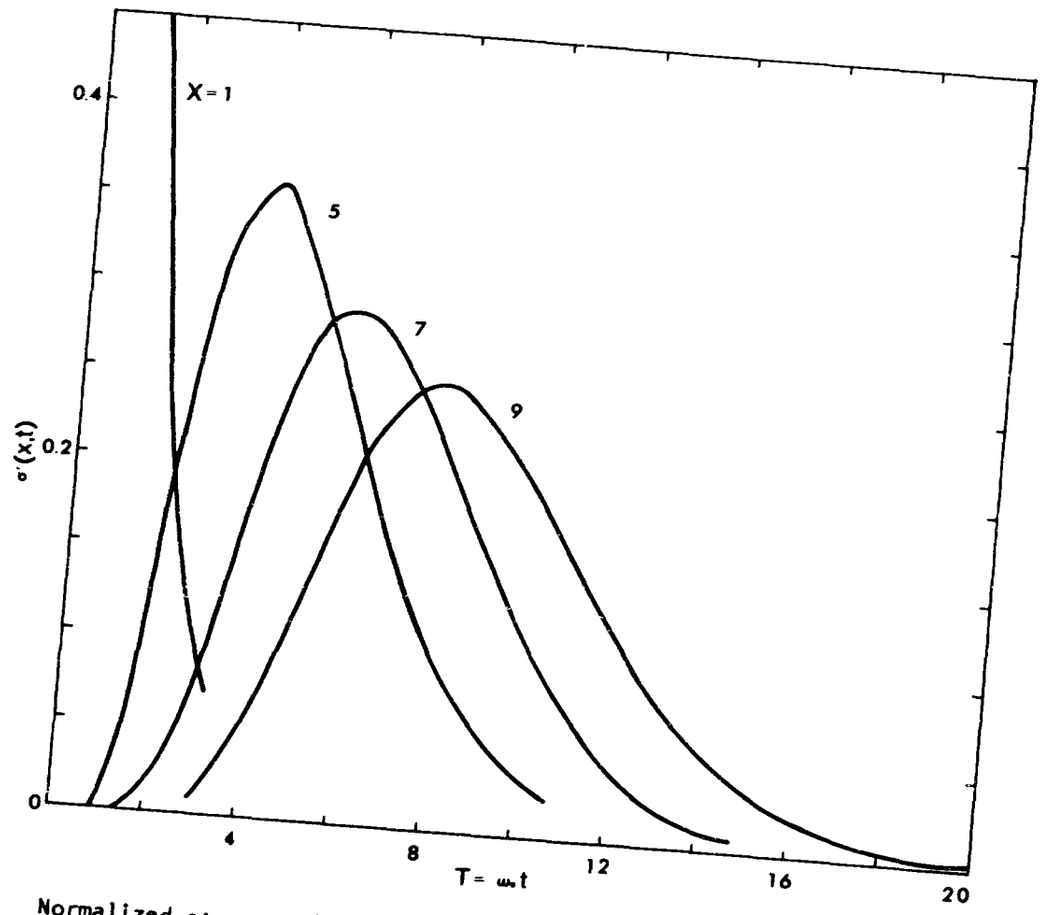

Fig. 6. Normalized stress $\sigma'(x,t) = \sigma(x,t) \div -\frac{E\omega_o}{\rho c^2\sqrt{\pi}}$ for $\delta(t)$ forcing function for plane Voigt wave.

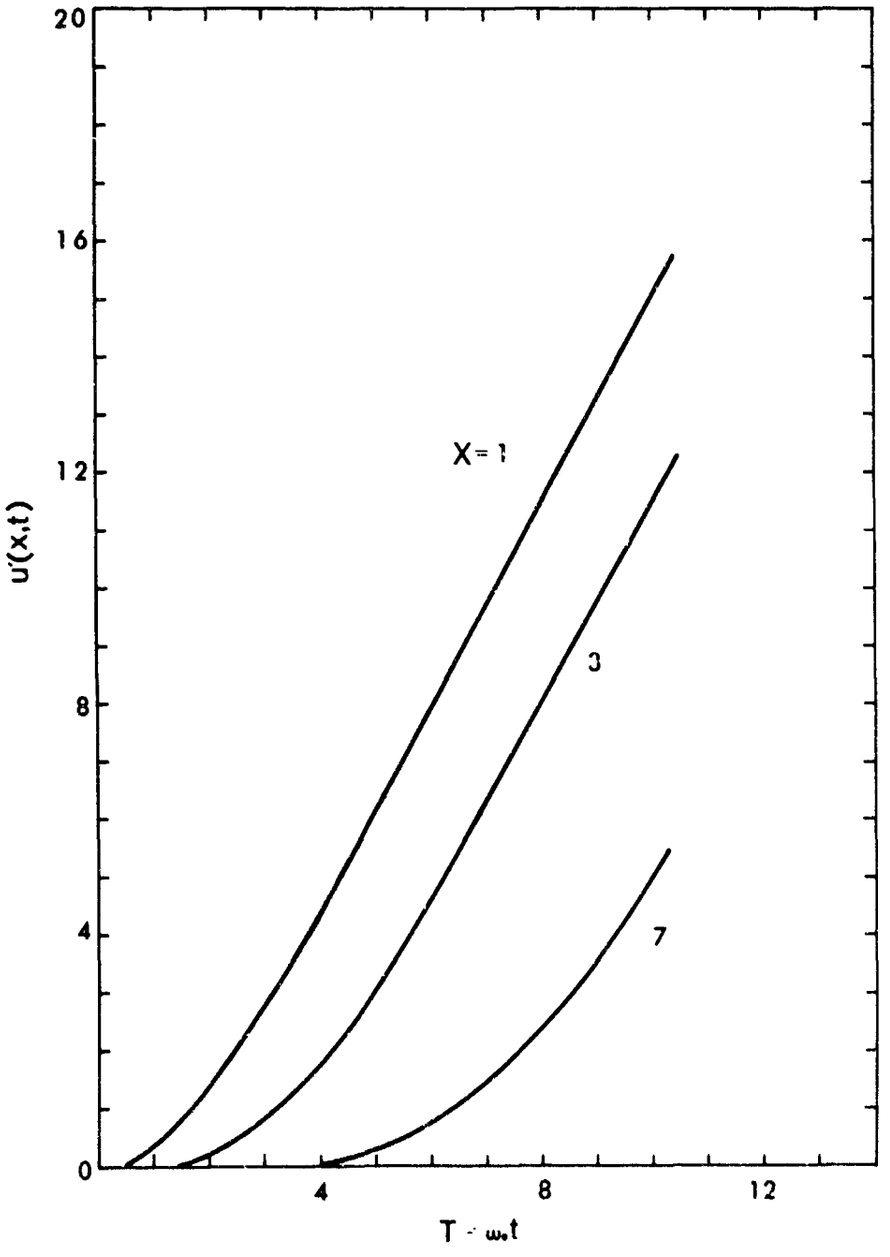

Fig. 7. Normalized displacement $u'(x,t) = u(x,t) \div \frac{1}{\rho c \omega_0 \sqrt{\pi}}$ for I(t) forcing function for plane Voigt wave.

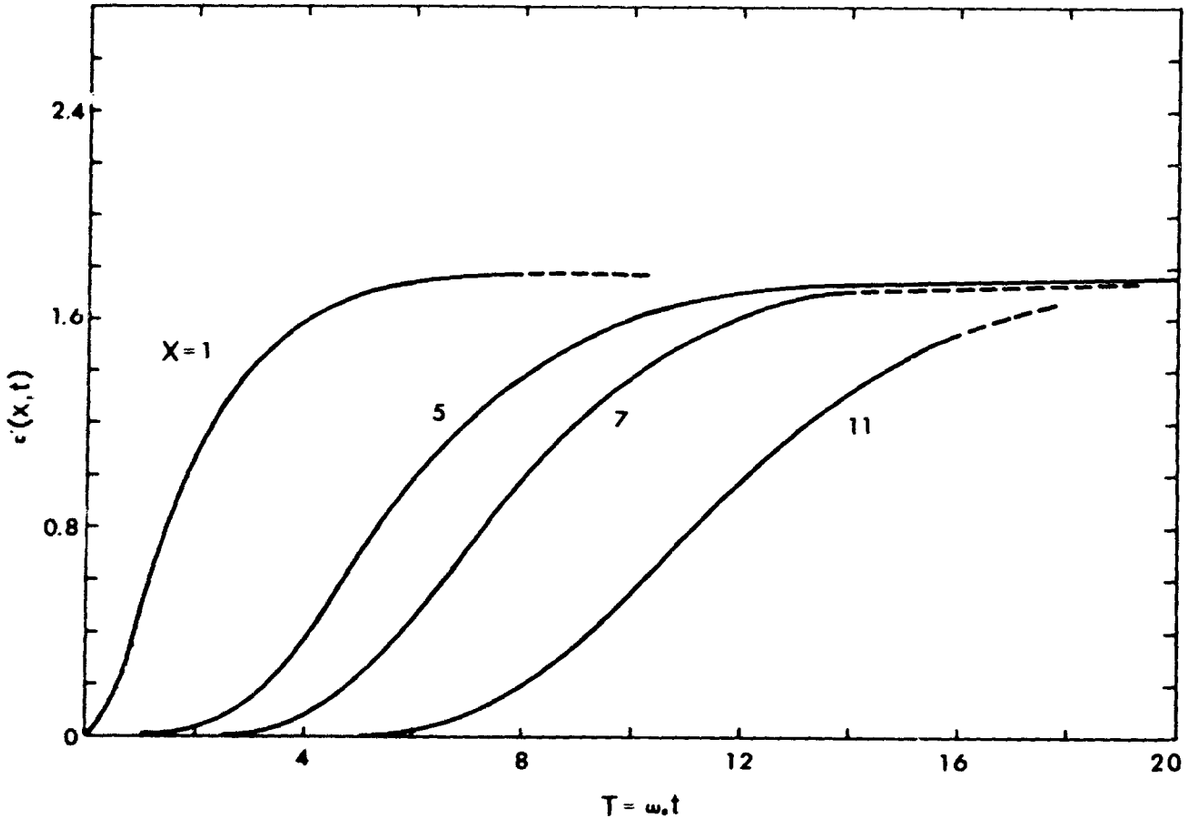

Fig. 8. Normalized strain $\varepsilon'(x,t) = \varepsilon(x,t) \div \frac{1}{\rho c^2 \sqrt{\pi}}$ for 1(t) forcing function for plane Voigt wave.

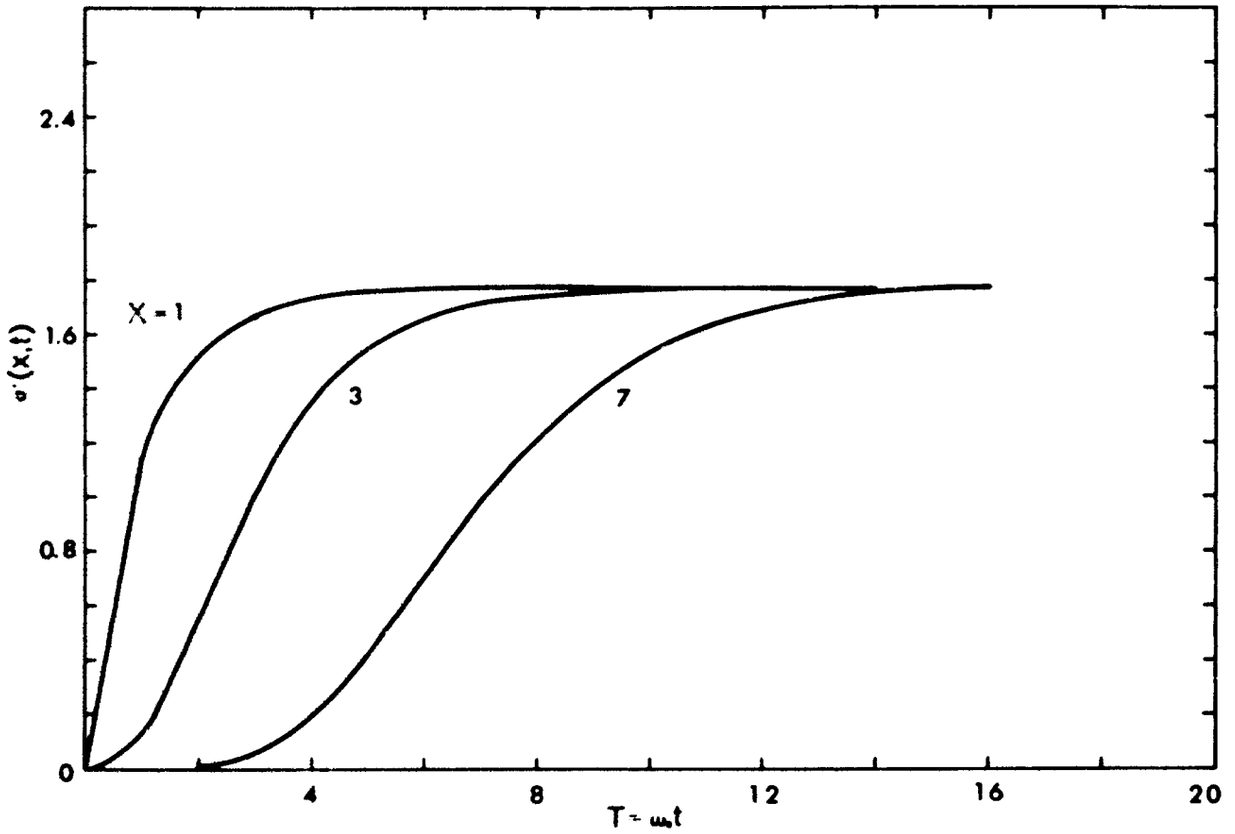

Fig. 9. Normalized stress $\sigma'(x,t) = \sigma(x,t) \div - \frac{E}{\rho c^2 \omega_o \sqrt{\pi}}$ for 1(t) forcing function for plane Voigt wave.

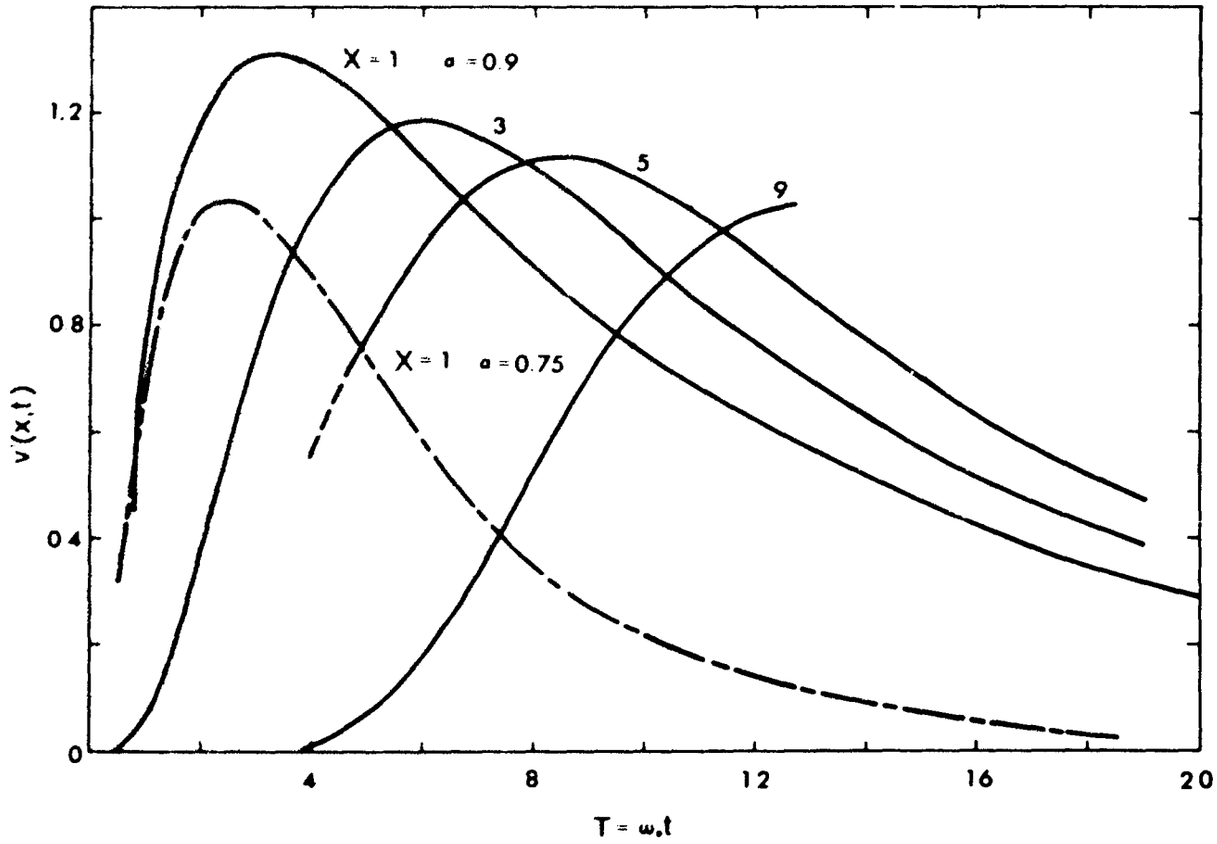

Fig. 10. Normalized velocity $v'(x,t) = v(x,t) \div \frac{P_o}{\rho c\sqrt{\pi}}$ for $P_o e^{-\beta t}$ forcing function for plane Voigt wave.

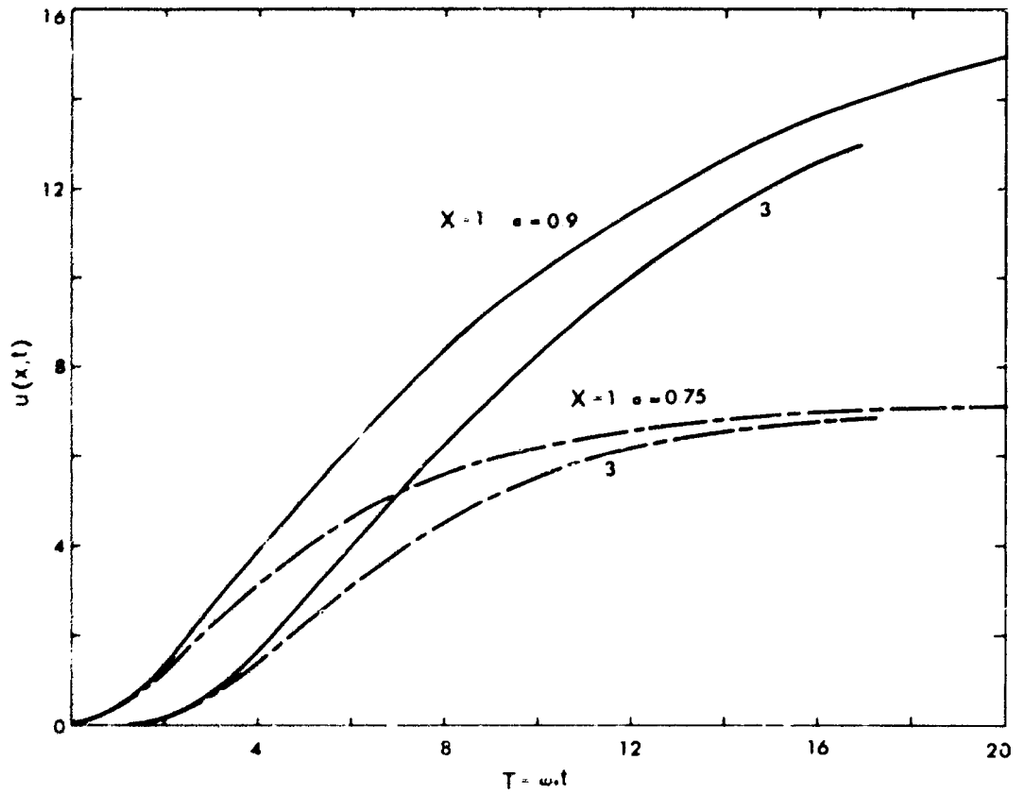

Fig. 11. Normalized displacement $u'(x,t) = u(x,t) : \frac{P_o}{\rho c \omega_o \sqrt{\pi}}$ for $P_o e^{-\beta t}$ forcing function for plane Voigt wave.

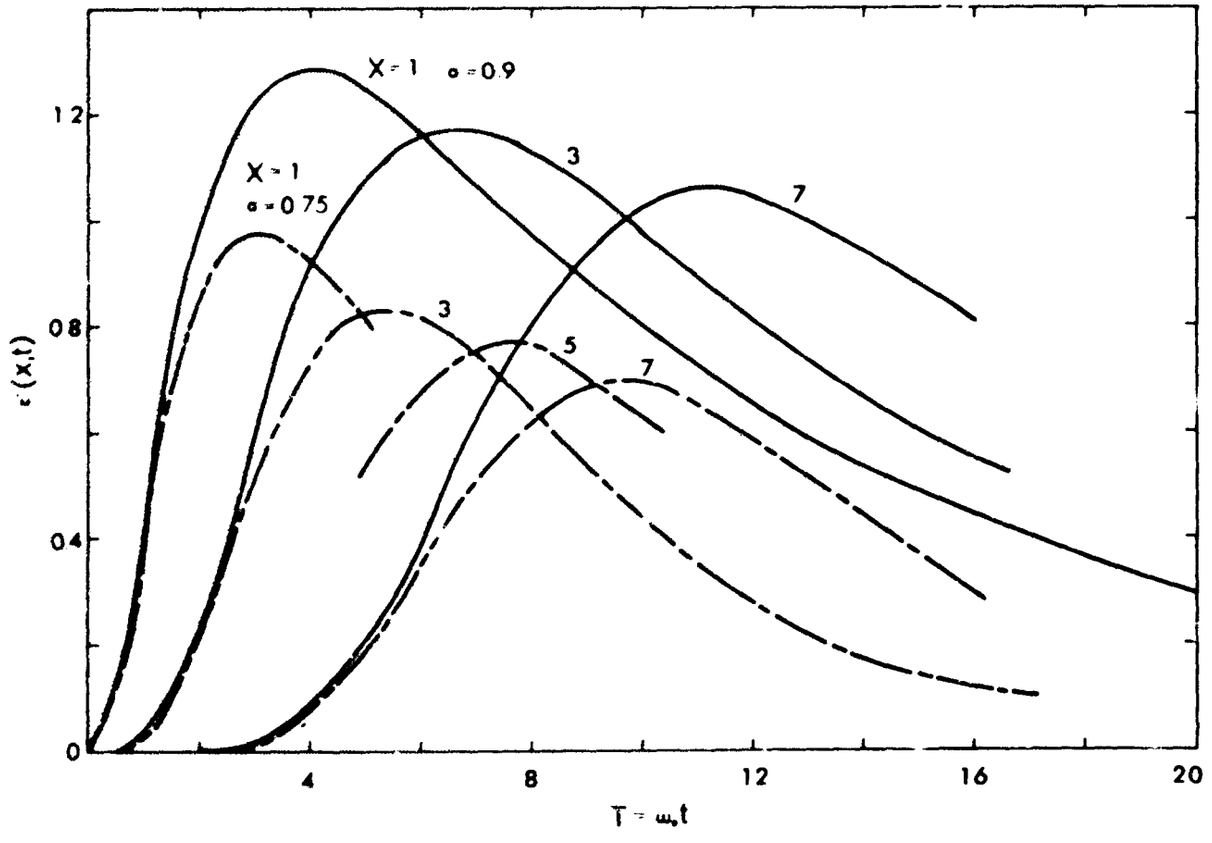

Fig. 12. Normalized strain $\varepsilon'(x,t) = \varepsilon(x,t) : -\frac{P_o}{\rho c^2 \omega_o \sqrt{\pi}}$ for $P_o e^{-\beta t}$ forcing function for Voigt plane wave.

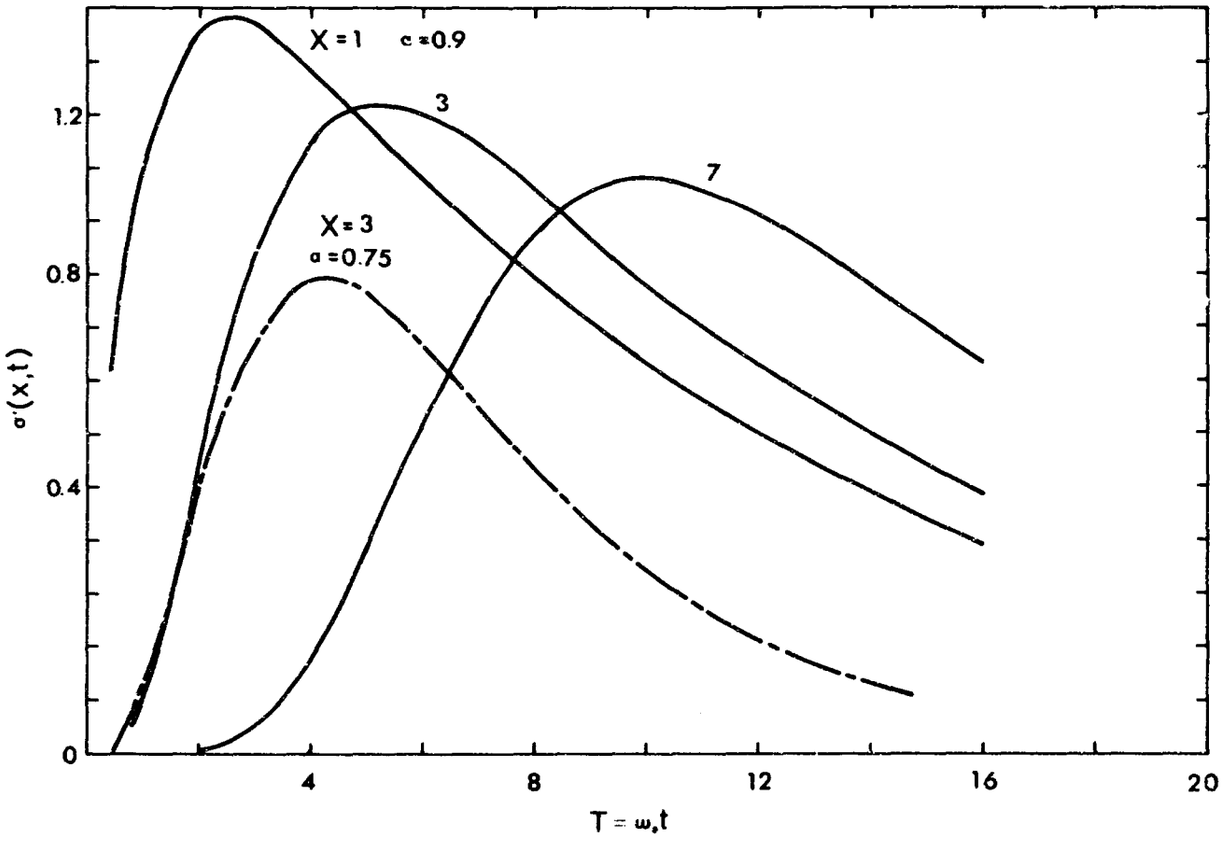

Fig. 13. Normalized stress $\sigma'(x,t) = \sigma(x,t) \div -\frac{EP_o}{\rho c^2\sqrt{\pi}}$

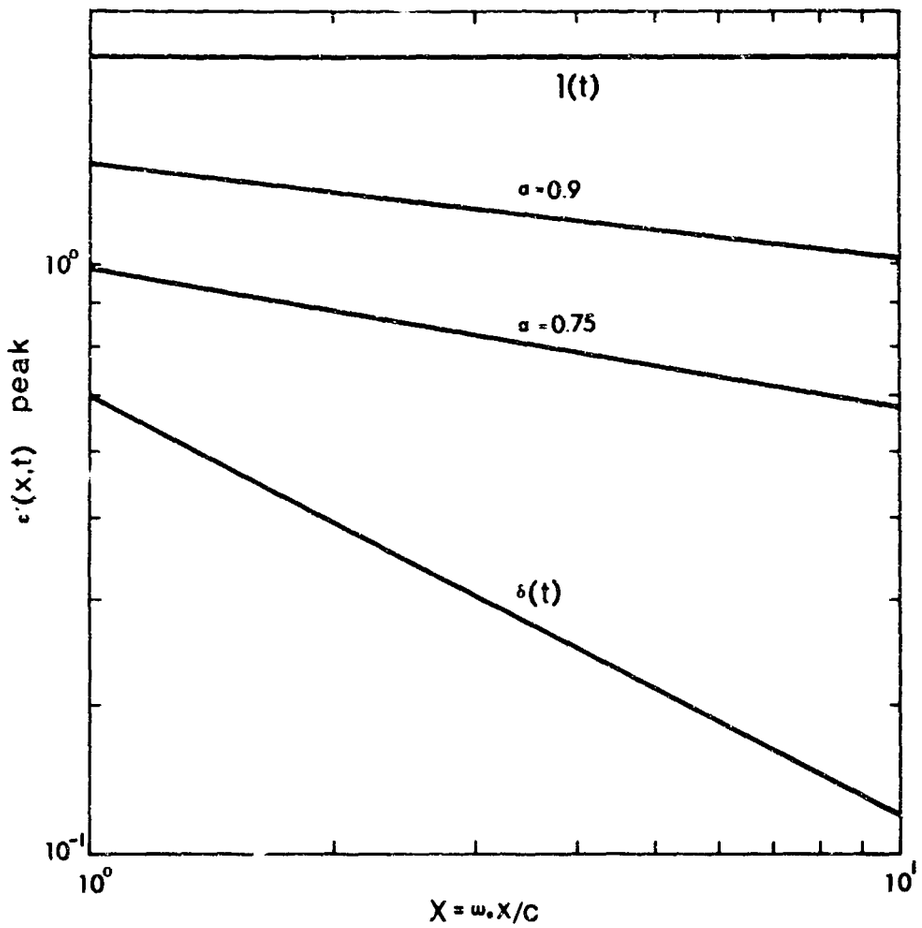

Fig. 14. Normalized peak strain for various forcing functions versus distance.

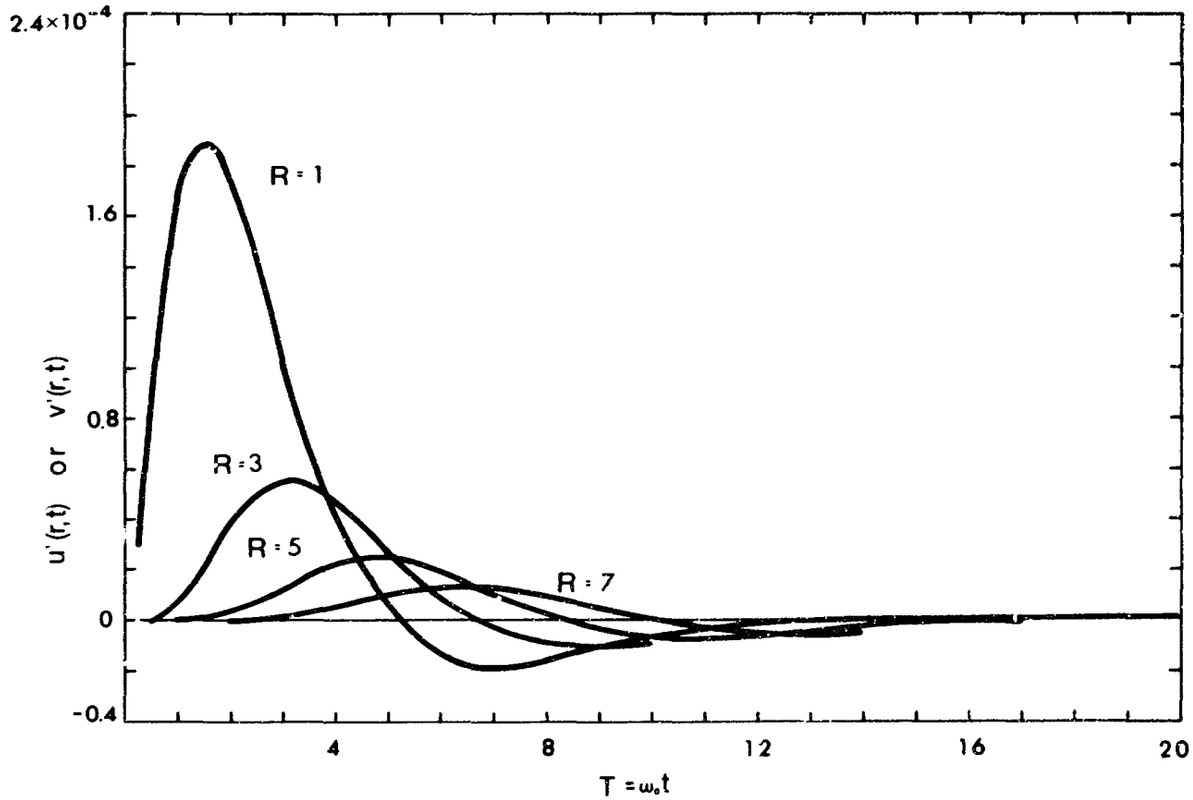

Fig. 15. Normalized displacement $u'(r,t) = u(r,t) \div \frac{P' r_o c^2}{3\mu\omega_o\sqrt{\pi}}$ for $P(t) = P'\delta(t)$ for spherical Voigt wave, r_o = 50 ft., ω_o = 600 and c = 20,000 ft/sec. Also, normalized velocity $v'(r,t) = v(r,t) \div \frac{P'' r_o c^2}{3\mu\omega_o\sqrt{\pi}}$ for $P(t) = P''1(t)$.

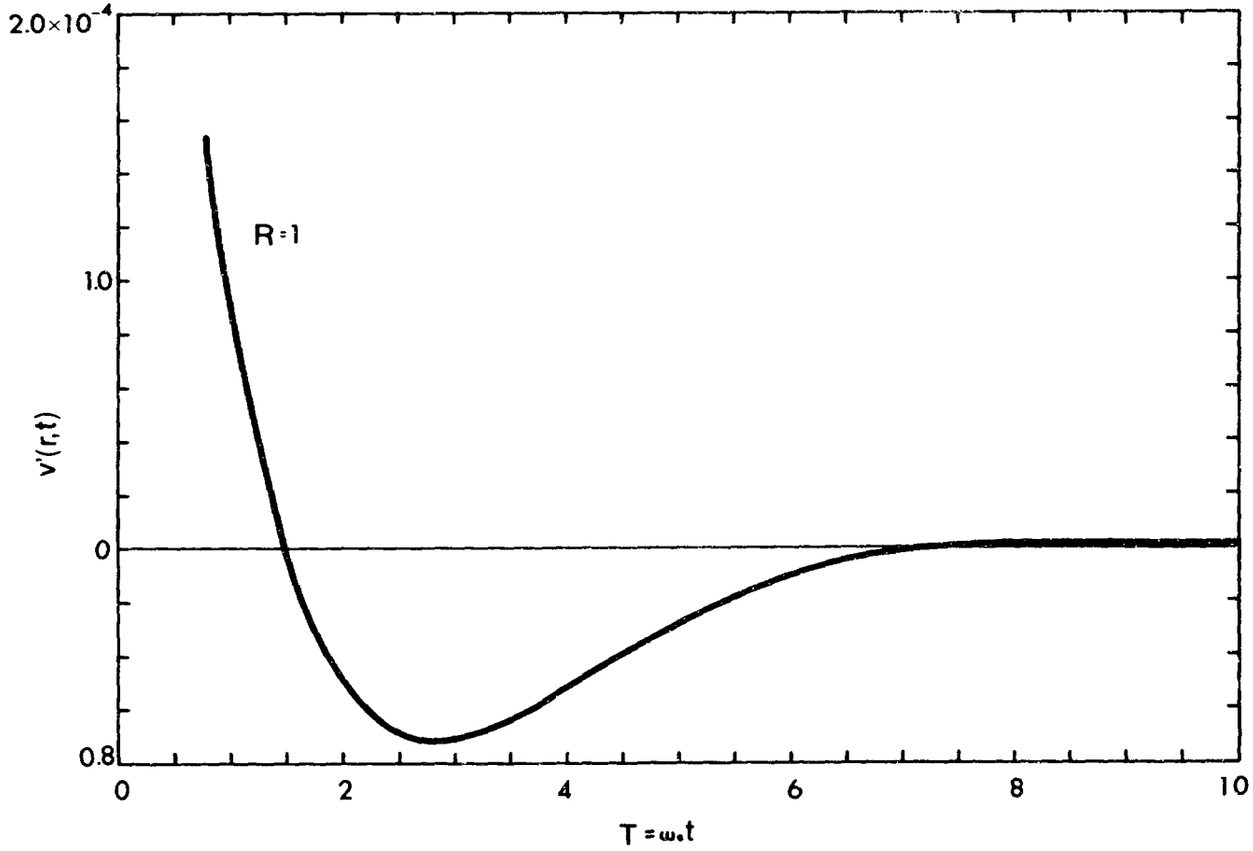

Fig. 16. Normalized particle velocity $v'(r,t) = v(r,t) \div \frac{P' r_o c^2}{3\mu\sqrt{\pi}}$ for $P(t) = P'\delta(t)$ for spherical Voigt wave, r_o = 50 ft., ω_o = 600 and c = 20,000 ft/sec.

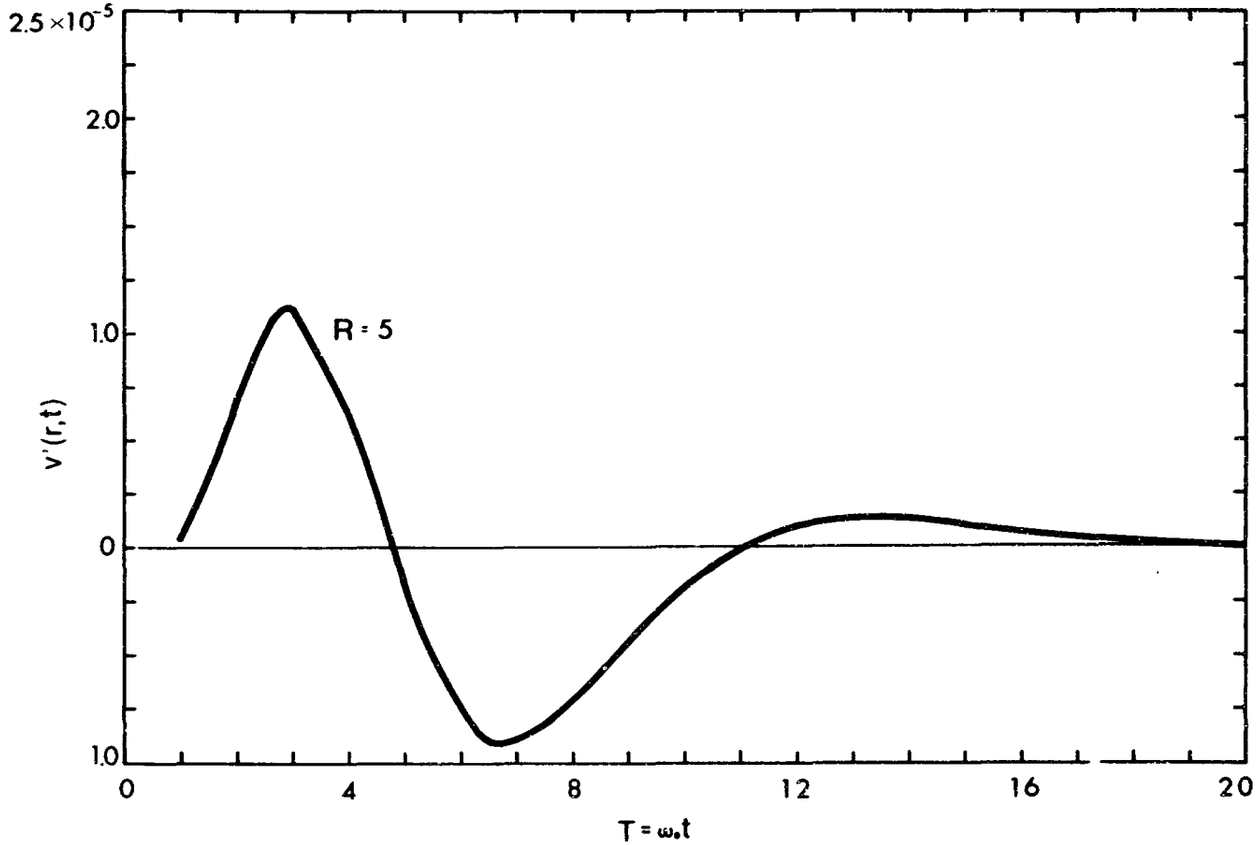

Fig. 17. Normalized particle velocity $v'(r,t) = v(r,t) \div \frac{P' r_o c^2}{3\mu\sqrt{\pi}}$ for $P(t) = P'\delta(t)$ for spherical Voigt wave, r_o = 50 ft., ω_o = 600 and c= 20,000 ft/sec.

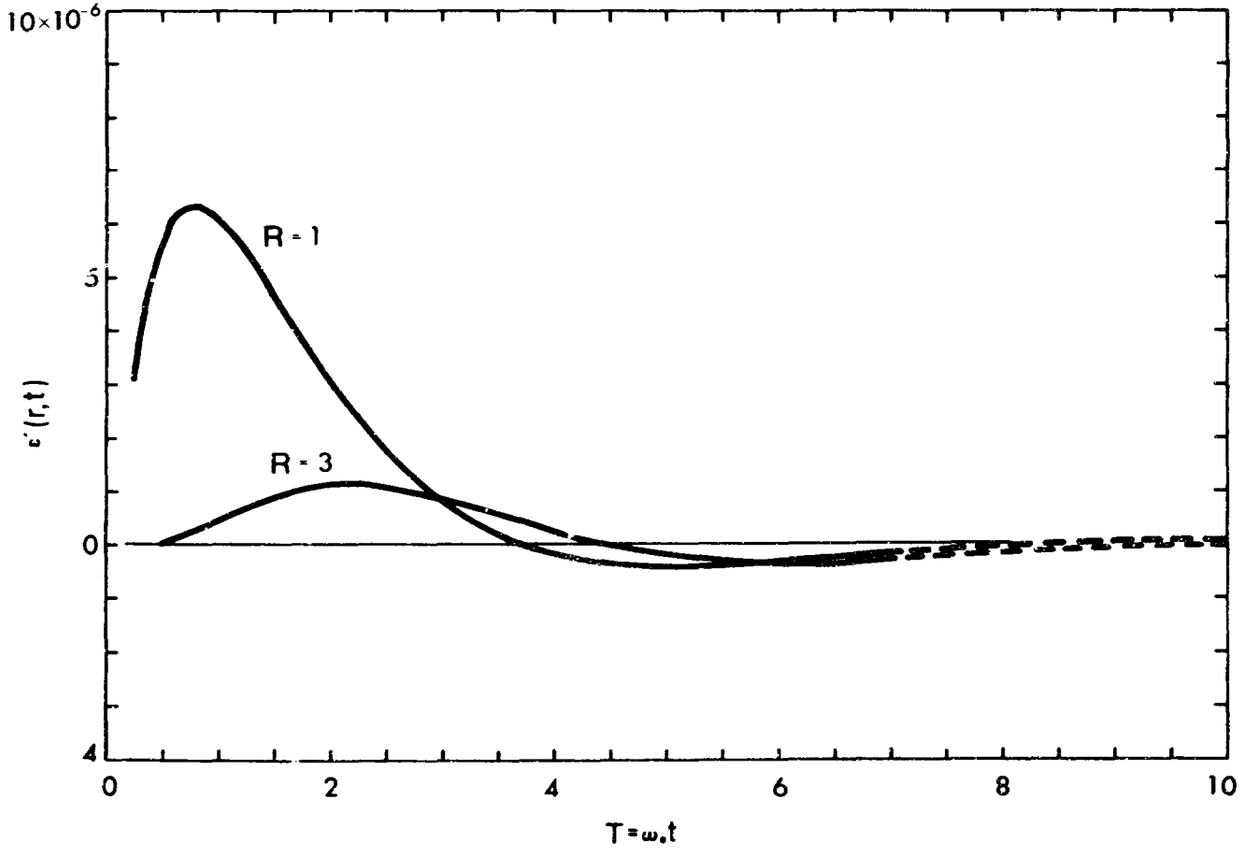

Fig. 18. Normalized strain $\varepsilon'(r,t) = \varepsilon(r,t) \div -\frac{P' r_o c^2}{3\mu\omega_o\sqrt{\pi}}$ for $P(t) = P'\delta(t)$ for spherical Voigt wave, r_o = 50 ft., ω_o = 600 and c = 20,000 ft/sec.

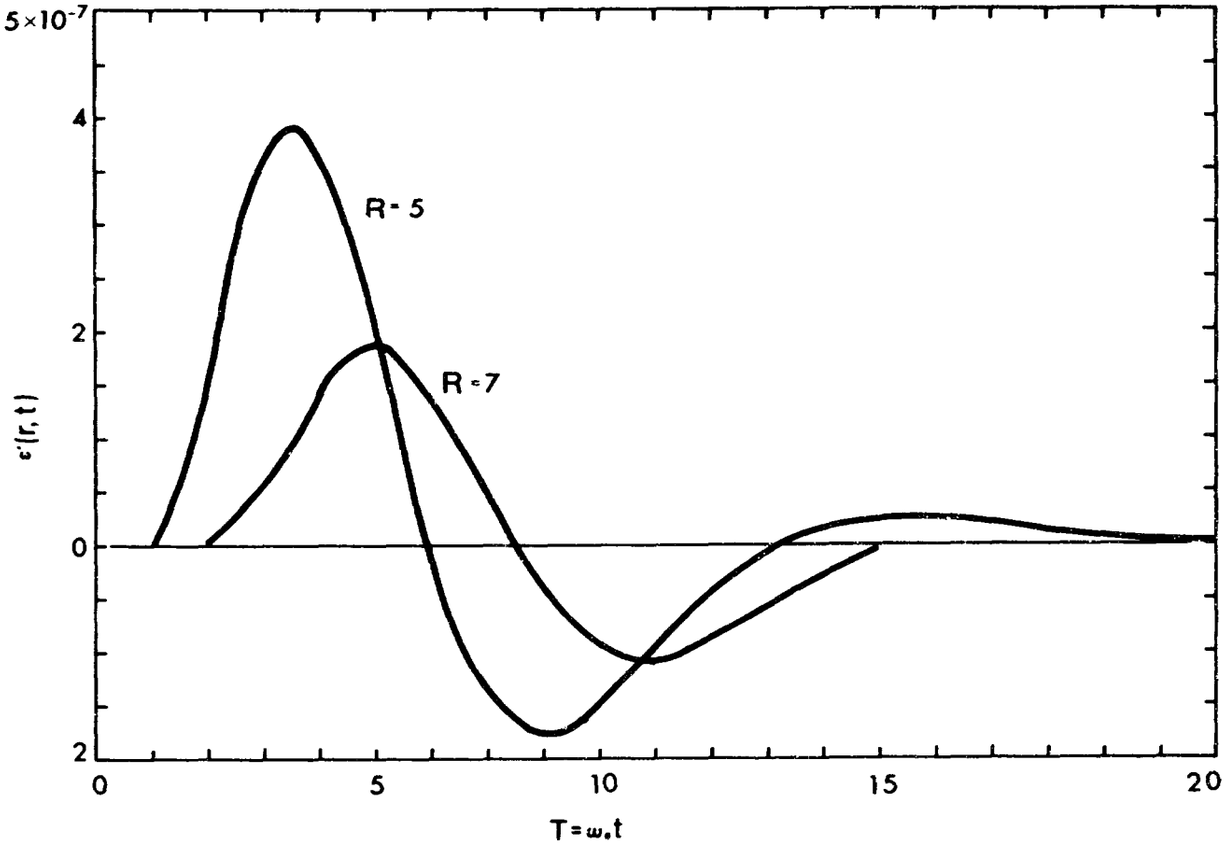

Fig. 19. Normalized strain $\varepsilon'(r,t) = \varepsilon(r,t) \div \frac{P' r_o c^2}{3\mu\omega_o\sqrt{\pi}}$ for $P(t) = P'\delta(t)$ for spherical Voigt wave, r_o = 50 ft., ω_o = 600, and c = 20,000 ft/sec.

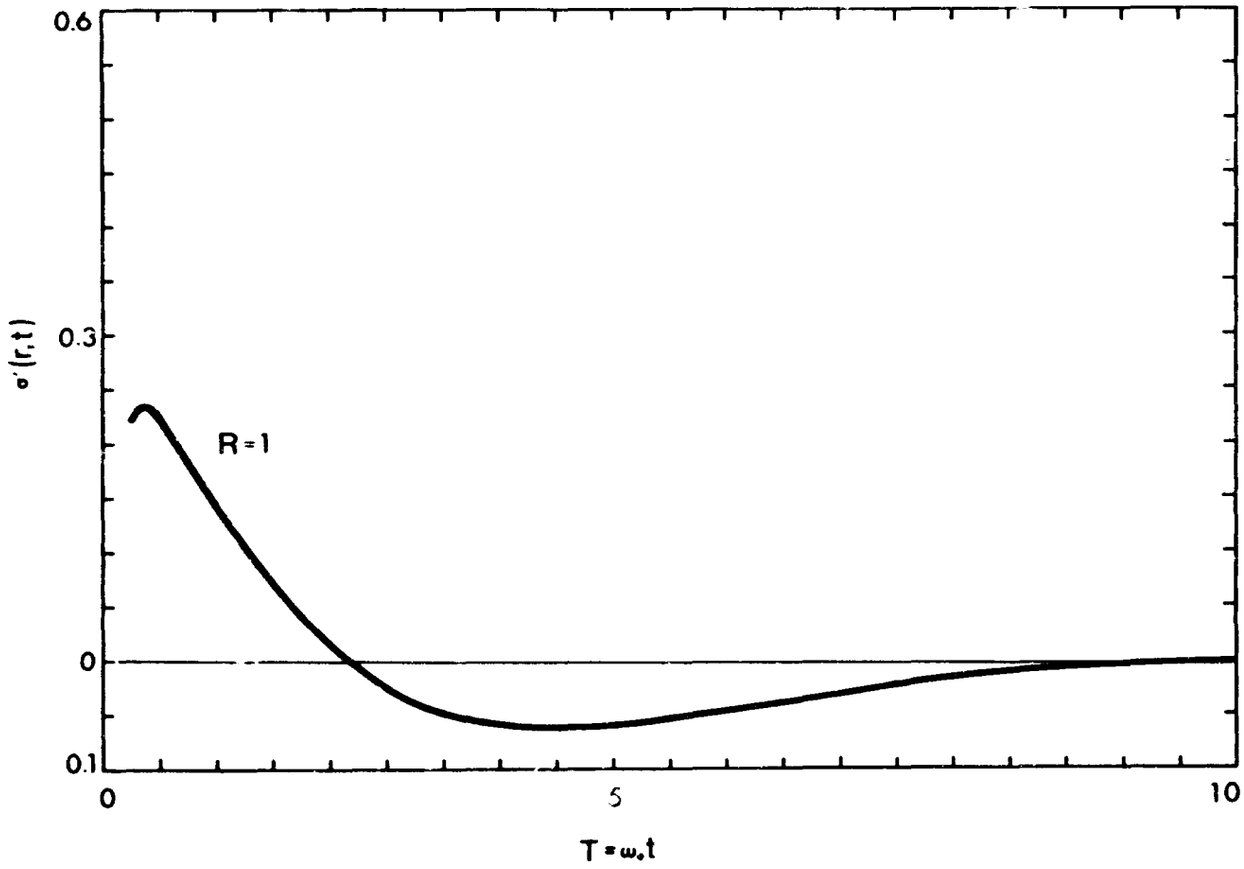

Fig. 20. Normalized stress $\sigma'(r,t) = \sigma(r,t) \div -\frac{P' r_o c^2}{3\omega_o \sqrt{\pi}}$ for $P(t) = P'\delta(t)$ for spherical Voigt wave, $r_o = 50$ ft., $\omega_o = 600$, and $c = 20{,}000$ ft/sec.

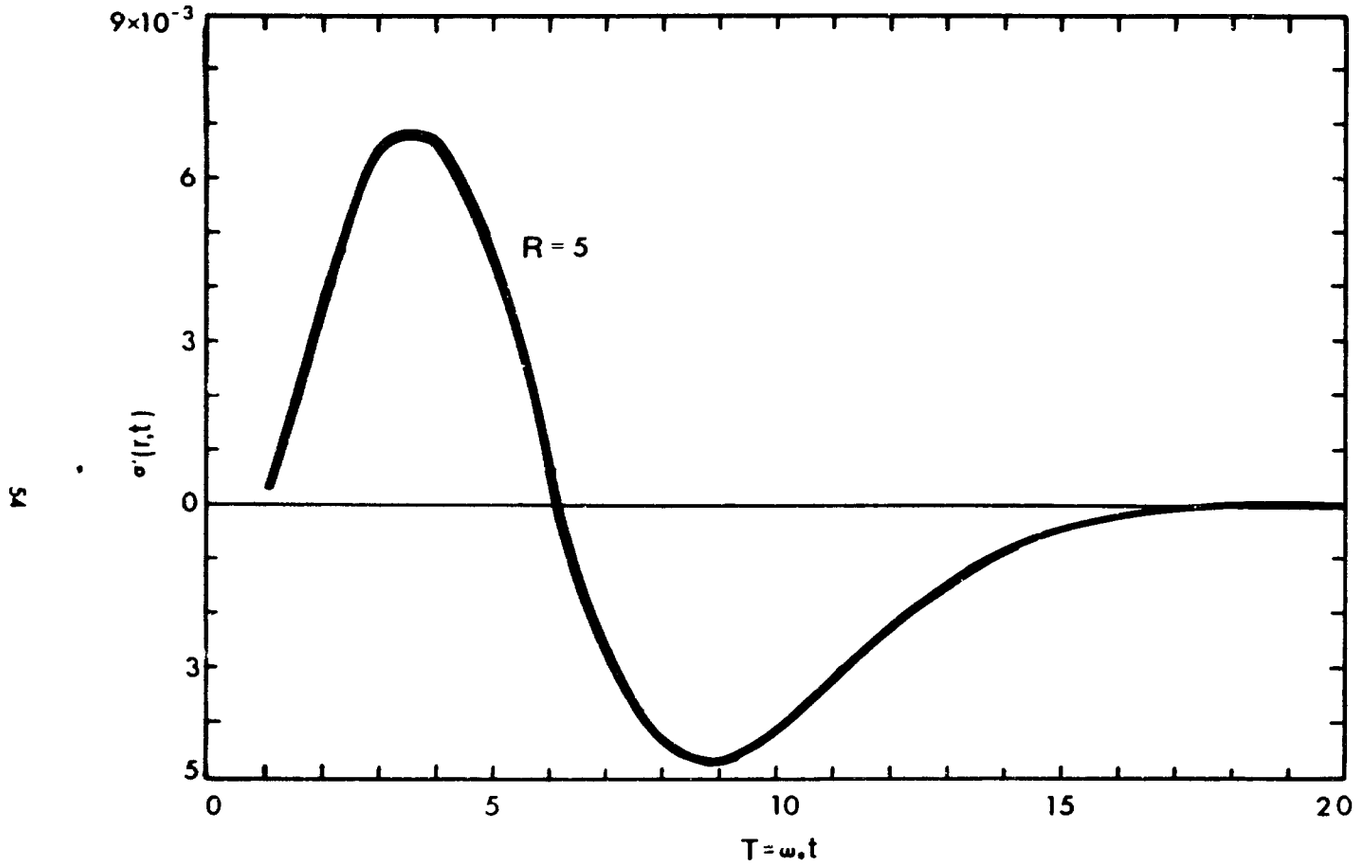

Fig. 21. Normalized stress $\sigma'(r,t) = \sigma(r,t) \div -\frac{P' r_o c^2}{3\omega_o \sqrt{\pi}}$ for $P(t) = P'\delta(t)$ for spherical Voigt wave, r_o = 50 ft., ω_o = 600, and c = 20,000 ft/sec.

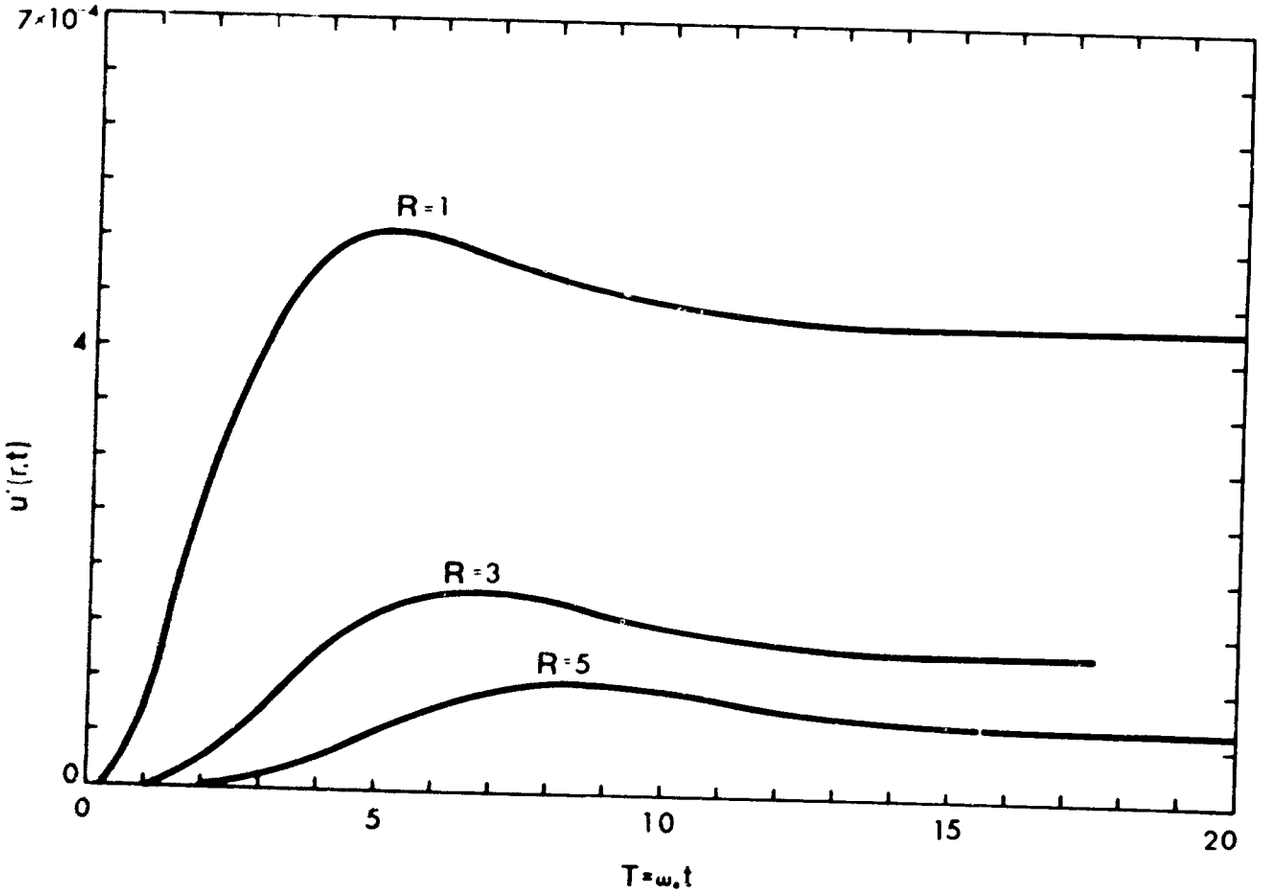

Fig. 22. Normalized displacement $u'(r,t) = u(r,t) \div \frac{P''r_o c^2}{3\mu\omega_o\sqrt{\pi}}$ for $P(t) = P''\,1(t)$ for spherical Voigt wave, r_o = 50 ft., ω_o = 600 and c = 20,000 ft/sec.

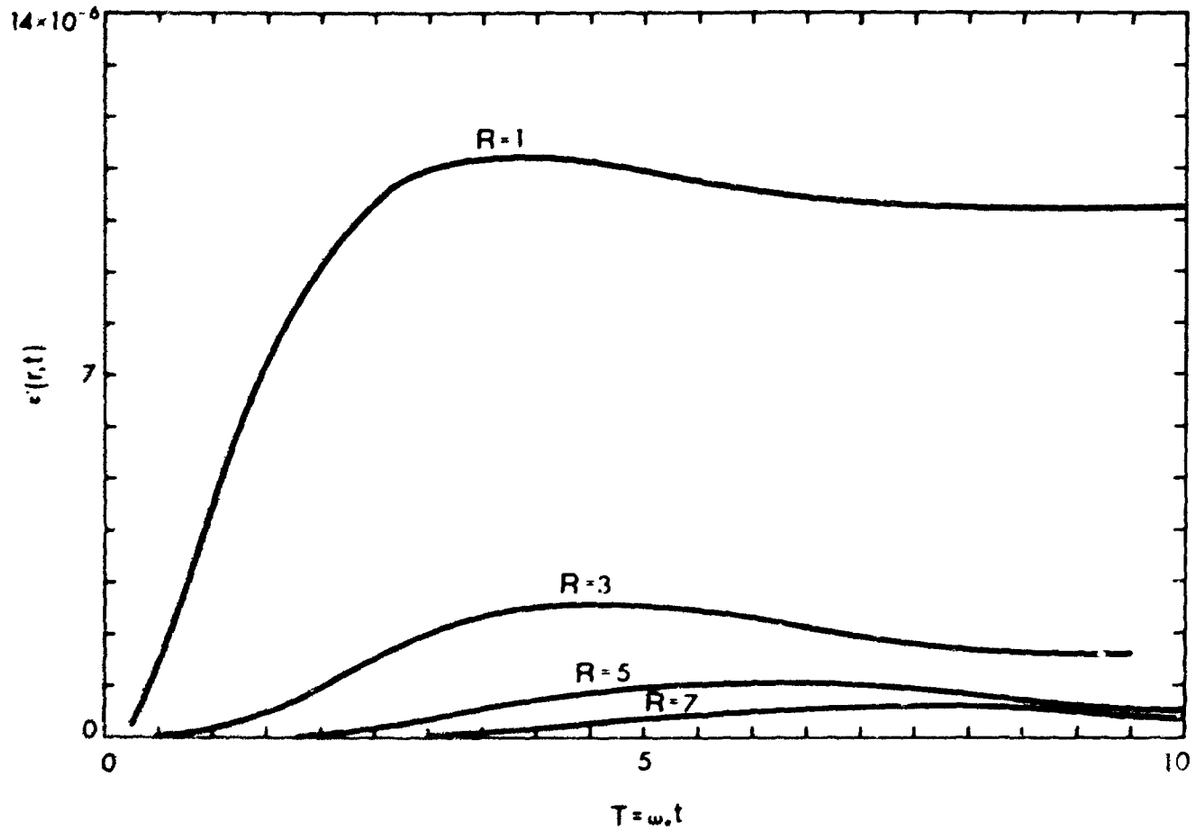

Fig. 23. Normalized strain $\varepsilon'(r,t) = \varepsilon(r,t) \div -\frac{P'' r_o c^2}{3\mu\omega_o^2\sqrt{\pi}}$ for $P(t) = P''\,1(t)$ for spherical Voigt wave, r_o = 50 ft., ω_o = 600 and c = 20,000 ft/sec.

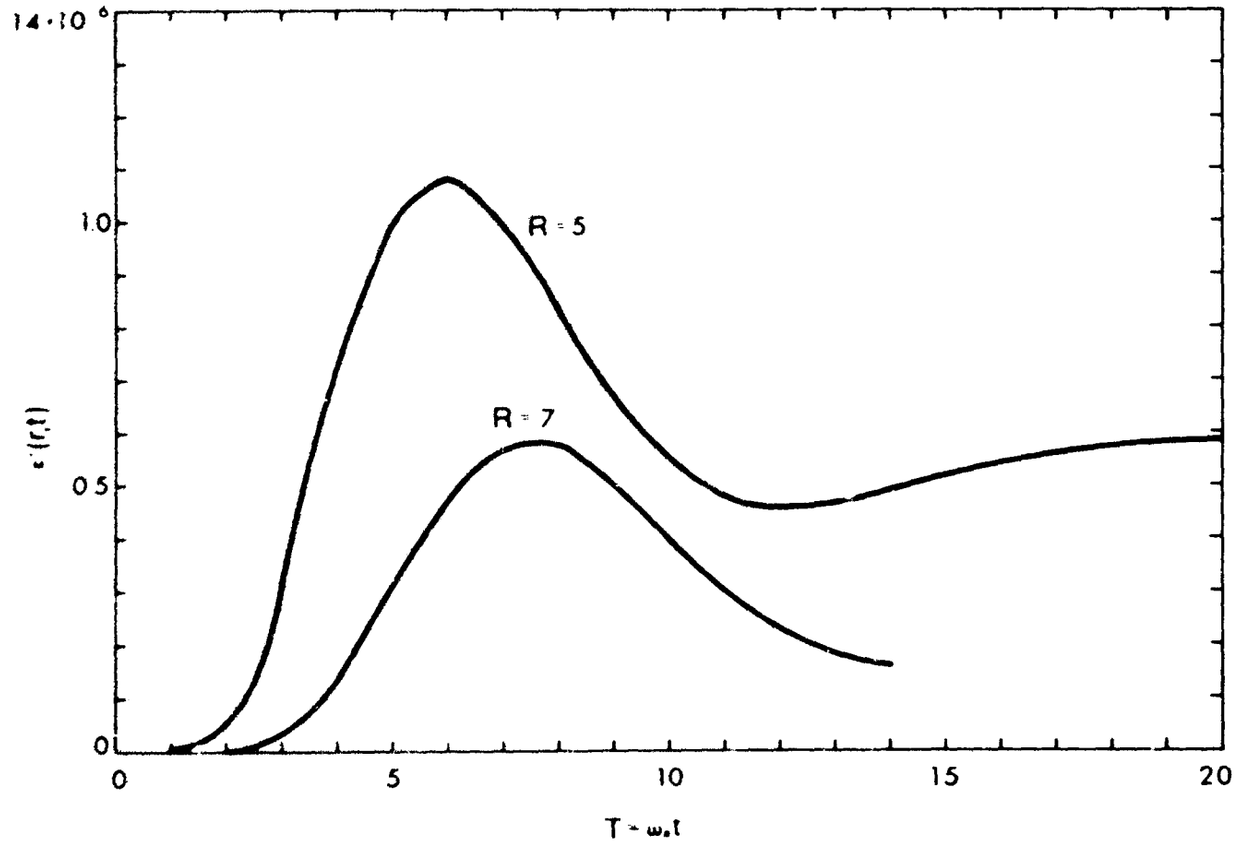

Fig. 24. Normalized strain $\varepsilon'(r,t) = \varepsilon(r,t) \div -\frac{P'' r_o c^2}{3\mu\omega_o^2\sqrt{\pi}}$ for $P(t) = P''\, 1(t)$ for spherical Voigt wave, r_o = 50 ft., ω_o = 600 and c = 20,000 ft/sec.

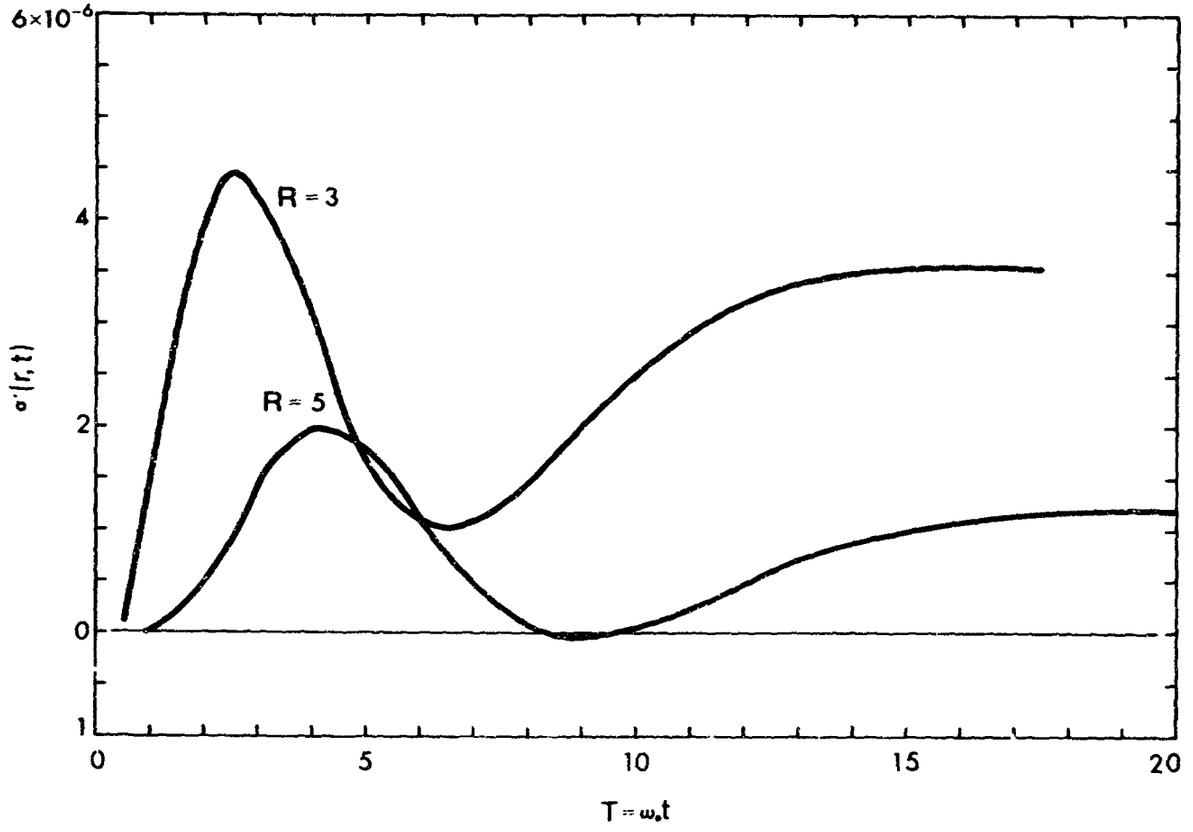

Fig. 25. Normalized stress $\sigma'(r,t) = \sigma(r,t) \div -\frac{P'' r_o c^2}{3\omega_o^2\sqrt{\pi}}$ for $P(t) = P''\, 1(t)$ for spherical Voigt wave, r_o = 50 ft., ω_o = 600 and c = 20,000 ft/sec.

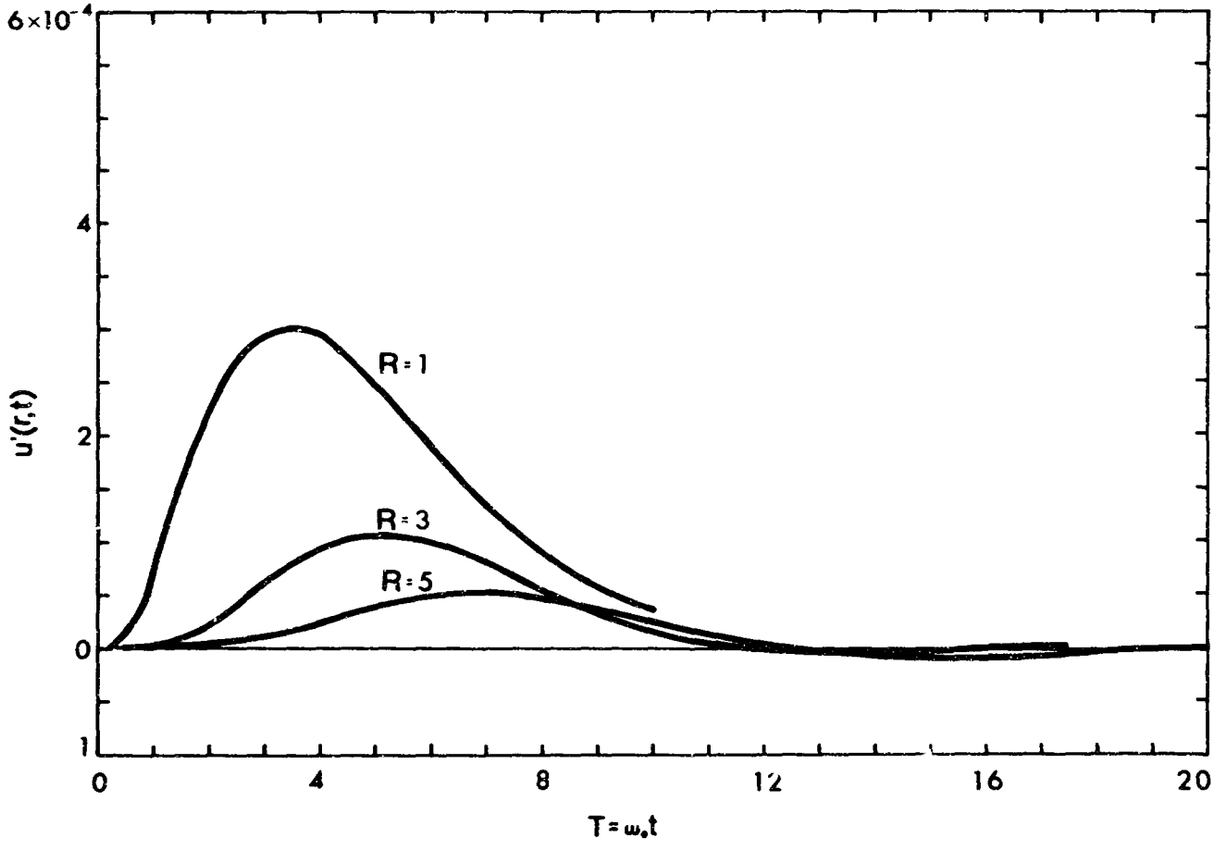

Fig. 26. Normalized displacement $u'(r,t) = u(r,t) \div \frac{P_o r_o c^2}{3\mu\omega_o^2\sqrt{\pi}}$ for $P(t) = P_o e^{-\beta t}$ for spherical Voigt wave, r_o = 50 ft., ω_o = 600 and c = 20,000 ft/sec.

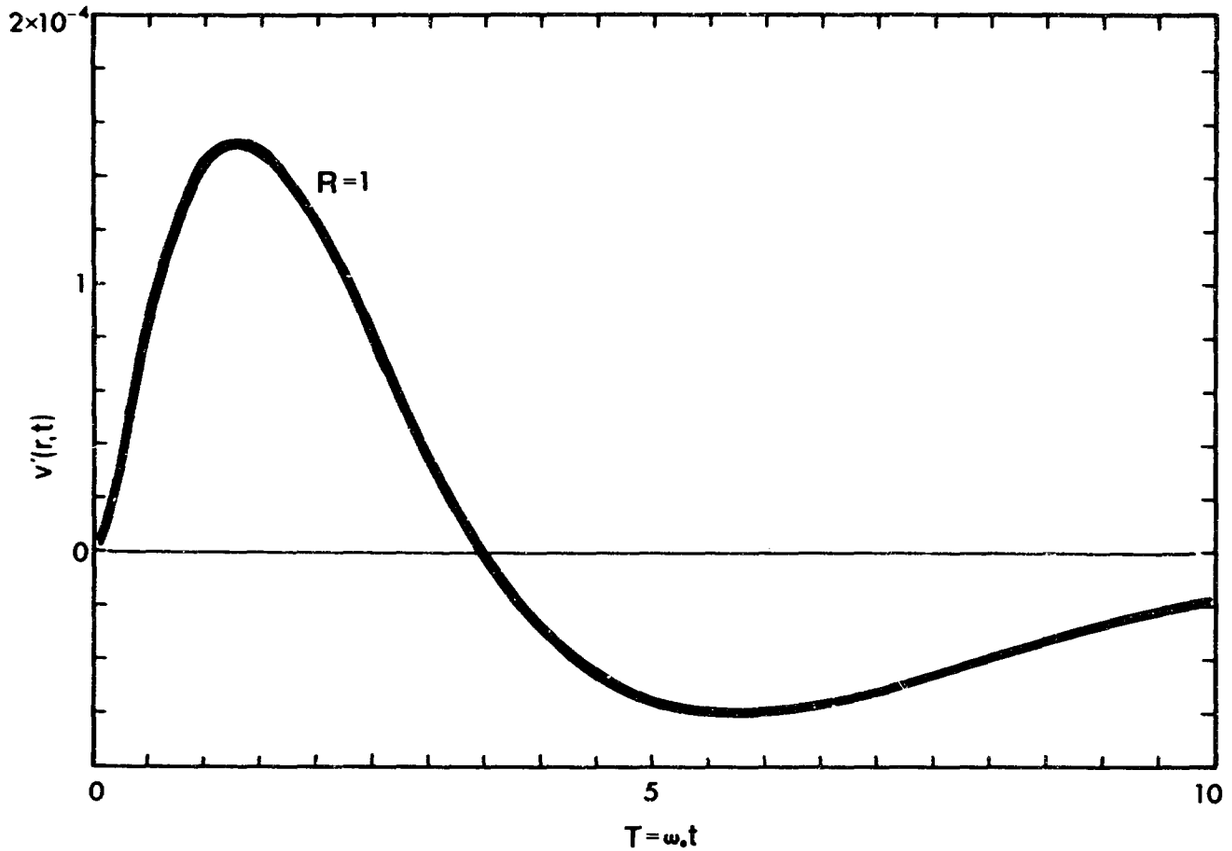

Fig. 27. Normalized velocity $v'(r,t) = v(r,t) \div \frac{P_o r_o c^2}{3\mu\omega_o\sqrt{\pi}}$ for $P(t) = P_o e^{-\beta t}$ for a spherical Voigt wave, r_o = 50 ft., ω_o = 600 and c = 20,000 ft/sec.

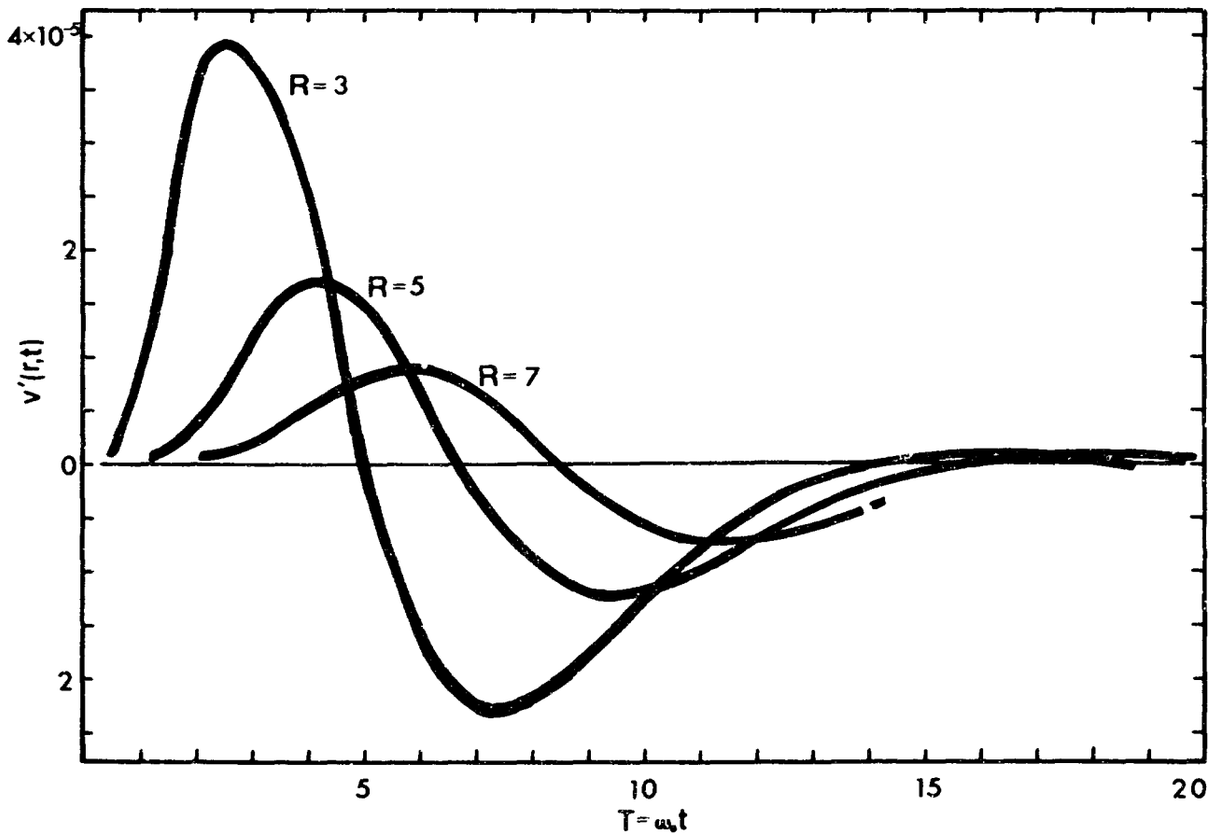

Fig. 28. Normalized particle velocity $v'(r,t) = v(r,t) \div \frac{P_o r_o c^2}{3\mu\omega_o\sqrt{\pi}}$ for $P(t) = P_o e^{-\beta t}$

for spherical Voigt wave, r_o = 50 ft., ω_o = 600 and c = 20,000 ft/sec.

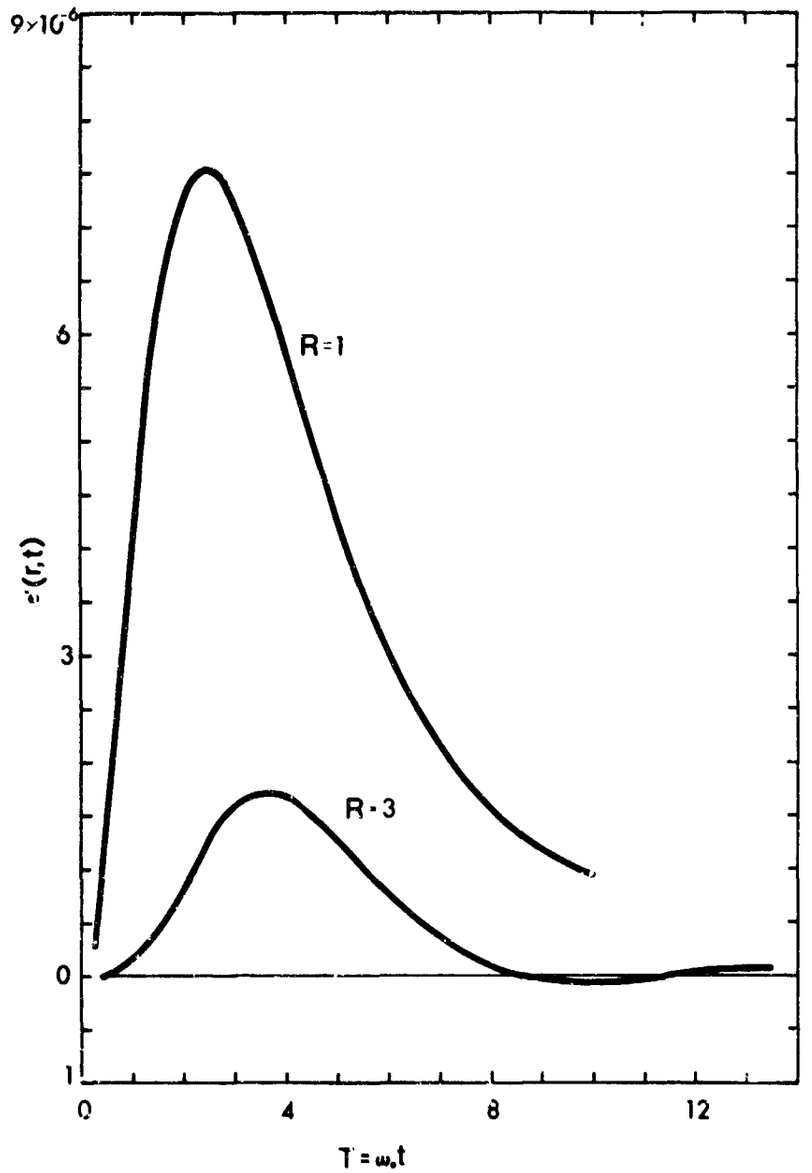

Fig. 29. Normalized strain $\varepsilon'(r,t) = \varepsilon(r,t) \div -\frac{P_o r_o c^2}{3\mu\omega_o^2\sqrt{\pi}}$ for $P(t) = P_o e^{-\beta t}$ for spherical Voigt wave, r_o = 50 ft., ω_o = 600 and c = 20,000 ft/sec.

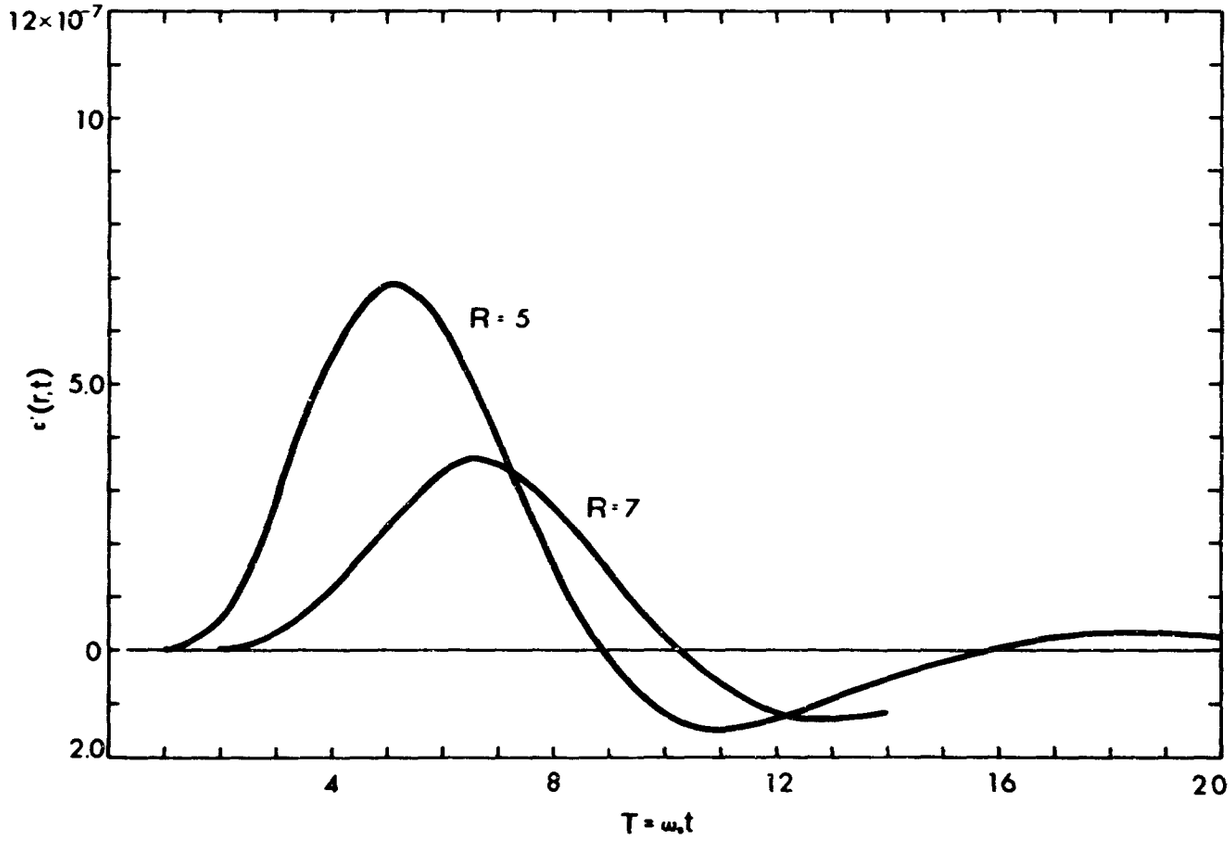

Fig. 30. Normalized strain $\varepsilon'(r,t) = \varepsilon(r,t) \div -\frac{P_o r_o c^2}{3\mu\omega_o^2\sqrt{\pi}}$ for $P(t) = P_o e^{-\beta t}$ for spherical Voigt wave, r_o = 50 ft., ω_o = 600 and c = 20,000 ft/sec.

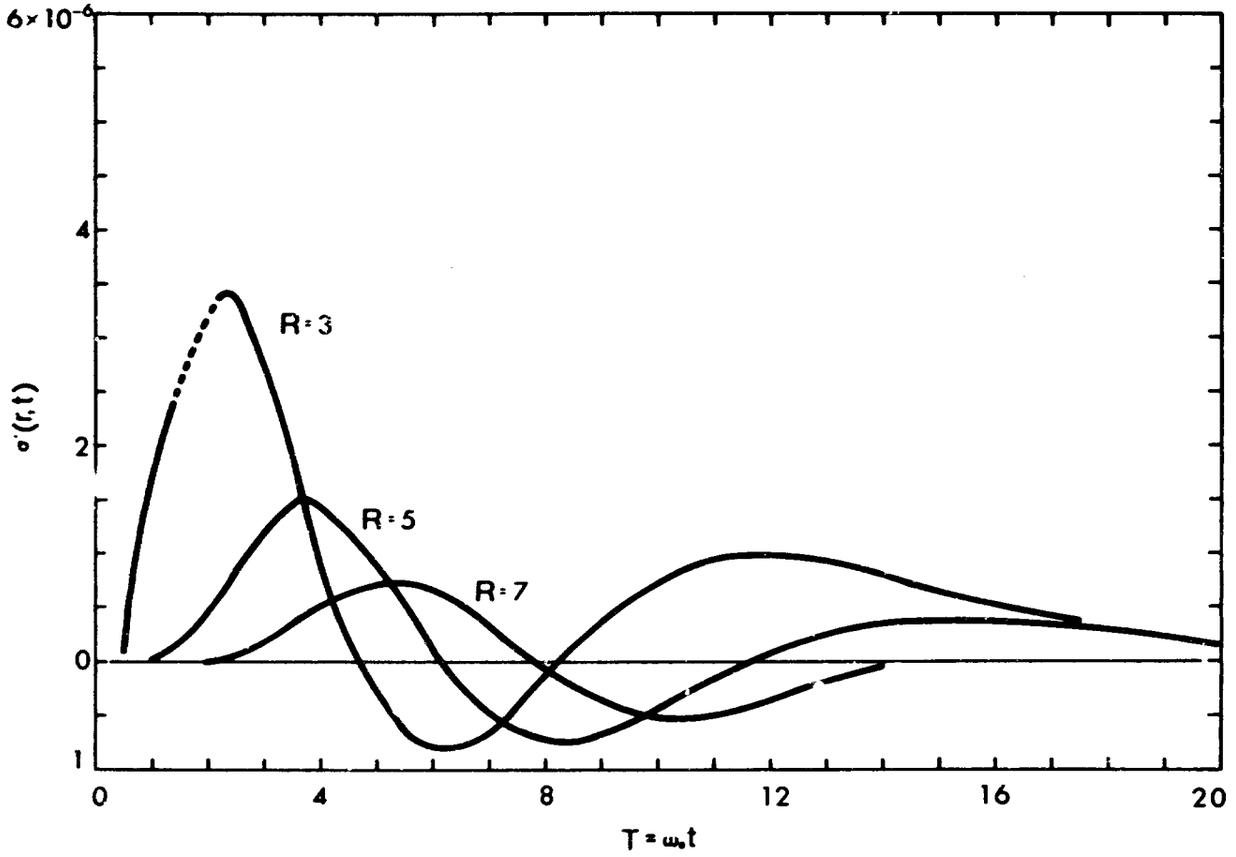

Fig. 31. Normalized stress $\sigma'(r,t) = \sigma(r,t) \div -\frac{P_o r_o c^2}{3\omega_o^2\sqrt{\pi}}$ for $P(t) = P_o e^{-\beta t}$ for spherical Voigt wave, r_o = 50 ft., ω_o = 600 and c = 20,000 ft/sec.

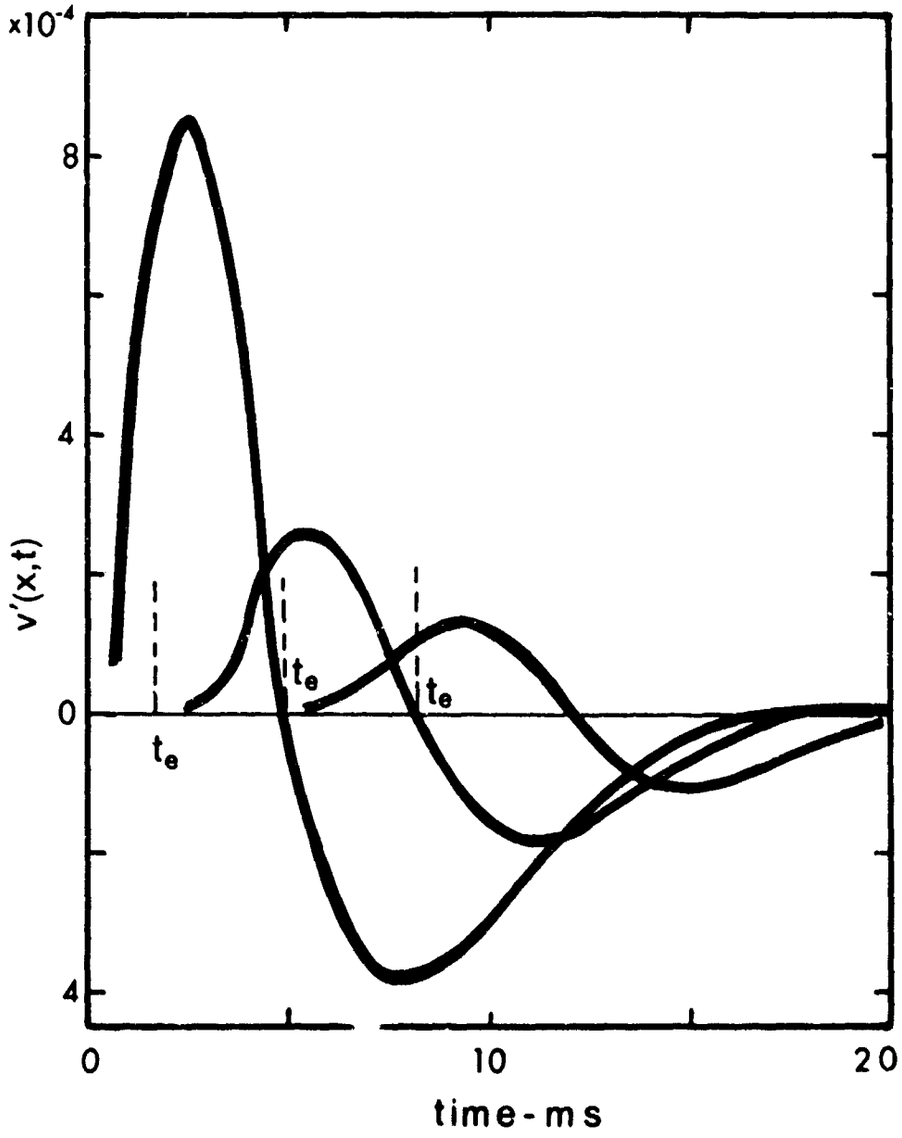

Fig. 32. Normalized particle velocity $v'(r,t) = v(r,t) : \frac{P_o r_o c^2}{3\mu\omega_o\sqrt{\pi}}$ for $P(t) = P_o e^{-\beta t}$ for spherical Voigt wave, $r_o = 50$ ft., $\omega_o = 2000$, $\beta = 150$ and $c = 20{,}000$ ft/sec. Notation t_e indicates arrival time of elastic wave.

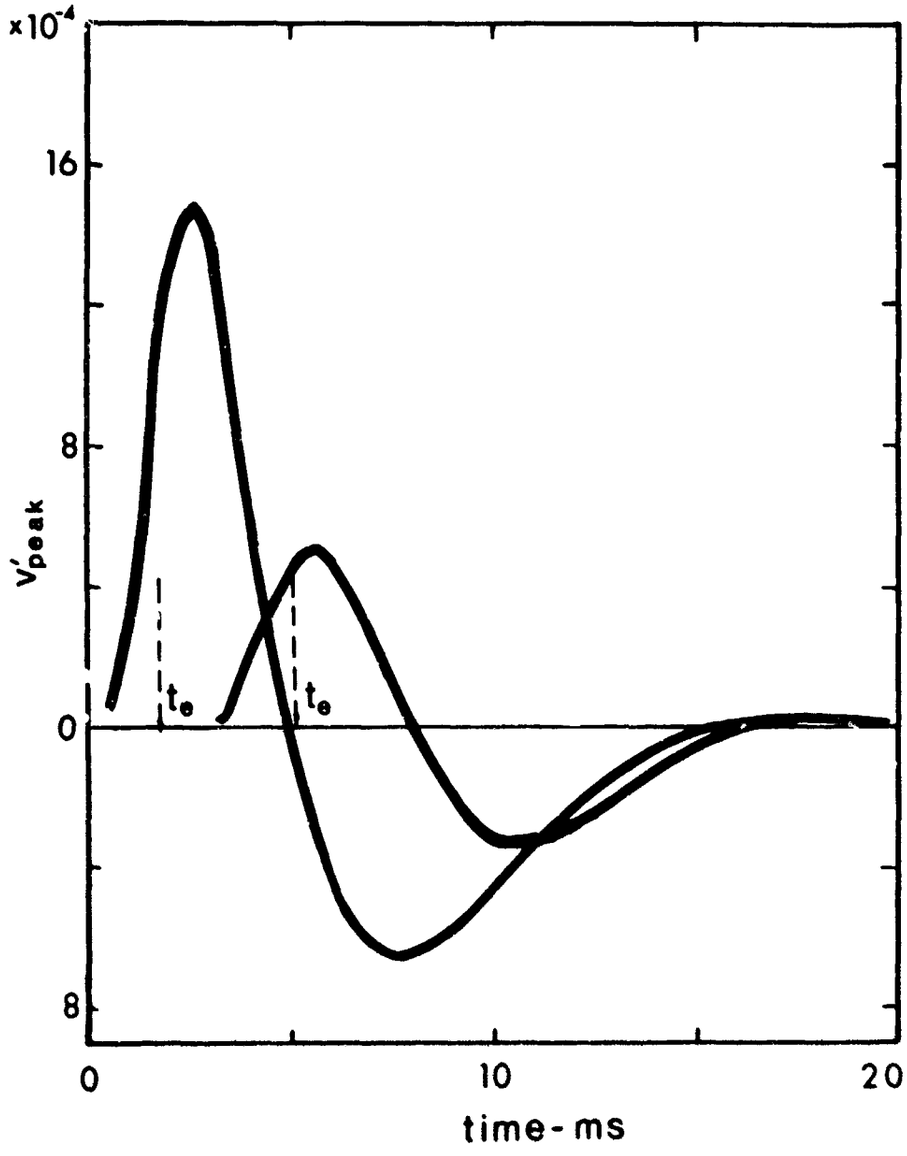

Fig. 33. Normalized particle velocity $v'(r,t) = v(r,t) \div \frac{P_o r_o c^2}{3\mu\omega_o\sqrt{\pi}}$ for $P(t) = P_o e^{-\beta t}$ for spherical Voigt wave, r_o = 50 ft., ω_o = 3000, β = 150, and c = 20,000 ft/sec. Notation t_e indicates arrival time of elastic wave.

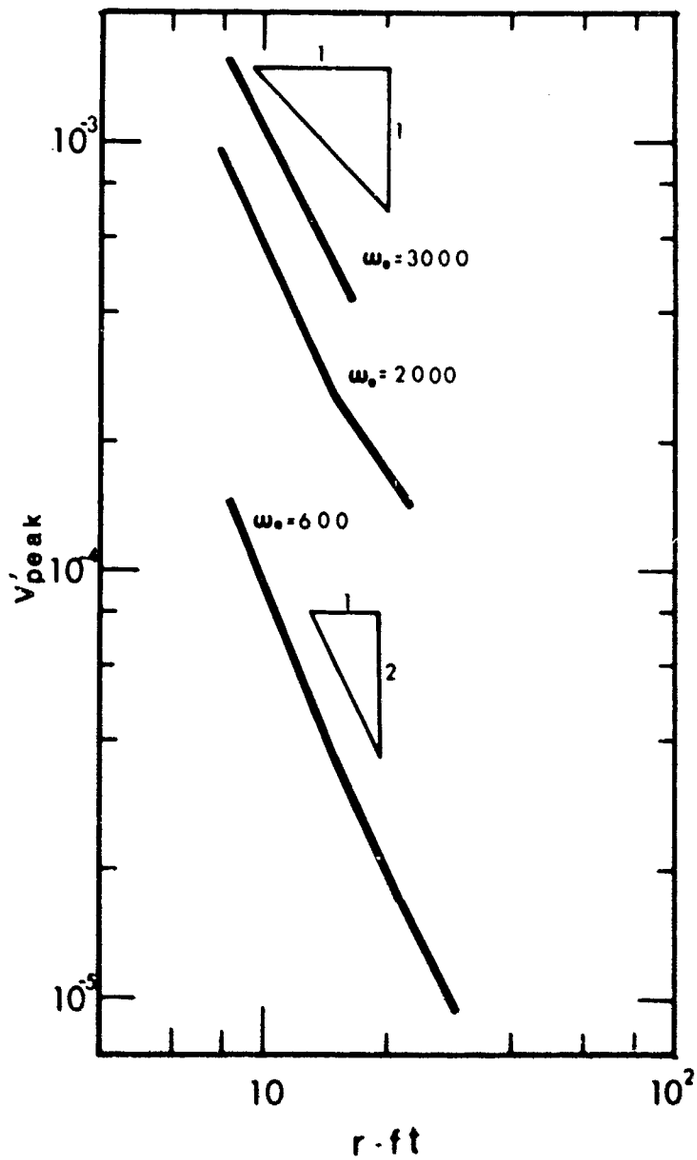

Fig. 34. Peak particle velocity versus travel distance for a spherical Voigt wave for three values of ω_o with forcing function $P(t) = P_o e^{-\beta t}$ and $\beta = 150$.

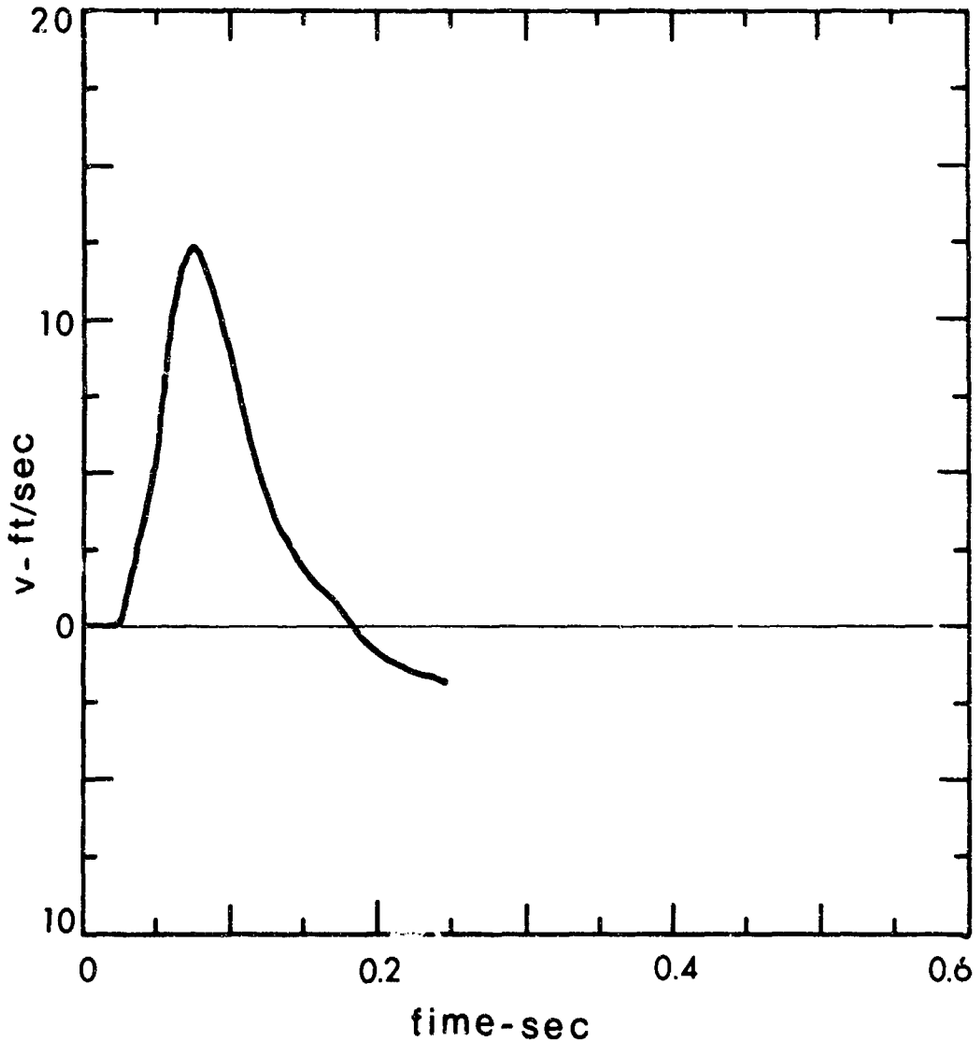

Fig. 35. Particle velocity pulse, Project AIRVENT, gage 60-A.

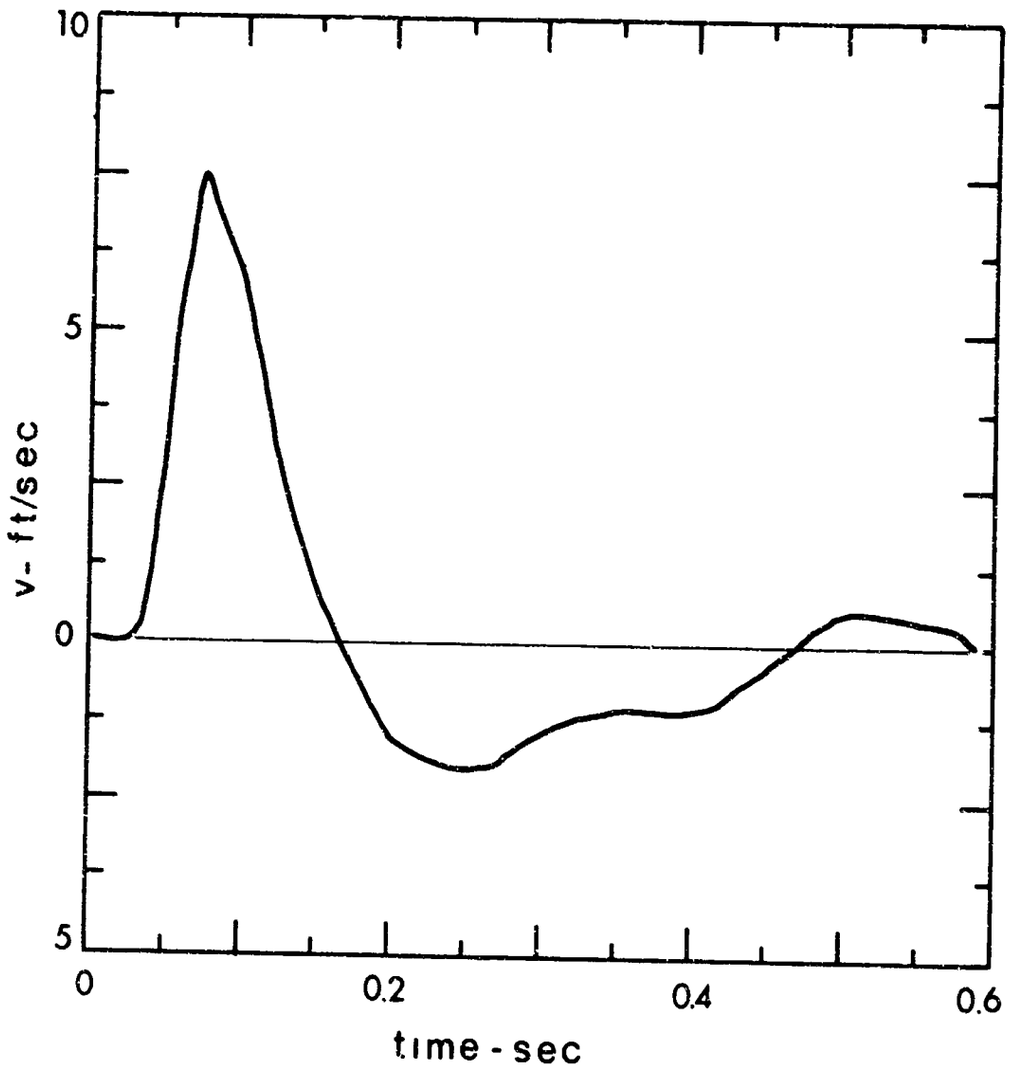

Fig. 36. Particle velocity pulse, Project AIRVENT, gage 60u.

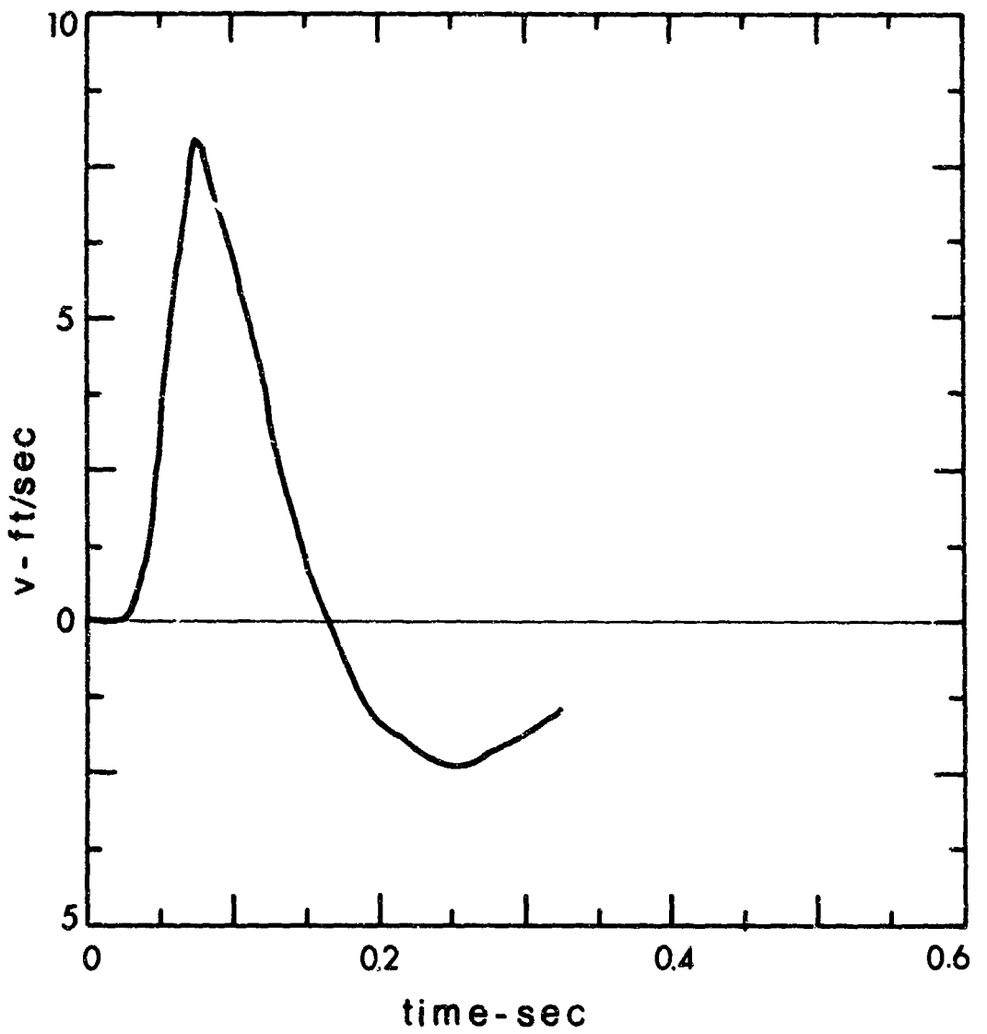

Fig. 37. Particle velocity pulse, Project AIRVENT, gage 70u.

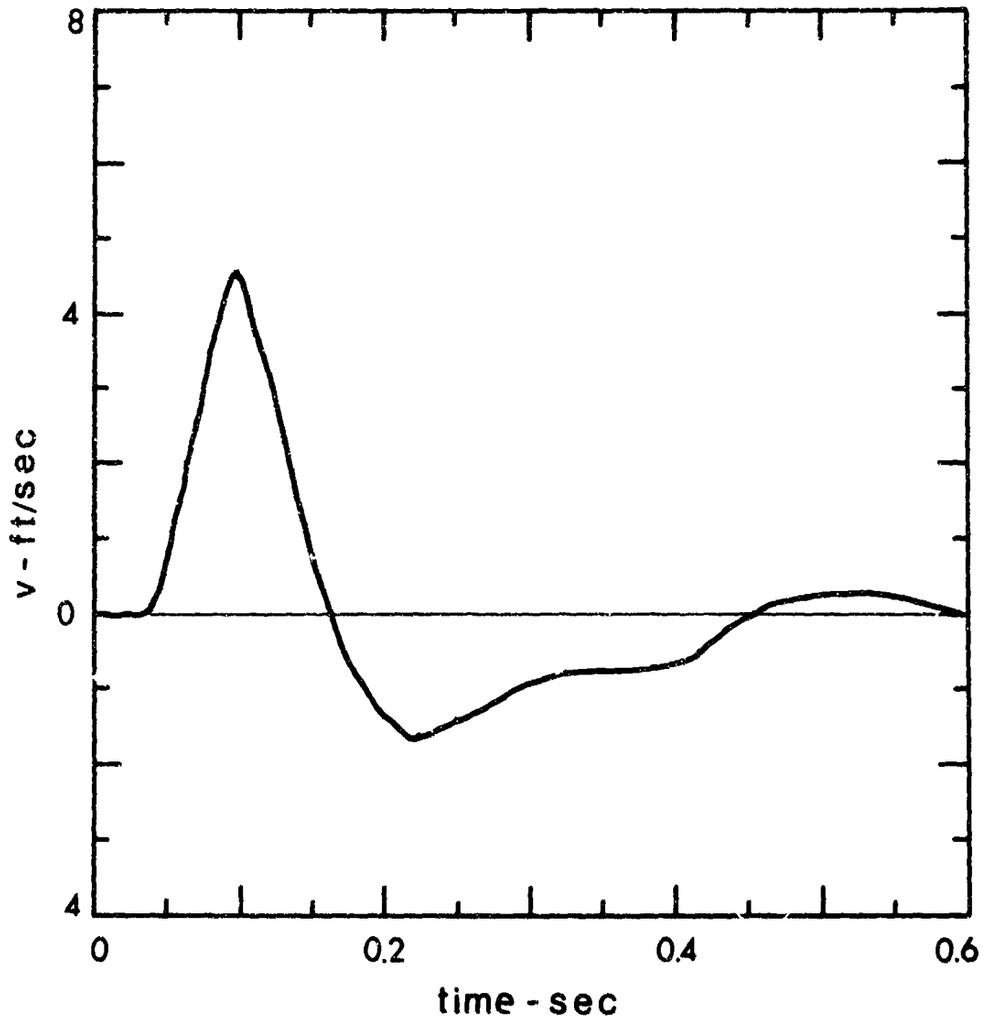

Fig. 38. Particle velocity pulse, Project AIRVENT, gage 90u.

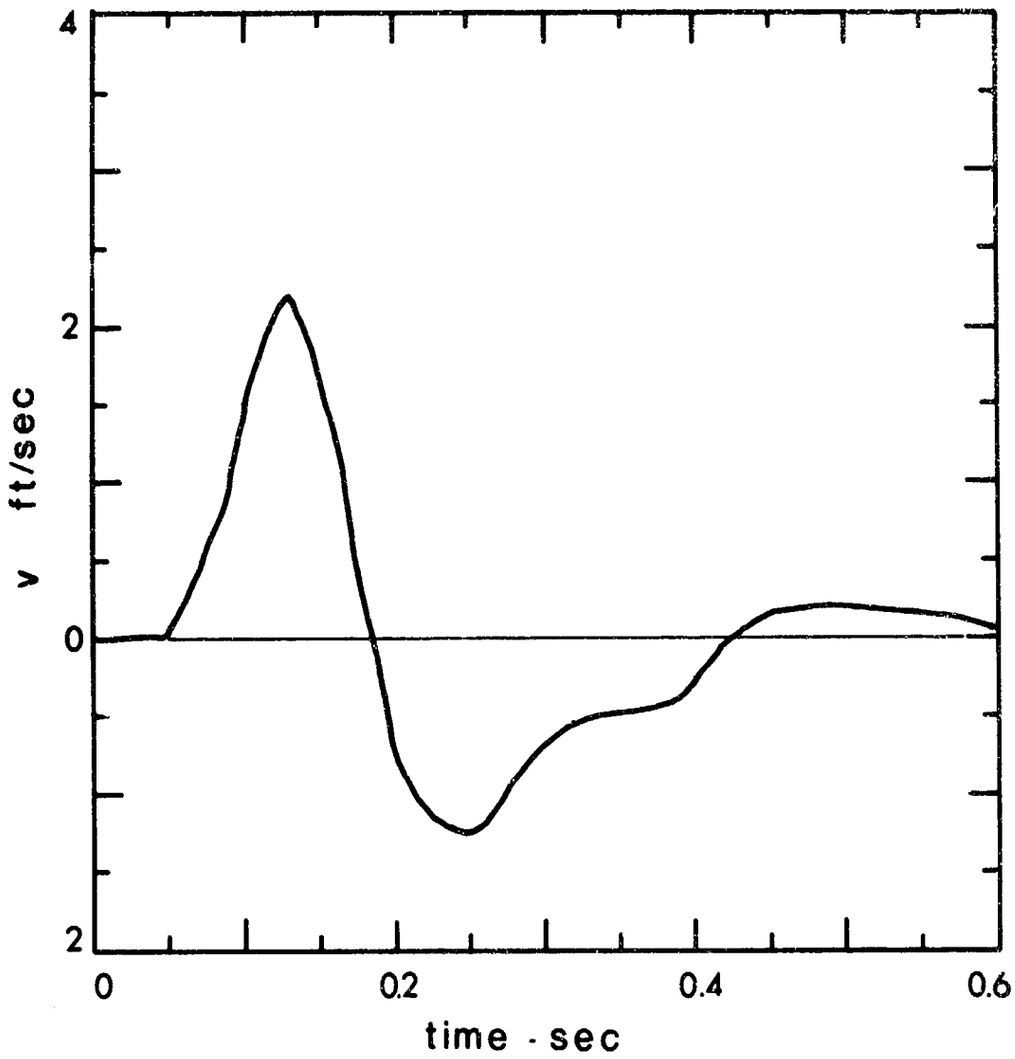

Fig. 39. Particle velocity pulse, Project AIRVENT, gage 130-u.

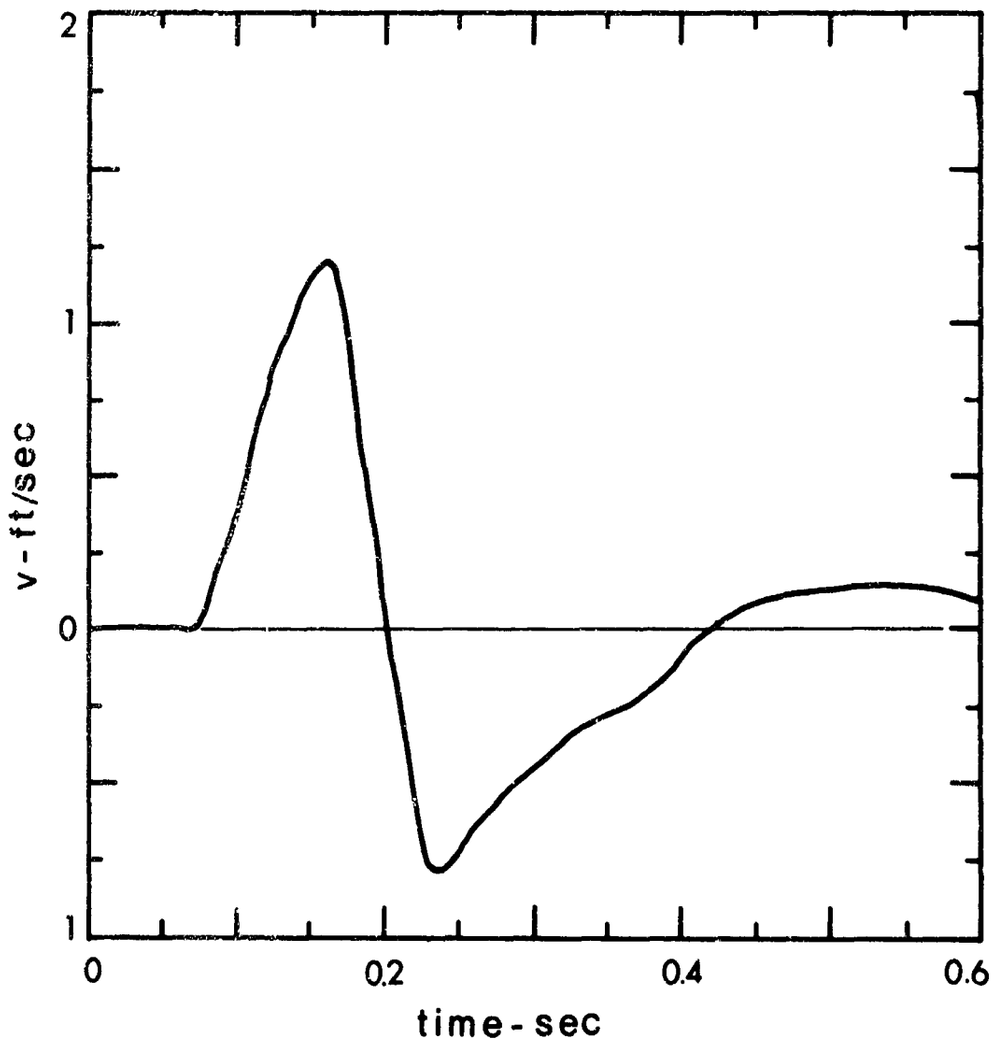

Fig. 40. Particle velocity pulse, Project AIRVENT, 170-u.

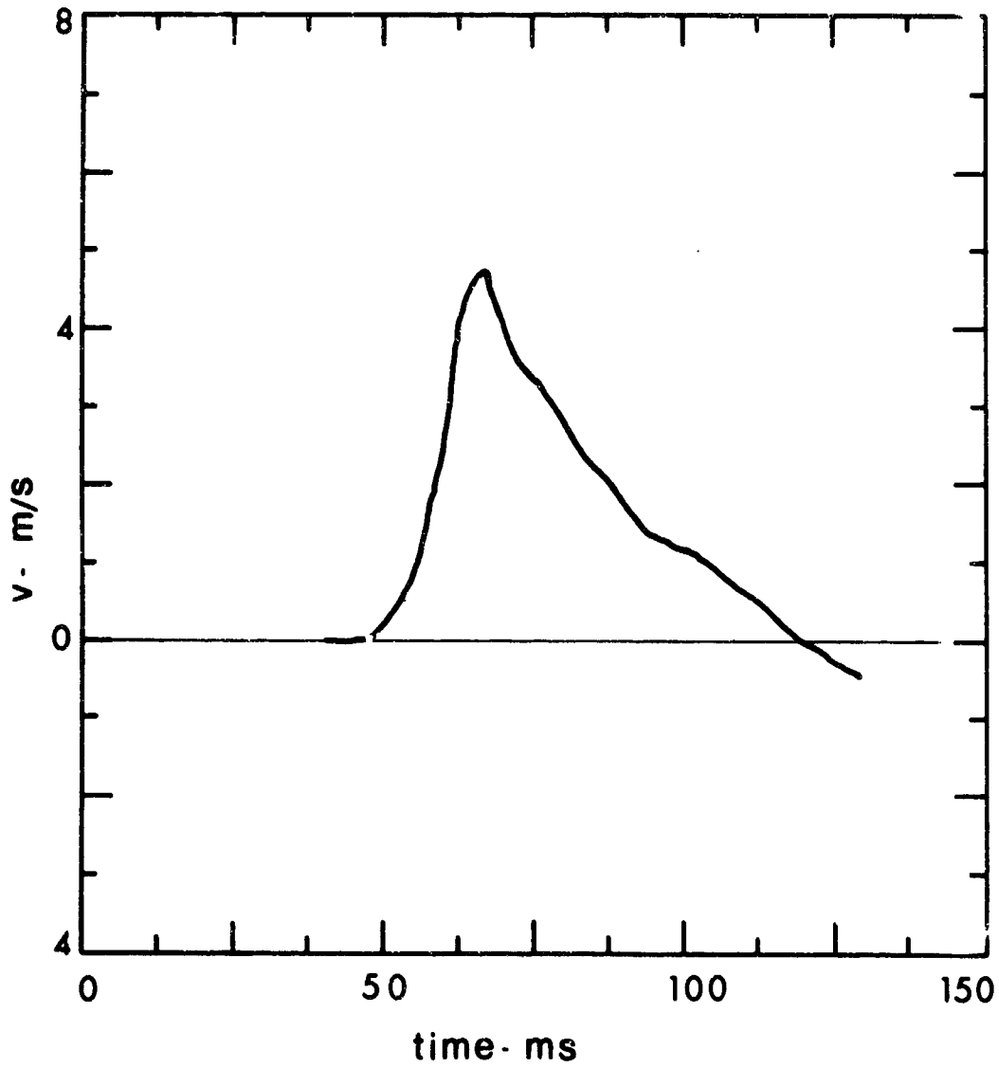

Fig. 41. Particle velocity pulse, Project GNOME, range 229 meters, 6-AH.

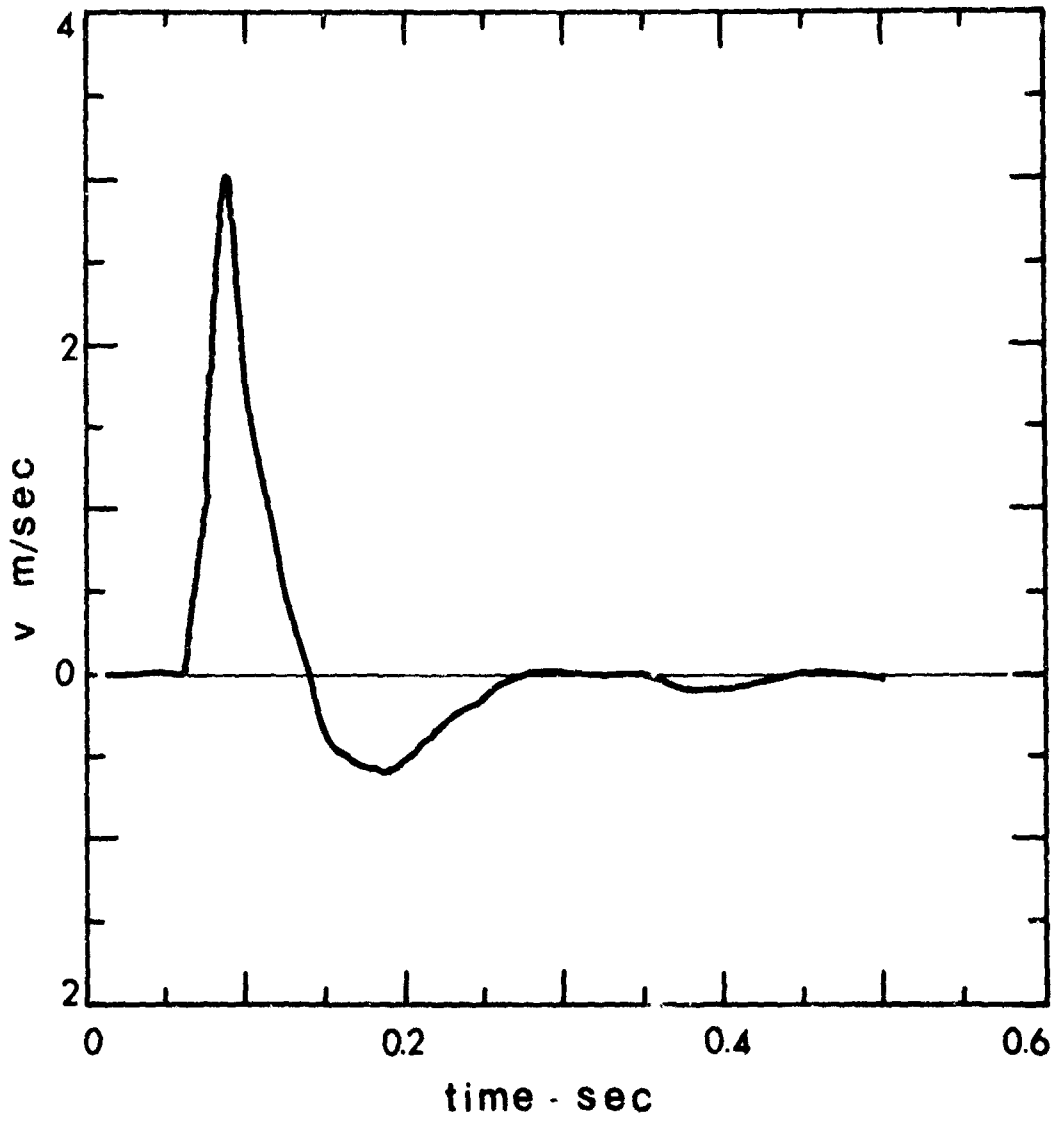

Fig. 42. Particle velocity pulse in salt, Project GNOME, range 298 meters, 7-ulH.

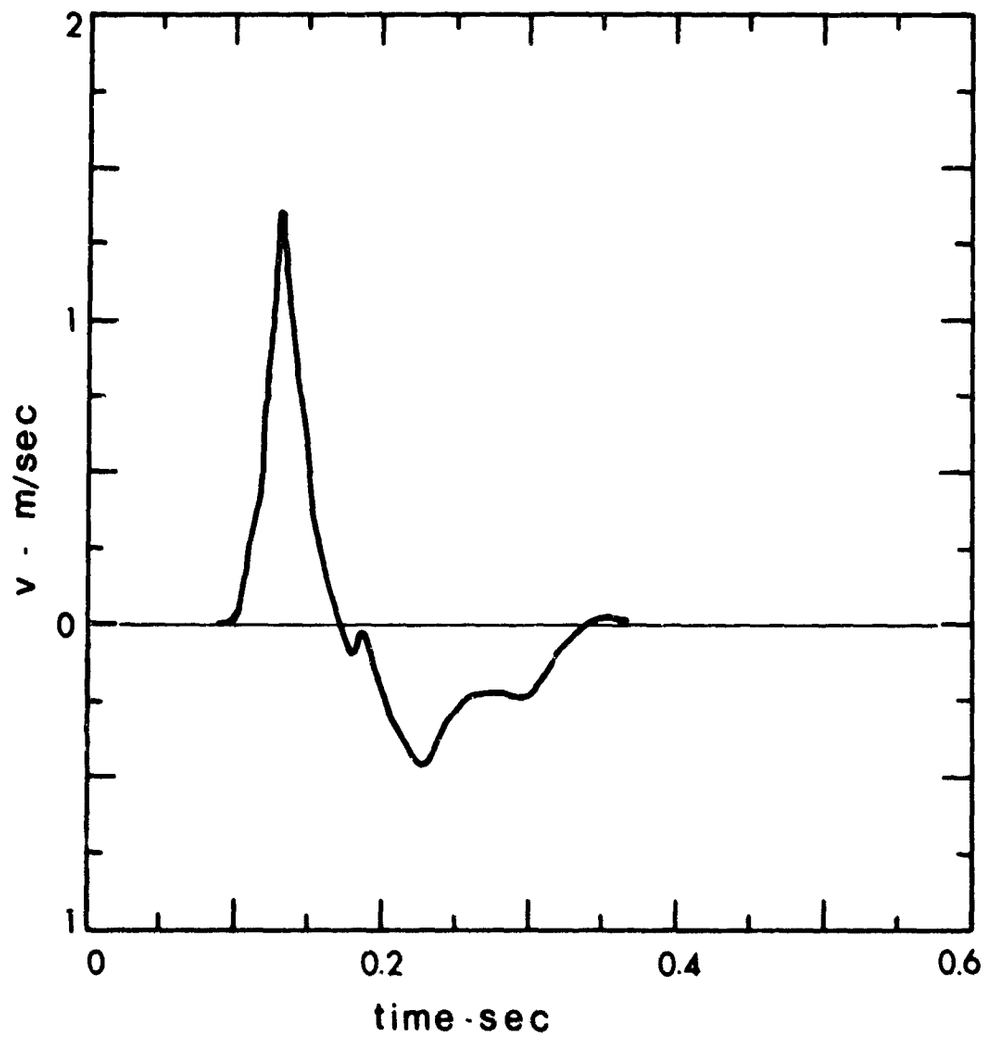

Fig. 43. Particle velocity pulse in salt, Project GNOME, range 477 meters, 21-AIH.

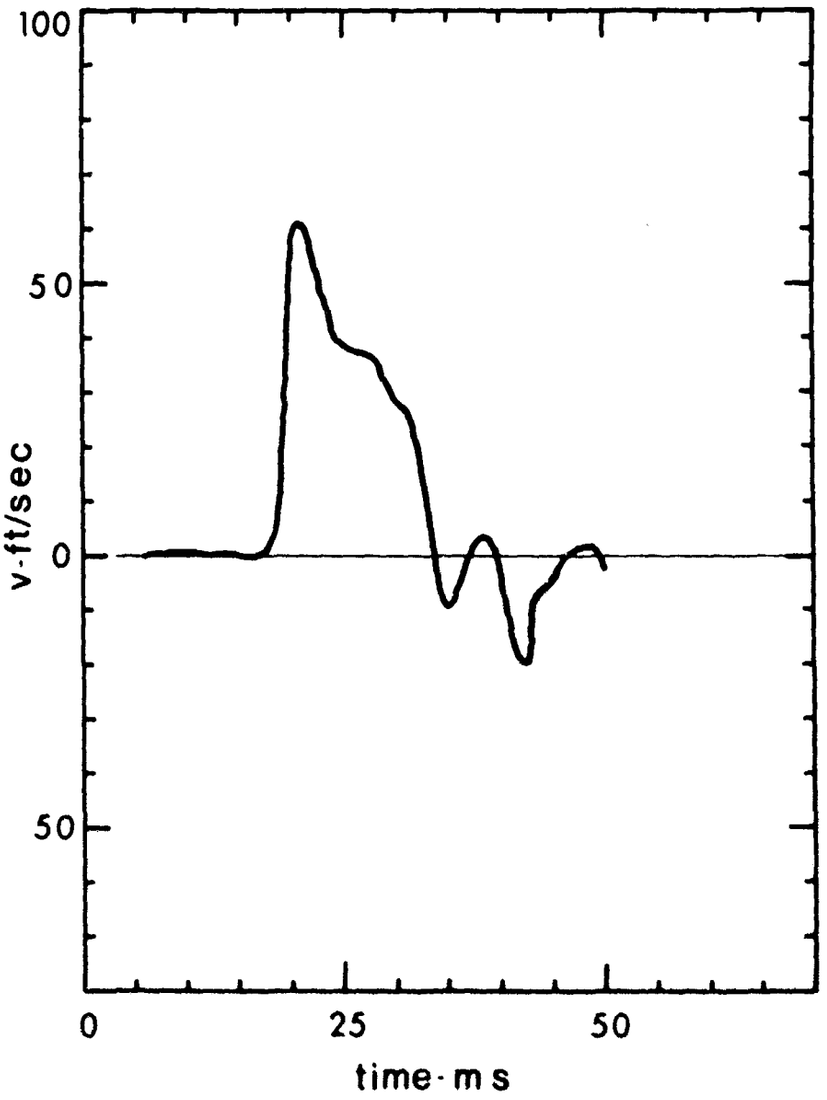

Fig. 44. Particle velocity pulse, Project HARDHAT, 306 ft., gage 6-A.

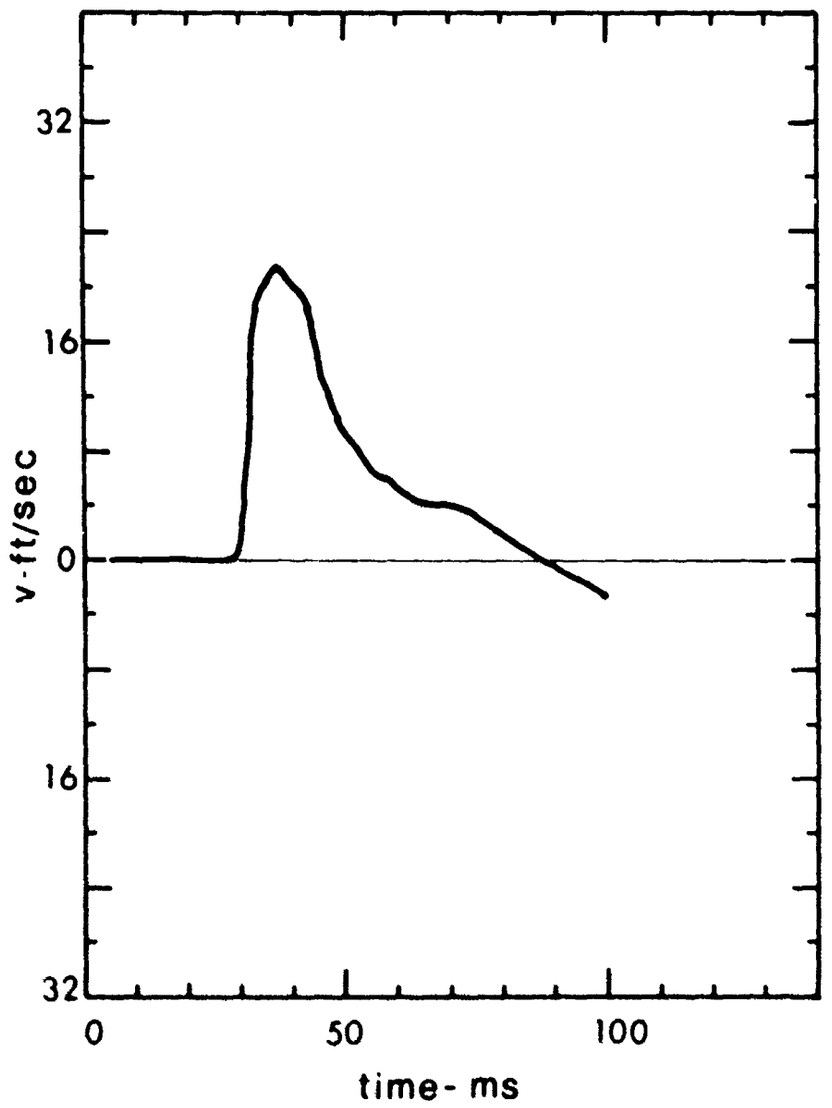

Fig. 45. Particle velocity pulse, Project HARDHAT, 505 ft., gage 9-A.

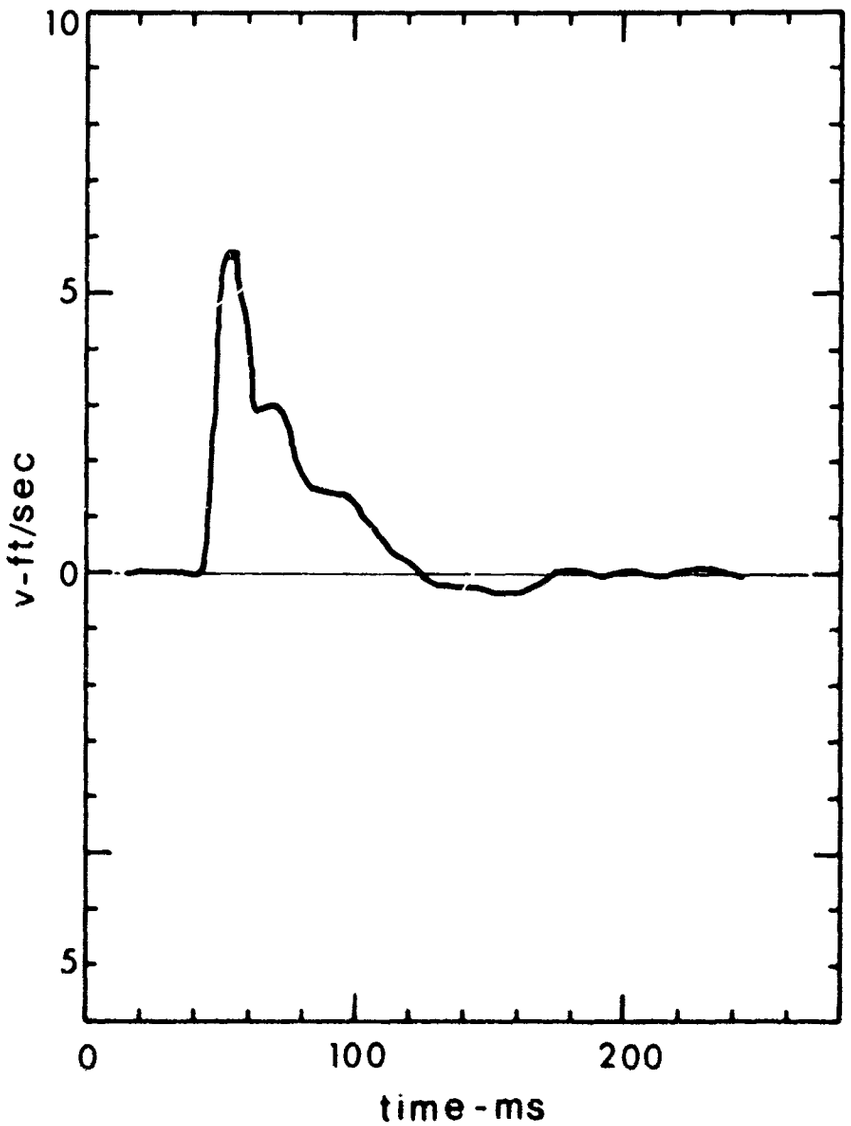

Fig. 46. Particle velocity pulse, Project HARDHAT, 784 ft., gage 12 AR.

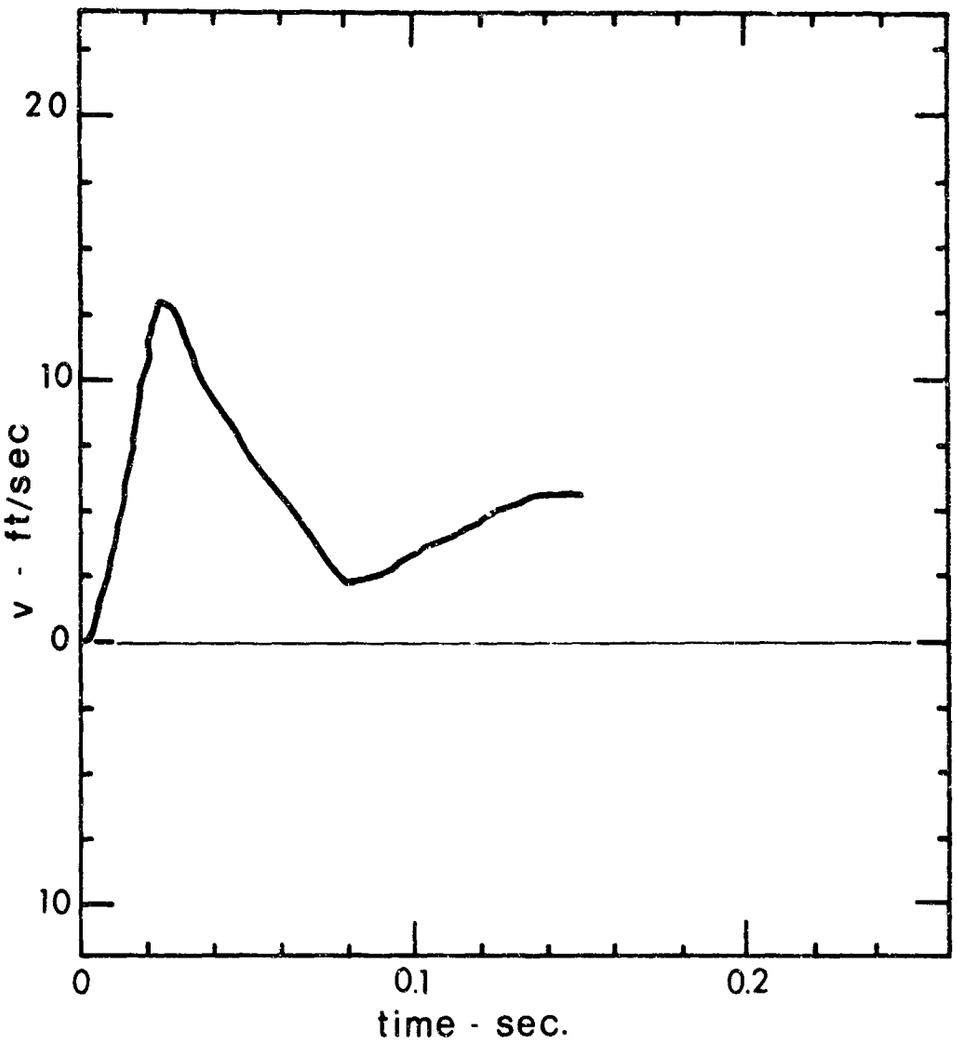

Fig. 47. Particle velocity pulse in andesite, Project LONGSHOT, 80 KT, horizontal range 20 ft., gage depth 500 ft., slant range 1800 ft., gage 3A.

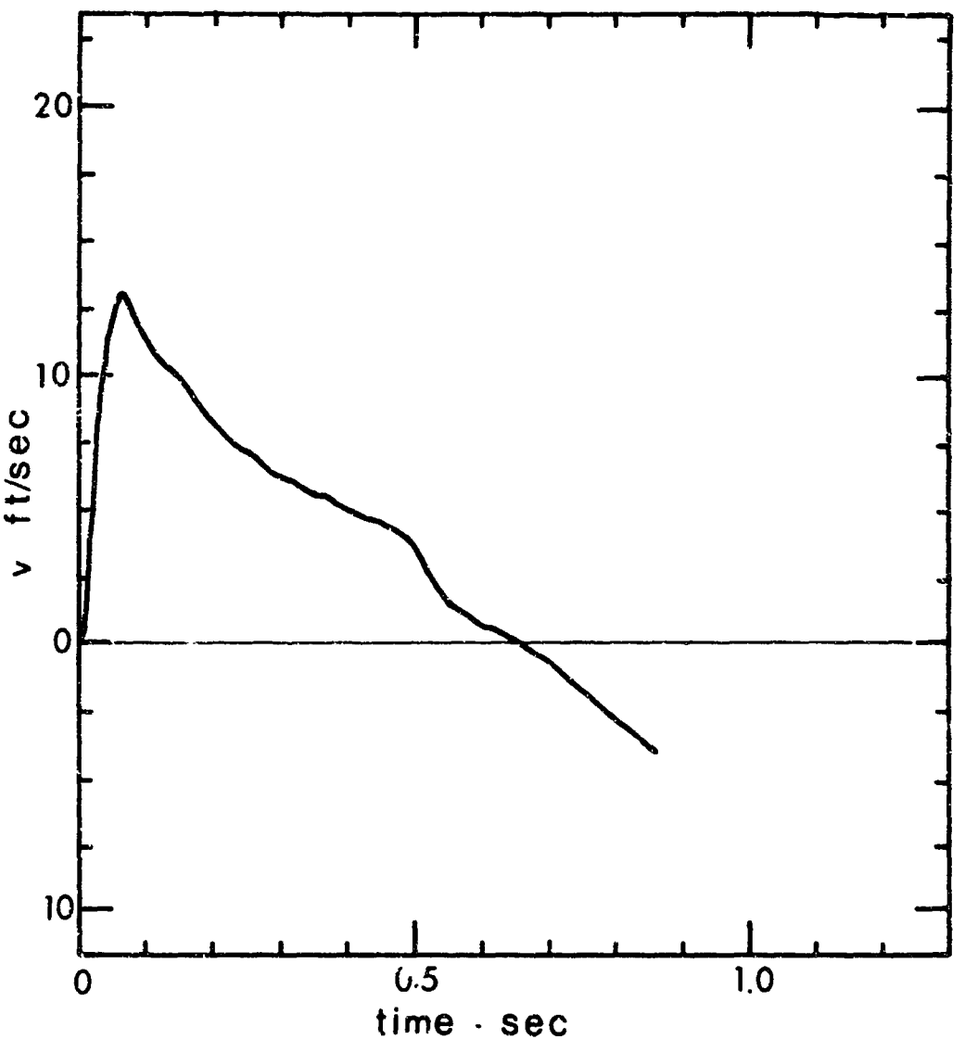

Fig. 48. Particle velocity pulse in andesite, Project LONGSHOT, 80 KT, horizontal range 600 ft., gage depth 100 ft., slant range 2291 ft., gage ?H, EH-?.

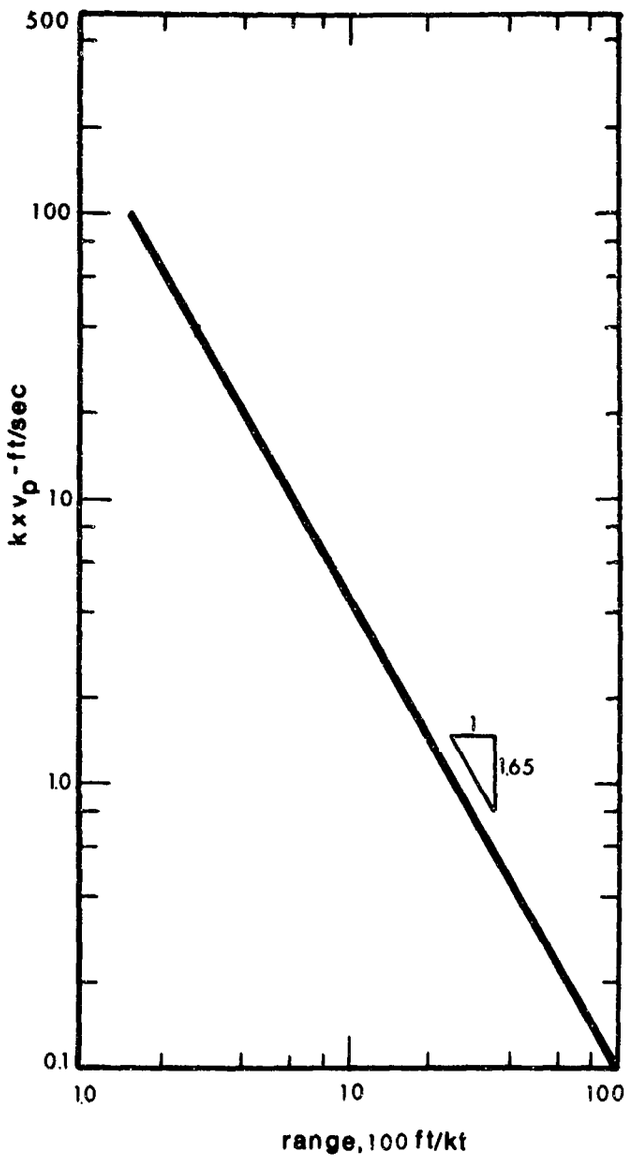

Fig. 49. Composite correlation of magnitude (peak) of radial velocity pulse in salt, granite and tuff, scaled to 1 KT (Ref. 15).

APPENDIX A

WAVE PARAMETER FORMULAS

Summation Symbols

Plane wave - single summation

$$\sum_y^{(s,P)} = \sum_{n=o}^{\infty} \frac{X^n}{n!} \frac{\exp(-X\sqrt{s})}{s^{n/2+y}}$$

$$\sum_z^{(t,P)} = \sum_{n=o}^{\infty} \frac{X^n}{n!} 2^{(n+z)/2} T^{(n+z-1)/2} D_{-n-z}\left(\frac{X}{\sqrt{2T}}\right) \cdot EXP$$

Plane wave - double summation

$$\sum\sum_y^{(s,P)} = \sum_{m=o}^{\infty} \sum_{n=o}^{\infty} b_m \frac{X^n}{n!} \frac{\exp(-X\sqrt{s})}{s^{m+n/2+y}}$$

$$\sum\sum_z^{(t,P)} = \sum_{m=o}^{\infty} \sum_{n=o}^{\infty} b_m \frac{X^n}{n!} 2^{m+(n+z)/2} T^{m+(n+z-1)/2} D_{-n-2m-z}\left(\frac{X}{\sqrt{2T}}\right) \cdot EXP$$

Spherical wave

$$\sum\sum_y^{(s,S)} = \sum_{m=o}^{\infty} \sum_{n=o}^{\infty} b_m \frac{R^n}{n!} \frac{\exp(-R\sqrt{s})}{s^{(m+n)/2+y}}$$

$$\sum\sum_z^{(t,S)} = \sum_{m=o}^{\infty} \sum_{n=o}^{\infty} b_m \frac{R^n}{n!} 2^{(m+n+z)/2} T^{(m+n+z-1)/2} D_{-n-m-z}\left(\frac{R}{\sqrt{2T}}\right) \cdot EXP$$

(s,P) = s variable, plane wave (s,S) = s variable, spherical wave
(t,P) = t variable, plane wave (t,S) = t variable, spherical wave

On the left side of the above equations the first letter in the superscript represents the s-plane or the t-plane, and the second a plane or spherical wave. The subscripts y and z are, respectively, the numerical values of the transform variable exponent other than the summation indices, and the subscript of the Weber function other than the summation indices. In all cases $z = 2y-1$, $EXP = \exp(-T-X^2/8T)$ for the plane wave, and $EXP = \exp(-T-R^2/8T)$ for the spherical wave.

In the following (1) is the transform solution, (2) the transform shifted and normalized, (3) the expanded transform, and (4) the inverse solution.

Plane Wave: $P(t) = P'\delta(t)$

Particle Velocity

$$(1)\quad v(x,t) \doteqdot \frac{P' \exp[-xs/c(s/\omega_o+1)^{\frac{1}{2}}]}{\rho c \qquad (s/\omega_o+1)^{\frac{1}{2}}}$$

$$(2)\quad (1/\omega_o)\ v(x,t/\omega_o)e^t \doteqdot \frac{P' \exp(-X\sqrt{s}+X\sqrt{s})}{\rho c \qquad \sqrt{s}}$$

$$(3)^*\quad (1/\omega_o)\ v(x,t/\omega_o)e^t \doteqdot \frac{P'}{\rho c} \int_{\frac{1}{2}}^{(s,P)}$$

$$(4)^*\quad v(x,t) = \frac{P'\omega_o}{\rho c\sqrt{\pi}} \int_o^{(t,P)}$$

Displacement

$$(1)\quad u(x,t) \doteqdot \frac{P' \exp[-xs/c(s/\omega_o+1)^{\frac{1}{2}}]}{\rho c \qquad s(s/\omega_o+1)^{\frac{1}{2}}}$$

$$(2)\quad (1/\omega_o)\ u(x,t/\omega_o)e^t \doteqdot \frac{P' \exp(-X\sqrt{s}+X/\sqrt{s})}{\rho c\omega_o \quad (s-1)\ \sqrt{s}}$$

$$(3)^*\quad u(x,t/\omega_o)e^t \doteqdot \frac{P'}{\rho c} \int\int_{3/2}^{s,P)}$$

$$(4)^*\quad u(x,t) = \frac{P'}{\rho c\sqrt{\pi}} \int\int_2^{(t,P)}$$

* In summations all $b_m = 1$

Strain

(1) $\varepsilon(x,t) \doteq -\frac{P' \exp[-xs/c(s/\omega_o+1)^{\frac{1}{2}}]}{\rho c^2 \quad (s/\omega_o+1)}$

(2) $(1/\omega_o)\ \varepsilon(x,t/\omega_o)e^t \doteq -\frac{P' \quad \exp(-X\sqrt{s}+X/\sqrt{s})}{\rho c^2 \qquad s}$

(3)* $(1/\omega_o)\ \varepsilon(x,t/\omega_o)e^t \doteq -\frac{P'}{\rho c^2}\sum_1^{(s,P)}$

(4)* $\varepsilon(x,t) = -\frac{P'\omega_o}{\rho c^2\sqrt{\pi}}\sum_1^{(t,P)}$

Stress

(1) $\sigma(x,t) \doteq -P'\exp[-xs/c(s/\omega_o+1)^{\frac{1}{2}}]$

(2) $(1/\omega_o)(x,t/\omega_o)e^t \doteq -P'\exp(-X\sqrt{s}+X/\sqrt{s})$

(3)* $(1/\omega_o)(x,t/\omega_o)e^t \doteq -P'\sum_o^{(s,P)}$

(4)* $\sigma(x,t) \doteq -P'\omega_o\sum_{-1}^{(t,P)}$

** In summations all $b_m = 1$

Plane Wave: $P(t) = P''1(t)$

Particle Velocity

(1) $$v(x,t) \doteq \frac{P''}{\rho c} \frac{\exp[-xs/c(s/\omega_o+1)^{\frac{1}{2}}]}{(s/\omega_o+1)^{\frac{1}{2}}}$$

(2) $$(1/\omega_o)\ v(x,t/\omega_o)e^t \doteq \frac{P''\ \exp(-X\sqrt{s}+X/\sqrt{s})}{\rho c\omega_o\ (s-1)\ \sqrt{s}}$$

(3)* $$v(x,t/\omega_o)e^t \doteq \frac{P''}{\rho c} \sum \int_{3/2}^{(s,P)}$$

(4)* $$v(x,t) = \frac{P''}{\rho c\sqrt{\pi}} \sum \int_{2}^{(t,P)}$$

Displacement

(1) $$u(x,t) \doteq \frac{P''}{\rho c} \frac{\exp[-xs/c(s/\omega_o+1)^{\frac{1}{2}}]}{s^2\sqrt{s/\omega_o+1}}$$

(2) $$u(x,t/\omega_o)e^t \doteq \frac{P''\ \exp(-X\sqrt{s}+X/\sqrt{s})}{\rho c\omega_o\ (s-1)^2\sqrt{s}}$$

(3)** $$u(x,t/\omega_o)e^t \doteq \frac{P''}{\rho c\omega_o} \sum \int_{3/2}^{(s,P)}$$

(4)** $$u(x,t) = \frac{P''}{\rho c\omega_o\sqrt{\pi}} \sum \int_{2}^{(t,P)}$$

* In summations all $b_m = 1$

** Summation on m is from $1 \to \infty$ for this case only and in summations $b_m = m$

Strain

(1) $\varepsilon(x,t) \doteq -\dfrac{P''}{\rho c^2}\dfrac{\exp[-xs/c(s/\omega_o+1)^{\frac{1}{2}}]}{s(s/\omega_o+1)}$

(2) $(1/\omega_o)\ \varepsilon(x,t/\omega_o)e^t \doteq -\dfrac{P''}{\rho c^2\omega_o}\dfrac{\exp(-X\sqrt{s}+X/\sqrt{s})}{s(s-1)}$

(3)* $(1/\omega_o)\ \varepsilon(x,t/\omega_o)e^t \doteq -\dfrac{P''}{\rho c^2}\sum\int_2^{(s,P)}$

(4)* $\varepsilon(x,t) = -\dfrac{P''}{\rho c^2\sqrt{\pi}}\sum\int_3^{(t,P)}$

Stress

(1) $\sigma(x,t) \doteq -\dfrac{P''}{s}\exp[-xs/c(s/\omega_o+1)^{\frac{1}{2}}]$

(2) $(1/\omega_o)\ \sigma(x,t/\omega_o)e^t \doteq -\dfrac{P''}{\omega_o(s-1)}\exp(-X\sqrt{s}+X/\sqrt{s})$

(3)* $\sigma(x,t/\omega_o)e^t \doteq -P''\sum\int_1^{(s,P)}$

(4)* $\sigma(x,t) = -P''\sum\int_1^{(t,P)}$

* In summations all $b_m = 1$

Plane Wave: $P(t) = P_o e^{-\beta t}$

Particle Velocity

(1) $v(x,t) \doteq_o \frac{P_o}{\rho c} \frac{\exp[-xs/c(s/\omega_o+1)^{\frac{1}{2}}}{(s+\beta)\ (s/\omega_o+1)^{\frac{1}{2}}}$

(2) $(1/\omega_o)\ v(x,t/\omega_o)e^t \doteq_o \frac{P_o \exp(-X\sqrt{s}+X/\sqrt{s})}{\rho c\omega_o\ (s-\alpha)\ \sqrt{s}}$

where $\alpha = (1-\beta/\omega_o)$

(3)* $v(x,t/\omega_o)e^t \doteq_o \frac{P_o}{\rho c} \sum \int_{3/2}^{(s,P)}$

(4)* $v(x,t) = \frac{P_o}{\rho c\sqrt{\pi}} \sum \int_{2}^{(t,P)}$

Displacement

(1) $u(x,t) \doteq_o \frac{P_o \exp[-xs/c(s/\omega_o+1)^{\frac{1}{2}}]}{\rho c \quad s(s+\beta)\ (s/\omega_o+1)^{\frac{1}{2}}}$

(2) $u(x,t/\omega_o)e^t \doteq_o \frac{P_o \exp(-X\sqrt{s}+X/\sqrt{s})}{\rho c\omega_o\ (s-1)\ (s-\alpha)\ \sqrt{s}}$

(3)** $u(x,t/\omega_o)e^t \doteq_o \frac{P_o}{\rho c\omega_o} \sum \int_{5/2}^{(s,P)}$

(4)** $u(x,t) = \frac{P_o}{\rho c\omega_o\sqrt{\pi}} \sum \int_{4}^{(t,P)}$

* In summation $b_m = a^m$

** In summation b_m obtained from expansion of $1/(s-1)(s-a)$

Strain

(1) $$\varepsilon(x,t) \doteq -\frac{P_o \exp[-xs/c(s/\omega_o+1)^{1/2}]}{\rho c^2 (s+\beta)(s/\omega_o+1)}$$

(2) $$\varepsilon(x,t/\omega_o)e^t \doteq -\frac{P_o \exp(-X\sqrt{s}+X/\sqrt{s})}{\rho c^2 s(s-\alpha)}$$

(3)* $$\varepsilon(x,t/\omega_o)e^t \doteq -\frac{P_o}{\rho c^2} \sum \sum_2^{(s,P)}$$

(4)* $$\varepsilon(x,t) = -\frac{P_o}{\rho c^2 \sqrt{\pi}} \sum \sum_3^{(t,P)}$$

Stress

(1) $$\sigma(x,t) \doteq -\frac{P_o \exp[-xs/c(s/\omega_o+1)^{1/2}]}{(s+\beta)}$$

(2) $$\sigma(x,t/\omega_o)e^t \doteq -\frac{P_o \exp(-X\sqrt{s}+X/\sqrt{s})}{(s-\alpha)}$$

(3)* $$\sigma(x,t/\omega_o)e^t \doteq -P_o \sum \sum_1^{(s,P)}$$

(4)* $$\sigma(x,t) = -\frac{P_o}{\sqrt{\pi}} \sum \sum_1^{(t,P)}$$

* In summations $b_m = a^m$

Spherical Wave: $P(t) = P'\delta(t)$

Displacement

(1) $$u(r,t) \underset{\omega_o}{\sim} \frac{P' r_o \exp[-s(r-r_o)/c(s/\omega_o+1)^{\frac{1}{2}}]}{\mu(s/\omega_o+1)\ [B]} \left[\frac{1}{r^2} + \frac{s}{rc(s/\omega_o+1)^{\frac{1}{2}}}\right]$$

(2) $$u(r,t/\omega_o)e^t \underset{\omega_o}{\sim} \frac{P' r_o c^2 \exp(-R\sqrt{s}+R/\sqrt{s})}{3\mu\omega_o\ [A]} \left[\frac{1}{r^2} + \frac{\omega_o(s-1)}{rc\sqrt{s}}\right]$$

(3)* $$u(r,t/\omega_o)e^t \underset{\omega_o}{\sim} \frac{P' r_o c}{3\mu\omega_o} \left[\frac{1}{r^2} \sum \sum_2^{(s,S)} + \frac{\omega_o}{rc} \sum \sum_{3/2}^{(s,S)} - \frac{\omega_o}{rc} \sum \sum_{5/2}^{(s,S)}\right]$$

(4)* $$u(r,t) = \frac{P' r_o c^2}{3\mu\omega_o\sqrt{\pi}} \left[\frac{1}{r^2} \sum \sum_3^{(t,S)} + \frac{\omega_o}{rc} \sum \sum_2^{(t,S)} - \frac{\omega_o}{rc} \sum \sum_4^{(t,S)}\right]$$

* In summations all b_m obtained from expansion of $1/[A]$

Particle Velocity

$$(1)\quad v(x,t) \doteq_{\infty} \frac{P' r_o s \exp[-s(r-r_o)/c(s/\omega_o+1)^{\frac{1}{2}}]}{\mu(s/\omega_o+1)\ [B]} \left[\frac{1}{r^2} + \frac{s}{rc(s/\omega_o+1)^{\frac{1}{2}}}\right]$$

$$(2)\quad v(r,t/\omega_o)e^{t} \doteq_{\infty} \frac{P' r_o c^2 (s-1)\ \exp(-R\sqrt{s}+R/\sqrt{s})}{3\mu[A]} \left[\frac{1}{2} + \frac{\omega_o(s-1)}{rc\sqrt{s}}\right]$$

$$(3)^*\quad v(r,t/\omega_o)e^{t} \doteq_{\infty} \frac{P' r_o c^2}{3\mu} \left\{\frac{1}{r^2}\left[\sum\sum{}_1^{(s,S)} - \sum\sum{}_2^{(s,S)}\right] + \frac{\omega_o}{rc}\left[\sum\sum{}_{1/2}^{(s,S)} - 2\sum\sum{}_{3/2}^{(s,S)} + \sum\sum{}_{5/2}^{(s,S)}\right]\right\}$$

$$(4)^*\quad v(r,t) = \frac{P' r_o c^2}{3\mu\sqrt{\pi}} \left\{\frac{1}{r^2}\left[\sum\sum{}_1^{(t,S)} - \sum\sum{}_3^{(t,S)}\right] + \frac{\omega_o}{rc}\left[\sum\sum{}_o^{(t,S)} - 2\sum\sum{}_2 + \sum\sum{}_4^{(t,S)}\right]\right\}$$

* In summations all b_m obtained from expansion of $1/[A]$

Strain

$$(1)\quad \varepsilon(r,t) \doteq -\frac{P' r_o \exp[-s(r-r_o)/c(s/\omega_o+1)^{\frac{1}{2}}]}{\mu(s/\omega_o+1)\ [B]} \times$$

$$\left[\frac{2}{r^3} + \frac{2s}{r^2 c(s/\omega_o+1)^{\frac{1}{2}}} + \frac{s^2}{rc^2(s/\omega_o+1)}\right]$$

$$(2)\quad \varepsilon(r,t/\omega_o)e^t \doteq -\frac{P' r_o c^2 \exp(-R\sqrt{s}+R/\sqrt{s})}{3\mu\omega_o[A]} \times$$

$$\left[\frac{2}{r^3} + \frac{2\omega_o(s-1)}{r^2 c\sqrt{s}} + \frac{\omega_o^2(s-1)^2}{rc^2 s}\right]$$

$$(3)^*\quad \varepsilon(r,t/\omega_o)e^t \doteq -\frac{P' r_o c^2}{3\mu\omega_o}\left\{\frac{2}{r^3}\sum\sum_2^{(s,S)} + \frac{2\omega_o}{r^2 c}\left[\sum\sum_{3/2}^{(s,S)} - \sum\sum_{5/2}^{(s,S)}\right]\right.$$

$$\left. + \frac{\omega_o^2}{rc^2}\left[\sum\sum_1^{(s,S)} - 2\sum\sum_2^{(s,S)} + \sum\sum_3^{(s,S)}\right]\right\}$$

$$(4)^*\quad \varepsilon(r,t) = -\frac{P' r_o c^2}{3\mu\omega_o\sqrt{\pi}}\left\{\frac{2}{r^3}\sum\sum_3^{(t,S)} + \frac{2\omega_o}{r^2 c}\left[\sum\sum_2^{(t,S)} - \sum\sum_4^{(t,S)}\right]\right.$$

$$\left. + \frac{\omega_o^2}{rc^2}\left[\sum\sum_1^{(t,S)} - 2\sum\sum_3^{(t,S)} + \sum\sum_5^{(t,S)}\right]\right\}$$

* In summations all b_m obtained from expansion of $1/[A]$

Stress

$$(1)\quad \sigma(r,t) \doteq -\frac{P' r_o \exp[-s(r-r_o)/c(s/\omega_o+1)^{\frac{1}{2}}]}{3[B]} \times$$

$$\left[\frac{4}{r^3} + \frac{4s}{r^2 c(s/\omega_o+1)^{\frac{1}{2}}} + \frac{3s^2}{rc^2(s/\omega_o+1)}\right]$$

$$(2)\quad \sigma_r(r,t)e^t \doteq -\frac{P' r_o c^2 s \exp(-R\sqrt{s}+R/\sqrt{s})}{3\omega_o\ [A]} \times$$

$$\left[\frac{4}{r^3} + \frac{4\omega_o(s-1)}{r^2 c\sqrt{s}} + \frac{3\omega_o^2(s-1)^2}{rc^2 s}\right]$$

$$(3)^*\quad \sigma_r(r,t)e^t \doteq -\frac{P' r_o c^2}{3\omega_o}\left\{\frac{4}{r^3}\sum\sum{}_1^{(s,S)} + \frac{4\omega_o}{r^2 c}\left[\sum\sum{}_{1/2}^{(s,S)} - \sum\sum{}_{3/2}^{(s,S)}\right]\right.$$

$$\left. + \frac{3\omega_o^2}{rc^2}\left[\sum\sum{}_0^{(s,S)} - 2\sum\sum{}_1^{(s,S)} + \sum\sum{}_2^{(s,S)}\right]\right\}$$

$$(4)^*\quad \sigma(r,t) \doteq -\frac{P' r_o c^2}{3\omega_o\sqrt{\pi}}\left\{\frac{4}{r^3}\sum\sum{}_1^{(t,S)} + \frac{4\omega_o}{r^2 c}\left[\sum\sum{}_0^{(t,S)} - \sum\sum{}_2^{(t,S)}\right]\right.$$

$$\left. + \frac{3\omega_o^2}{rc^2}\left[\sum\sum{}_1^{(t,S)} - 2\sum\sum{}_1^{(t,S)} + \sum\sum{}_3^{(t,S)}\right]\right\}$$

* In summations all b_m calculated from expansion of 1/[A]

Spherical Wave: $P(t) = P''\,1(t)$

Displacement

(1) $$u(r,t) \doteq \frac{P''r_o \exp[-s(r-r_o)/c(s/\omega_o+1)^{\frac{1}{2}}]}{\mu s(s/\omega_o+1)\ [B]} \left[\frac{1}{r^2} + \frac{s}{rc(s/\omega_o+1)^{\frac{1}{2}}}\right]$$

(2) $$u(r,t/\omega_o)e^t \doteq \frac{P''r_o c^2 \exp(-R\sqrt{s}+R/\sqrt{s})}{3\mu\omega_o{}^2(s-1)\ [A]} \left[\frac{1}{r^2} + \frac{\omega_o(s-1)}{rc\sqrt{s}}\right]$$

(3)* $$u(r,t/\omega_o)e^t \doteq \frac{P''r_o c^2}{3\mu\omega_o{}^2} \left\{\frac{1}{r^2} \sum \sum_3^{(s,S)} + \frac{\omega_o}{rc}\left[\sum \sum_{5/2}^{(s,S)} - \sum \sum_{7/2}^{(s,S)}\right]\right\}$$

(4)* $$u(r,t) = \frac{P''r_o c^2}{3\mu\omega_o\sqrt{\pi}} \left\{\frac{1}{r^2} \sum \sum_5^{(t,S)} + \frac{\omega_o}{rc}\left[\sum \sum_4^{(t,S)} - \sum \sum_6^{(t,S)}\right]\right\}$$

* In summations b_m calculated from expansion of $1/(s-1)$ [A]

Particle Velocity

$$(1)\quad v(r,t) \doteq \frac{P''r_o \exp[-s(r-r_o)/c(s/\omega_o+1)^{\frac{1}{2}}]}{\mu(s/\omega_o+1)\ [B]}\left[\frac{1}{r^2} + \frac{s}{rc(s/\omega_o+1)^{\frac{1}{2}}}\right]$$

$$(2)\quad v(r,t/\omega_o)e^t \doteq \frac{P''\omega_o r_o \exp(-R\sqrt{s}+/\sqrt{s})}{3\mu\omega_o\ [A]}\left[\frac{1}{r^2} + \frac{\omega_o(s-1)}{rc\sqrt{s}}\right]$$

$$(3)^*\quad v(r,t/\omega_o)e^t \doteq \frac{P''r_o c^2}{3\mu\omega_o}\left\{\frac{1}{r^2}\sum\sum{}_2^{(s,S)} + \frac{\omega_o}{rc}\left[\sum\sum{}_{3/2}^{(s,S)} - \sum\sum{}_{5/2}^{(s,S)}\right]\right\}$$

$$(4)^*\quad v(r,t) = \frac{P''r_o c^2}{3\mu\omega_o\sqrt{\tau}}\left\{\frac{1}{r^2}\sum\sum{}_3^{(t,S)} + \frac{\omega_o}{rc}\left[\sum\sum{}_2^{(t,S)} - \sum\sum{}_4^{(t,S)}\right]\right\}$$

* In summations b_m calculated from expansion of 1/[A]

Strain

(1) $$\varepsilon(r,t) \doteq -\frac{P'' r_o \exp[-s(r-r_o)/c(s/\omega_o+1)^{\frac{1}{2}}]}{\mu(s/\omega_o+1)\ [B]}$$

$$\left[\frac{2}{r^3} + \frac{2s}{r^2 c(s/\omega_o+1)^{\frac{1}{2}}} + \frac{s^2}{rc^2(s/\omega_o+1)}\right]$$

(2) $$\varepsilon(r,t/\omega_o)e^t \doteq -\frac{P'' r_o c^2 \exp(-R\sqrt{s}+R/\sqrt{s})}{3\mu\omega_o^2\ (s-1)\ [A]}$$

$$\left[\frac{2}{r^2} + \frac{2\omega_o(s-1)}{r^2 c\sqrt{s}} + \frac{\omega_o^2(s-1)^2}{rc^2 s}\right]$$

(3)* $$\varepsilon(r,t/\omega_o)e^t \doteq -\frac{P'' r_o c^2}{3\mu\omega_o^2}\left\{\frac{2}{r^3}\sum\sum_3^{(s,S)} + \frac{2\omega_o}{r^2 c}\left[\sum\sum_{5/2}^{(s,S)} - \sum\sum_{7/2}^{(s,S)}\right]\right.$$

$$\left. + \frac{\omega_o^2}{rc^2}\left[\sum\sum_2^{(s,S)} - 2\sum\sum_3^{(s,S)} + \sum\sum_4^{(s,S)}\right]\right\}$$

(4)* $$\varepsilon(r,t) = -\frac{P'' r_o c^2}{3\mu\omega_o^2\sqrt{\pi}}\left\{\frac{2}{r^3}\sum\sum_5^{(t,S)} + \frac{2\omega_o}{r^2 c}\left[\sum\sum_4^{(t,S)} - \sum\sum_6^{(t,S)}\right]\right.$$

$$\left. + \frac{\omega_o^2}{rc^2}\left[\sum\sum_3^{(t,S)} - 2\sum\sum_5^{(t,S)} + \sum\sum_7^{(t,S)}\right]\right\}$$

* In summations all b_m calculated from expansion of 1/[A]

Stress

$$(1)\quad \sigma(r,t) \doteq -\frac{P''\exp[-s(r-r_o)/c(s/\omega_o+1)^{\frac{1}{2}}]}{s\ [B]} \times \left[\frac{4}{r^3} + \frac{4s}{r^2c(s/\omega_o+1)^{\frac{1}{2}}} + \frac{3s^2}{rc^2(s/\omega_o+1)}\right]$$

$$(2)\quad \sigma(r,t/\omega_o)e^t \doteq -\frac{P''r_oc^2s\exp(-R\sqrt{s}+R/\sqrt{s})}{3\omega_o^2\ (s-1)\ [A]} \times \left[\frac{4}{r^3} + \frac{4\omega_o(s-1)}{r^2c\sqrt{s}} + \frac{3\omega_o^2(s-1)^2}{rc^2s}\right]$$

$$(3)^*\quad \sigma(r,t/\omega_o)e^t \doteq -\frac{P''r_oc^2}{3\omega_o^2}\left\{\frac{4}{r^3}\sum\sum_2^{(s,S)} + \frac{4\omega_o}{r^2c}\left[\sum\sum_{3/2}^{(s,S)} - \sum\sum_{5/2}^{(s,S)}\right] + \frac{3\omega_o^2}{rc^2}\left[\sum\sum_1^{(s,S)} - 2\sum\sum_2^{(s,S)} + \sum\sum_3^{(s,S)}\right]\right\}$$

$$(4)^*\quad \sigma(r,t) = -\frac{P''r_oc^2}{3\omega_o^2\sqrt{\pi}}\left\{\frac{4}{r^3}\sum\sum_3^{(t,S)} + \frac{4\omega_o}{r^2c}\left[\sum\sum_2^{(t,S)} - \sum\sum_4^{(t,S)}\right] + \frac{3\omega_o^2}{rc^2}\left[\sum\sum_1^{(t,S)} - 2\sum\sum_3^{(t,S)} + \sum\sum_5^{(t,S)}\right]\right\}$$

* In summations all b_m calculated from expansion of 1/[A]

Spherical Wave: $P(t) = P_o e^{-\beta t}$

Displacement

(1) $$u(r,t) \fallingdotseq \frac{P_o r_o \exp[-s(r-r_o)/c(s/\omega_o+1)^{\frac{1}{2}}]}{\mu(s+\beta)\ (s/\omega_o+1)\ [B]} \left[\frac{1}{r^2} + \frac{s}{rc(s/\omega_o+1)^{\frac{1}{2}}}\right]$$

(2) $$u(r,t/\omega_o)e^t \fallingdotseq \frac{P_o r_o c^2 \exp(-R\sqrt{s}+R/\sqrt{s})}{3\mu\omega_o^2\ (s-\alpha)\ [A]} \left[\frac{1}{r^2} + \frac{\omega_o(s-1)}{rc\sqrt{s}}\right]$$

$$\alpha = (1-\beta/\omega_o)$$

(3)* $$u(r,t/\omega_o)e^t \fallingdotseq \frac{P_o r_o c^2}{3\mu\omega_o^2}\left\{\frac{1}{r^2}\sum\int_3^{(s,S)} + \frac{\omega_o}{rc}\left[\sum\int_{5/2}^{(s,S)} - \sum\int_{7/2}^{(s,S)}\right]\right\}$$

(4)* $$u(r,t) = \frac{P_o r_o c^2}{3\mu\omega_o^2\sqrt{\pi}}\left\{\frac{1}{r^2}\sum\int_5^{(t,S)} + \frac{\omega_o}{rc}\left[\sum\int_4^{(t,S)} - \sum\int_6^{(t,S)}\right]\right\}$$

* In summations b_m calculated from expansion of $1/(s-\alpha)[A]$

Particle Velocity

$$(1)\quad v(r,t) \doteq \frac{P_o r_o s \exp[-s(r-r_o)/c(s/\omega_o+1)^{\frac{1}{2}}]}{\mu(s+\beta)\ (s/\omega_o+1)\ [B]} \left[\frac{1}{r^2} + \frac{s}{rc(s/\omega_o+1)^{\frac{1}{2}}}\right]$$

$$(2)\quad v(r,t/\omega_o)e^t \doteq \frac{P_o r_o c^2\ (s-1)\ \exp(-R\sqrt{s}+R/\sqrt{s})}{3\mu\omega_o\ \ (s-\alpha)\ [A]} \left[\frac{1}{r^2} + \frac{\omega_o(s-1)}{rc\sqrt{s}}\right]$$

$$(3)^*\quad v(r,t/\omega_o)e^t \doteq \frac{P_o r_o c^2}{3\mu\omega_o}\left\{\frac{1}{r^2}\left[\sum\sum{}_2^{(s,S)} - \sum\sum{}_3^{(s,S)}\right] + \frac{\omega_o}{rc}\left[\sum\sum{}_{3/2}^{(s,S)} - 2\sum\sum{}_{5/2}^{(s,S)} + \sum\sum{}_{7/2}^{(s,S)}\right]\right\}$$

$$(4)^*\quad v(r,t) = \frac{P_o r_o c^2}{3\mu\omega_o\sqrt{\pi}}\left\{\frac{1}{r^2}\left[\sum\sum{}_3^{(t,S)} - \sum\sum{}_5^{(t,S)}\right] + \frac{\omega_o}{rc}\left[\sum\sum{}_2^{(t,S)} - 2\sum\sum{}_4^{(t,S)} + \sum\sum{}_6^{(t,S)}\right]\right\}$$

* In summations b_m calculated from expansion of $1/(s-\alpha)$ [A]

Strain

(1) $$\varepsilon(r,t) \doteq -\frac{P_o r_o \exp[-s(r-r_o)/c(s/\omega_o+1)^{\frac{1}{2}}]}{\mu(s+\beta)\ (s/\omega_o+1)\ [B]} \times$$

$$\left[\frac{2}{r^3} + \frac{2s}{r^2 c(s/\omega_o+1)^{\frac{1}{2}}} + \frac{s^2}{rc^2(s/\omega_o+1)}\right]$$

(2) $$\varepsilon(r,t/\omega_o)e^t \doteq -\frac{P_o r_o \exp(-R\sqrt{s}+R/\sqrt{s})}{3\mu(s-\alpha)\ [A]}\left[\frac{2}{r^3} + \frac{2\omega_o(s-1)}{r^2 c\sqrt{s}} + \frac{\omega_o^2(s-1)^2}{rc^2 s}\right]$$

(3)* $$\varepsilon(r,t/\omega_o)e^t \doteq -\frac{P_o r_o c^2}{3\mu\omega_o^2}\left\{\frac{2}{r^3}\sum\sum_3^{(s,S)} + \frac{2\omega_o}{r^2 c}\left[\sum\sum_{5/2}^{(s,S)} - \sum\sum_{7/2}^{(s,S)}\right]\right.$$

$$\left. + \frac{\omega_o^2}{rc^2}\left[\sum\sum_2^{(s,S)} - 2\sum\sum_3^{(s,S)} + \sum\sum_4^{(s,S)}\right]\right\}$$

(4)* $$\varepsilon(r,t) = -\frac{P_o r_o c^2}{3\mu\omega_o^2\sqrt{\pi}}\left\{\frac{2}{r^3}\sum\sum_5^{(t,S)} + \frac{2\omega_o}{r^2 c}\left[\sum\sum_4^{(t,S)} - \sum\sum_6^{(t,S)}\right]\right.$$

$$\left. + \frac{\omega_o^2}{rc^2}\left[\sum\sum_3^{(t,S)} - 2\sum\sum_5^{(t,S)} + \sum\sum_7^{(t,S)}\right]\right\}$$

* In summations b_m calculated from expansion of $1/(s-\alpha)$ [A]

Stress

$$(1)\quad \sigma(r,t) \doteq -\frac{P_o r_o \exp[-s(r-r_o)/c(s/\omega_o+1)^{\frac{1}{2}}]}{(s+\beta)\ [B]} \times$$

$$\left[\frac{4}{r^3} + \frac{4s}{r^2 c(s/\omega_o+1)^{\frac{1}{2}}} + \frac{3s^2}{rc^2(s/\omega_o+1)}\right]$$

$$(2)\quad \sigma(r,t/\omega_o)e^{t} \doteq -\frac{P_o r_o c^2 s \exp(-R\sqrt{s}+R/\sqrt{s})}{3\omega_o^2\ (s-\alpha)\ [A]} \times$$

$$\left[\frac{4}{r^3} + \frac{4\omega_o(s-1)}{r^2 c\sqrt{s}} + \frac{3\omega_o^2(s-1)^2}{rc^2 s}\right]$$

$$(3)^*\quad \sigma(r,t/\omega_o)e^{\bar{t}} \doteq -\frac{P_o r_o c^2}{3\omega_o^2}\left\{\frac{4}{r^3}\ \sum\sum_{2}^{(s,S)} + \frac{4\omega_o}{r^2 c}\left[\sum\sum_{3/2}^{(s,S)} - \sum\sum_{5/2}^{(s,S)}\right]\right.$$

$$\left. + \frac{3\omega_o^2}{rc^2}\left[\sum\sum_{1}^{(s,S)} - 2\sum\sum_{2}^{(s,S)} + \sum\sum_{3}^{(s,S)}\right]\right\}$$

$$(4)^*\quad \sigma(r,t) = -\frac{P_o r_o c^2}{3\omega_o^2\sqrt{\pi}}\left\{\frac{4}{r^3}\ \sum\sum_{3}^{(t,S)} + \frac{4\omega_o}{r^2 c}\left[\sum\sum_{2}^{(t,S)} - \sum\sum_{4}^{(t,S)}\right]\right.$$

$$\left. + \frac{3\omega_o^2}{rc^2}\left[\sum\sum_{1}^{(t,S)} - 2\sum\sum_{3}^{(t,S)} + 2\sum\sum_{5}^{(t,S)}\right]\right\}$$

* In summations b_m calculated from expansion of $1/(s-\alpha)[A]$

References

1. Collins, F., Plane Compressional Voigt Waves, Geoph., Vol. 25, pp. 483-492, 1960.

2. Hanin, M., Propagation of an Aperiodic Wave in a Compressible Viscous Medium, Jl. of Math. and Phys., Vol. 36, p. 234, 1956.

3. Lee, T.M., Spherical Waves in Viscoelastic Media, Jl. Acoustical Soc. of Am., Vol. 36, pp. 2402-2407, December 1964.

4. Clark, G.B., Rupert, G.B., and Jamison, J.E., Transient Plane Voigt Waves, submitted to Quarterly of Applied Math.

5. Rupert, G.B., A Study of Plane and Spherical Waves in a Voigt Viscoelastic Medium, Ph.D. thesis, U. of Mo. at Rolla, 1964.

6. Voigt, W., Ann. d. Phys., Vol. 47, 1892.

7. Kolsky, H., Stress Waves in Solids, Oxford, 1953.

8. Erdelyi, A., Tables of Integral Transforms, Vol. 1, McGraw-Hill, 1954.

9. Kaplan, W., Operational Methods for Linear Systems, p. 328, Addison Wesley, 1962.

10. Carslaw, H.S., and Jeager, J.C., Operational Methods for Applied Mathematics, p. xii, Dover, 1963.

11. Abramowitz, M., and Stegun, I.A., Handbook of Math. Functions, Nat. Bur. of Stand., Appl. Math. Series 55, pp. 298-299.

12. Day, J.D., and Murrell, D.W., Operation LONG SHOT, Ground and Water Shock Measurements, POR, Project 1.01, U.S.A. Waterways Exp. Sta., August 1966.

13. Perrett, W.R., Operation NOUGAT, Shot HARD HAT, POR, Project 3.3, Free Field Motion Studies in Granite, Sandia Corp., POR-1803 (WT-1803) April 1963.

14. Weart, W.D., Project GNOME, Particle Motion Near a Nuclear Detonation in Halite, Sandia Corp., PNE-108P, March 1962.

15. Sauer, F.M., et al., Empirical Analysis of Ground Motion and Cratering, Nuclear Geoplosics, Pt. IV, DASA-1285(IV), May 1964.

Unclassified
Security Classification

DOCUMENT CONTROL DATA - R & D

(Security classification of title, body of abstract and indexing annotation must be entered when the overall report is classified)

1 ORIGINATING ACTIVITY (Corporate author)	2a. REPORT SECURITY CLASSIFICATION
George B. Clark and Associates Rolla, Missouri	Unclassified
	2b. GROUP

3 REPORT TITLE

A COMPARISON OF PLANE AND SPHERICAL TRANSIENT VOIGT WAVES WITH EXPLOSION GENERATED WAVES IN ROCK MASSES

4 DESCRIPTIVE NOTES (Type of report and inclusive dates)
Final Report

5 AUTHOR(S) (First name, middle initial, last name)

G. B. Clark, G. B. Rupert, and J. E. Jamison

6 REPORT DATE	7a. TOTAL NO. OF PAGES	7b. NO. OF REFS
April 1967	115	15

8a. CONTRACT OR GRANT NO.	9a. ORIGINATOR'S REPORT NUMBER(S)
DA-22-079-eng-464 b. PROJECT NO c. NWER Subtask 13.191C d	9b. OTHER REPORT NO(S) (Any other numbers that may be assigned this report) U. S. Army Engineer Waterways Experiment Station Contract Rpt No. 1-170

10 DISTRIBUTION STATEMENT

Distribution of this document is unlimited.

11 SUPPLEMENTARY NOTES	12 SPONSORING MILITARY ACTIVITY
Conducted for U. S. Army Engineer Waterways Experiment Station, Corps of Engineers, Vicksburg, Miss.	Defense Atomic Support Agency, Washington, D. C.

13 ABSTRACT

Plane and spherical waves in a Voigt medium were investigated to compare the calculated wave forms with observed waves generated by large contained HE and NE explosions. Interest is centered on wave forms in what is usually considered to be the elastic region around an explosion. Plane waves do not apply at this distance because of geometry. The plane Voigt wave equation has been previously solved for particle velocity, stress and strain for a unit impulse forcing function. However, solutions for the displacement for a unit impulse and for the four wave parameters for a unit step and a decay exponential involve multipliers in the operational form for which no transform pairs have been published. A method of solution is presented which utilizes a Heaviside expansion of the multipliers in the transform plane which results in products of two infinite series which may be inverted term by term. These may be further resolved as single series with polynomial coefficients for purposes of computation. A similar method of solution of Voigt spherical waves was found for unit impulse, unit step and decay exponential forcing functions for displacement, particle velocity, strain and radial stress. Appropriate recursion formulas make them readily adaptable to computer evaluation. Oscillations occur for a spherical wave whereas for a plane wave they do not. Calculations were performed for particle velocity for three values of the Voigt viscoelastic parameter ϵ_0 and comparisons made with pulse forms for waves in granite, tuff and salt.

DD FORM 1473 REPLACES DD FORM 1473, 1 JAN 64, WHICH IS OBSOLETE FOR ARMY USE

Unclassified
Security Classification

14. KEY WORDS	LINK A		LINK B		LINK C	
	ROLE	WT	ROLE	WT	ROLE	WT
Explosions						
Mechanical waves						
Rock (Geology)						
Shock waves						

DEPARTMENT OF THE ARMY
WATERWAYS EXPERIMENT STATION, CORPS OF ENGINEERS
VICKSBURG, MISSISSIPPI 39181

IN REPLY REFER TO:

24 January 1968

Errata Sheet

No. 1

A COMPARISON OF PLANE AND SPHERICAL TRANSIENT VOIGT WAVES WITH EXPLOSION GENERATED WAVES IN ROCK MASSES

Contract Report No. 1-170

April 1967

Please make the following revisions:

1. Insert on page 33:

"AIRVENT* - playa

Density - wet 1.44-1.85

Density - dry 1.15-1.67

Porosity - estimated 5070

Hugoniot Data

ρ_o = 1.41-1.47 gm/cm^3

V = 2.58-5.24 mm/μsec

u = 1.04-3.54 mm/μsec

P = 30-271 kb

v/v_o = 0.302-640"

2. Page 28, line 10 - Delete "AIRVENT"

Insert after line 10 - "AIRVENT was a 40,000 lb. TNT event detonated at 17 ft. depth in desert playa."

3. Page 29, line 26 - Delete "No data were available for AIRVENT."

4. Page 30, line 37 - Substitute "playa" for "andesite."

---

* Kintzinger, P. R., AIRVENT Phase I, Project I, Earth Particle Motion. SC-RR-64-549, Sandia Corporation, October 1964.